TARGETED THERAPY FOR LIVER FIBROSIS AND CANCER

by

Yifei Zhang

BS in Pharmaceutical Sciences, Peking University, 2006

MS in Pharmaceutics, Peking University, 2008

Submitted to the Graduate Faculty of

School of Pharmacy in partial fulfillment

of the requirements for the degree of

Doctor of Philosophy

University of Pittsburgh

2014

UNIVERSITY OF PITTSBURGH

SCHOOL OF PHARMACY

This dissertation was presented

by

Yifei Zhang

It was defended on

May 28, 2014

and approved by

Chandrashekhar Gandhi, PhD, Professor
Department of Pediatrics; Division of Gastroenterology, Hepatology and Nutrition
Cincinnati Children's Hospital Medical Center and University of Cincinnati

Raman Venkataramanan, PhD, Professor
Pharmaceutical Science, School of Pharmacy, University of Pittsburgh

Wen Xie, MD, PhD, Professor
Pharmaceutical Science, School of Pharmacy, University of Pittsburgh

Dissertation Advisor: Song Li, MD, PhD, Professor
Center for Pharmacogenetics, Department of Pharmaceutical Sciences,
School of Pharmacy, University of Pittsburgh

TARGETED THERAPY FOR LIVER FIBROSIS AND CANCER

Yifei Zhang, PhD

University of Pittsburgh, 2014

Liver fibrosis is a chronic disorder that leads to accumulation of excessive amounts of extracellular matrix (ECM), and the first part of my dissertation work is about the effect of microRNA miR-29a in inhibiting the ECM gene expression at post-transcriptional or translational level. Our data indicates that transfection of hepatic stellate cells (HSCs) with miR-29a significantly inhibited the expression of ECM-related genes, which was mediated by the putative targeting sites at their 3'-UTR. We have also found that miR-29a plays a role in mediating the antifibrotic effect of the nuclear receptor Farnesoid X receptor (FXR). In addition, we have uncovered that miR-29b indirectly inhibits ECM synthesis at post-translational level. By targeting the 3'-UTR of Heat shock protein 47 (HSP47) and lysyl oxidase (LOX) which are known to be essential for post-translational modification of ECM proteins, overexpression of miR-29b led to abnormal ECM structure as shown by electron-microscopy.

The second part of my work was to improve the therapeutic outcome via formulation strategy. A drug-interactive motif (Fmoc) was introduced into the PEG_{5K}-VE_2 micelle system (PEG-FVE_2), and the drug loading capacity was evaluated using paclitaxel (PTX) as a model drug. The Fmoc/PTX physical interaction was demonstrated by a fluorescence quenching assay. PTX-loaded PEG-FVE_2 micelles exerted higher antitumor effect than the Taxol formulation both in vitro and in vivo.

As an overall approach, the targeting efficiency of drug carriers was further improved by conjugation with a ligand for the Sigma-2 receptor, which is over-expressed in multiple types of solid tumors. SV119 is a synthetic small molecule which binds to sigma-2 receptors with high affinity and specificity. The final part of my study showed that incorporation of SV119-PEG-DOA significantly increased the cellular uptake of liposomes by tumor cells but not normal cells. This study suggests that SV119-modified liposomes might be another promising drug carrier for tumor targeted drug delivery.

In summary, our study suggests that miR-29 holds potential as a novel therapeutic agent for the treatment of liver fibrosis. In addition, we have developed a novel formulation that enhances the therapeutic efficacy of existing anticancer agents such as paclitaxel.

TABLE OF CONTENTS

LIST OF TABLES

LIST OF FIGURES

PREFACE

I would like to express a wealth of gratitude to my advisor, Dr. Song Li, a dedicated scientist and an excellent mentor who guided me through my PhD study. Throughout these years Dr. Li has offered me many opportunities on various projects and aspects which have greatly enriched my training experience. I am also very grateful for his open-mindedness and belief in my potential. He constantly encourages me to be fearless since he believes that I could always accomplish more, and he is always there when I need help. Dr. Li's laboratory not only provided me a wonderful environment for the development of nanocarriers for drug delivery, but also equipped me with the ability and confidence to explore other fields such as molecular biology. Without his encouragement and generous help, it would not be possible for me to make achievements on both fields.

I would also like to thank my committee members, Dr. Wen Xie, Dr. Raman Venkataramanan and Dr. Chandrashekhar Gandhi for their numerous advices and help in my research. Special thanks to Dr. Jiang Li for his invaluable guidance on my research and life; to Dr. Xiang Gao for his wealth of knowledge and passion for science that he is always willing to share; to Dr. Yixian Huang for his help with organic synthesis and insightful scientific discussions; to Dr. Lisa Rohan, Dr. Sean Xie, Dr. Donna B Stolz and Ming Sun for their the lab equipments and techniques.

I would like to extend my hearty thanks to all my colleagues and friends in Li Lab as well (Dr. Jiang Li, Dr. Xiang Gao, Dr. Yixian Huang, Peng Zhang, Jianqin Lu, Mohammed Ghazwani, Jilong Li, Xiaolan Zhang, Yichao Chen and Jieni Xu), who inspired me to strive for excellence. The work would be much less fun without them.

Many thanks go to the faculties from Center for Pharmacogenetics and the School of Pharmacy at the University of Pittsburgh. Special thanks to Dr. Patricia Dowley Kroboth, Dr. Randall B. Smith, Dr. Barry Gold, Dr. Robert B Gibbs, Dr. Maggie Folan, Lori Schmotzer and William C. Smith for their endless support and help all these years.

This dissertation is dedicated to my husband, Morigen, for his endless love, support and encouragement; and to my parents who are always supportive and proud of me. They have been a constant source of motivation for me to work hard and achieve my goals.

1.0 INTRODUCTION

1.1 INTRODUCTION ABOUT LIVER FIBROSIS AND MIRNA

1.1.1 AN OVERVIEW OF LIVER FIBROSIS

Liver fibrosis or cirrhosis is a serious problem worldwide. It ranks as the seventh leading cause of death in the United States. This advanced form of chronic liver disease is a result of pathological response to initial liver injuries of various causes, such as viral infections, drug overdoses, alcohol abuses, or bile-duct obstruction, and so on (Vitaglione et al. 2004, Chua et al. 2005, Prescott et al. 2005, Popov et al. 2009). The development of this chronic disease is characterized by a complex array of biologic processes that lead to the increased production of extracellular matrix (ECM) (Manabe et al. 2002, Popov et al. 2009). The scar tissue slowly replaces the normal liver tissue, leading to the loss of normal liver functions such as metabolism, detoxification, and endocrine functions (Triger et al. 1988). These fibrotic changes also lead to increases in intrahepatic vascular resistance and the development of portal hypertension (Thabut et al. 2010).

The mechanism of the pathogenesis of liver fibrosis is complicated and may differ dependent on the underlying etiology (Bataller et al. 2005). However, transactivation of hepatic stellate cells (HSCs) plays an important role in the development of liver fibrosis (Zhao et al.

2012). Hepatic stellate cells are located in the perisinusoidal space of Disse. Under quiescent condition, HSCs store 80% of the total body's vitamin A within their cytoplasm. Liver injury triggers the initiating and subsequent perpetuating signals that activate the quiescent HSCs (Ye et al. 2007). Initiating signals include oxidative stress signals, apoptotic bodies, TLR4 ligands (lipopolysaccharide) and paracrine stimuli from neighboring Kupffer cells, sinusoidal endothelial cells, and hepatocytes. These lead to the transformation of HSCs into proliferating, myofibroblast-like cells (Ghiassi-Nejad et al. 2008). They also gain several new phenotypes, such as enhanced cell migration and adhesion, expression of a-smooth muscle actin (a-SMA), loss of retinoid storing capacity, and, most importantly, acquisition of fibrogenic capacity (Friedman 2008). The buildup of excessive ECM proteins leads to fibrotic liver with impaired organ function (Friedman 2008). In addition to the pro-fibrogenic activities, activated HSCs acquire contractile property and respond to various vasoconstrictors, particularly endothelin-1 (ET-1), which contributes to the reduction of sinusoidal blood flow and the development of portal hypertension (Iwakiri 2012). A number of therapies are currently being tested in the clinic and these include angiotensin II antagonists, interferon-g, PPAR-g ligands, and drugs that inhibit collagen synthesis (pirfenidone) or secretion (colchicine) (Rockey 2008).

1.1.2 RNA interference and liver fibrosis

1.1.2.1 siRNA and miRNA for RNA interference

Over the past few years, studies of small RNAs have exploded and gained increasing attention. It is apparent that small RNAs play a very significant role in various biological processes (Liao et al. 1995, Sage et al. 1997, Suzuki et al. 2005). These tiny RNAs (21–26 nt) include short interfering (si) RNAs, microRNAs (miRNAs), heterochromatic siRNAs, tiny noncoding RNAs

and small temporal (st) RNAs (Lau et al. 2001, Poy et al. 2004, Sugiyama et al. 2005). SiRNA and miRNA are central to RNA interference (RNAi), which can modulate mRNA and protein expression (Kutter et al. 2008).

SiRNAs are a class of dsRNA molecules, typically 20–25 nucleotides in length, and play a variety of roles in biology (Coburn et al. 2003, Sioud 2004). SiRNAs were originally discovered as an important gene-silencing mechanism in plants (Agrawal et al. 2003). Shortly thereafter, specific gene silencing was demonstrated in mammalian cells with synthetic siRNAs (Zhou et al. 2002b). SiRNAs have a well defined structure: a short (usually 21-nt) dsRNA with 2-nt 3' overhangs on either end. Each strand has a 5' phosphate group and a 3' hydroxyl (-OH) group (Vargason et al. 2003). This structure is the result of processing by dicer, an enzyme that converts either long dsRNAs or small hairpin RNAs (shRNAs) into siRNAs (Paddison et al. 2004). Synthetic siRNAs can also be exogenously introduced into cells by various transfection methods to bring about the specific knockdown of a gene of interest (Walters et al. 2002). Each siRNA is unwound into two single-stranded (ss) ssRNAs, namely the passenger strand and the guide strand. The passenger strand will be degraded, and the guide strand is incorporated into the RNA-induced silencing complex (RISC). When the guide strand base pairs with a complementary sequence of a mRNA molecule, Argonaute, the catalytic component of the RISC complex, will be able to cleave RNA, leading to post-transcriptional gene silencing. In essence, any gene whose sequence is known can be targeted with an appropriately designed siRNA. This has made siRNAs an important tool for gene function and drug target validation studies in the postgenomic era.

MiRNAs are short RNA molecules with an average length of about 22 nucleotides (Ambros 2001). Mature miRNAs are post-transcriptional regulators that promote messenger

RNA transcripts (mRNAs) degradation and gene silencing or translational repression by annealing to complementary sequences in mRNA 3'-untranslated regions (3'-UTR) (Grosshans et al. 2002). In the human genome, over 1000 miRNAs have been reported, which may target 20–30% of all human mRNAs and regulate many major processes such as development, apoptosis, cell proliferation, immune response, and tumorigenesis (Perera et al. 2007).

MiRNAs are found in almost all species such as viruses, rats, mice and humans (Taccioli et al. 2009). Some of them lie in the introns of protein and nonprotein coding genes or even in exons of long nonprotein-coding transcripts, and are regulated together with their host genes (Mattick et al. 2005); others are found in intergenic regions, which contain their own miRNA gene promoter and regulatory units (Lai 2002). MiRNA genes are usually transcribed by RNA polymerase II (Pol II) as a huge double-stranded primary transcript (pri-miR) (Lee et al. 2004a). Pri-miR is recognized by a nuclear protein known as DiGeorge Syndrome Critical Region 8 (DGCR8 or "Pasha" in invertebrates), which is associated with the enzyme Drosha to form the "Microprocessor" complex (Kadener et al. 2009). In this complex, pri-miR is converted into a double-stranded miRNA precursor of 70 nucleotide (pre-miR), which is then transported into the cytoplasm by a mechanism involving the nucleocytoplasmic shuttle Exportin-5. Finally, Dicer enzyme processes the pre-miR into the 22-nucleotide doublestranded mature miRNA. Although either strand of the duplex may potentially act as a functional miRNA, only the leading strand (the "guide strand") is incorporated into the RISC, binding to the 3'-UTR of target mRNAs causing a block of translation or mRNA degradation depending on the level of complementarity (Moss 2002, Karkare et al. 2004, Lee et al. 2004b).

Figure 1 shows the biogenesis of siRNA and miRNA and their mechanisms of action in RNAi. The similarities and differences between the two are summarized in Table 1. Given

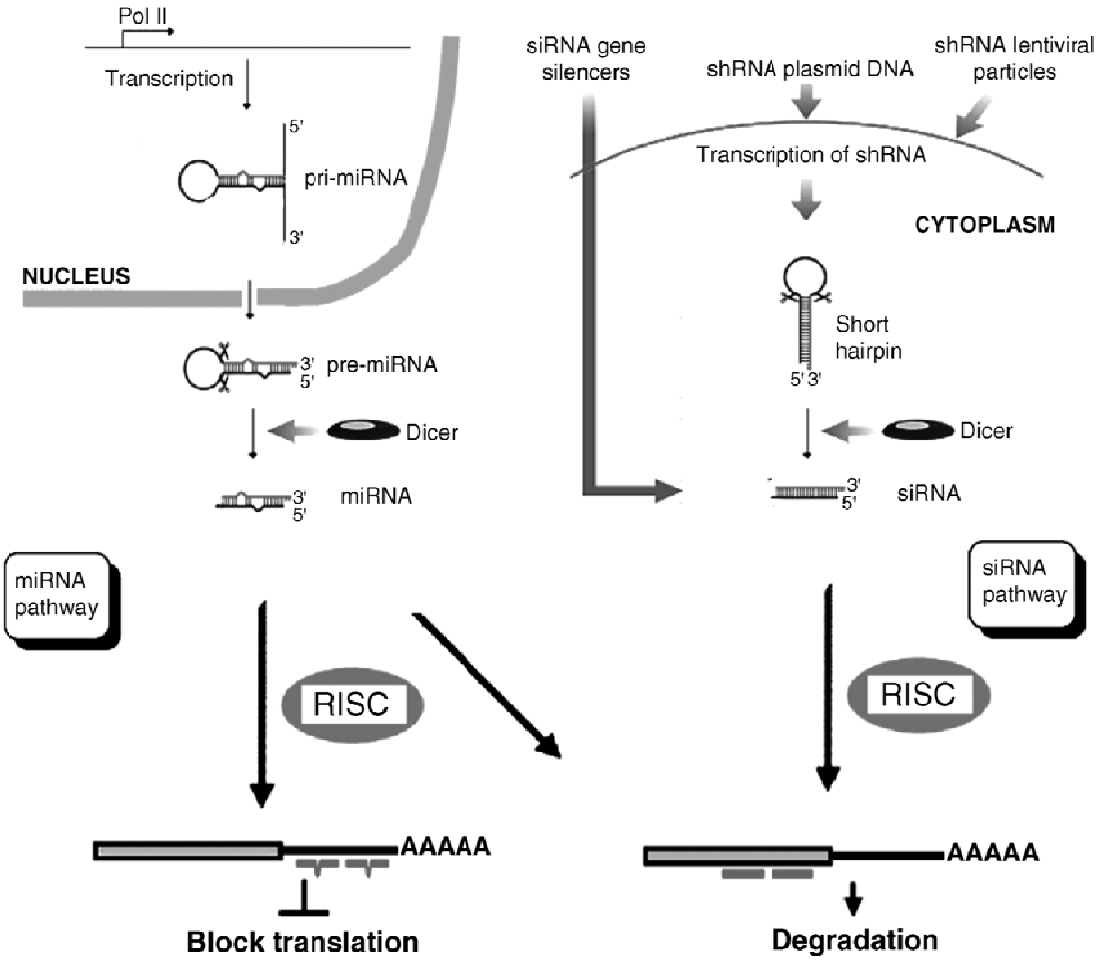

Figure 1 siRNA and miRNA biogenesis and RNAi mechanism.

the importance of siRNAs and miRNAs in regulating various molecular events and signaling pathways, it is not surprising that a vast amount of data has been published demonstrating the important function of siRNAs and miRNAs in various human diseases (Qin et al. 2003, Zamore et al. 2003, Barad et al. 2004, Miller et al. 2004, Scherr et al. 2004, Takamizawa et al. 2004, Gong et al. 2005, Mendell 2005).

Table 1 Comparison of miRNA and siRNA.

	miRNA	siRNA
Origin of discovery	Mammalian cells	Plant, virus
Length (bases)	21-28	21-25
Synthesis	Endogenous	Endogenous or exogenously derived from virus/ chemically synthesized
Mode of action	Inhibition of translation (major)/mRNA degradation	mRNA degradation (major)/chromatin condensation and methylation
Location of targeting sequence	3'-UTR	Coding sequence (can be anywhere)
Source of synthesis	Double-stranded segments of matched mRNA	An unmatched segment of mRNA precursor featuring a hairpin turn
Synthesis enzymes	Dicer	same
Match sequence	7-8 base-pair "seed" match	19-21 base-pair
Specificity	Low (target several genes)	High (one gene/each)
Detectable in cells	Yes	No (most of time)
Expression regulated in cells	Yes	No (most of time)
Significance in disease diagnosis	Yes	No
Significance in prognosis	Yes	No
Application in gene therapy	Yes	Yes

1.1.2.2 RNAi of Liver Fibrosis via siRNA/shRNA

There has been considerable interest in using siRNA to treat liver fibrosis in recent years. Most of the targeted genes are those critical for HSC activation, proliferation and/or collagen synthesis and deposition, which are markedly upregulated during hepatic fibrogenesis, including CTGF, TGF-β1, PDGF, tissue inhibitor of metalloproteinases (TIMPs) and plasminogen activator inhibitor-1 (PAI-1).

One of the promising targets is TGF-β1. As a very potent ECM production stimulator and activator of HSCs, TGF-β1 is believed to be the key pro-fibrogenic factor in liver fibrosis. Studies aiming at disrupting TGF-β1 signaling pathway have shown promising effects on the

attenuation of liver fibrosis in experimental animal models. Lang et al. designed siRNA specifically targeting TGF-β1. TGF-β1 siRNA treatment group (0.125 mg/kg) showed significant reduction of pathological changes and mRNA and/or protein expression of TGF-β1, type I collagen and type III collagen (Lang et al. 2011).

Jin's group designed CTGF siRNA and examined its effect on the liver fibrosis model induced by CCl_4 and ethanol (Li et al. 2006). They found that CTGF expression was reduced by intraportal vein injection of CTGF siRNA. Long-term treatment with this siRNA markedly attenuated the induction of CTGF, type I, III collagen, laminin, TIMP-1 and TGF-β1 genes, all of which are related to the development of liver fibrosis.

It is believed that liver fibrosis develops as a loss of the balance between ECM production, deposition and ECM degradation. Targeting genes affecting matrix degradation could also provide another therapeitic opportunity. One of those genes is plasminogen activator inhibitor-1 (PAI-1), the key inhibitor of both uPA and tissue-type plasminogen activator (tPA). PAI-1 is a powerful pro-fibrotic molecule and is a promising therapeutic target for fibrotic diseases. The study from Xie et al. has shown that an adenoviral expression vector for PAI-1-specific shRNA shows protective effect on hepatocytes and ameliorates liver fibrogenesis in rats. The treatment has led to the correction of the levels of matrix metalloproteinases (MMPs) and its inhibitors (TIMPs) through upregulation of MMP9 and MMP13, as well as downregulation of TIMP-1 (Hu et al. 2009).

TIMP-2, a specific inhibitor of MMP2, has a strong correlation with the progression of liver fibrosis. In CCl_4-treated rats, hepatic fibrosis was markedly attenuated by the administration of siRNA against TIMP-2, through upregulation of MMP activity. In addition to a reduction in collagen deposition, fewer HSCs were activated in the treatment group.

To date, siRNA-based therapy for liver fibrosis remains at the stage of preclinical study. Several issues need to be addressed before it can be translated into clinical application. One of them is the potency. Liver fibrosis is caused by multiple factors and various mechanisms are involved in the initiation and progression of this disease. Downregulation of a single gene or protein may not be sufficient to achieve therapeutic benefit. Other practical issues include lack of a suitable delivery system that specifically targets HSCs, off-target effects of siRNA, and the chronic nature of the disease. Targeted delivery of siRNA to the liver or specific cell population especially HSCs is therefore an important strategy to reduce possible adverse effects and improve therapeutic efficacy.

1.1.2.3 RNAi of Liver Fibrosis via miRNAs

MiRNAs have been shown to be critically involved in various steps of liver fibrosis. Roderburg and colleagues systematically analyzed the regulation of miRNAs in CCl_4- and common bile duct ligation (CBDL)-induced liver fibrosis in mice by gene array analysis. They revealed a panel of miRNAs that were dysregulated in livers of mice undergoing hepatic fibrosis (Roderburg et al. 2011). MiR-29 family is one of those that were significantly downregulated in both fibrotic models. MiR-29 is encoded in two separate genomic loci yielding four mature miRNAs (29a, 29b1, 29b2, and 29c) (Chau et al. 2011). All members of the miR-29 family play a critical role in the regulation of various types of ECM proteins such as COL1A1, COL3A1, fibrillin and elastin as shown by us and others (Li et al. 2011a). One major mechanism for miR-29-mediated regulation of these fibrosis-related genes is through direct binding to their target sequences located at the 3'-UTR of these mRNAs. Interestingly, several molecules that are critically involved in collagen maturation, such as LOX and HSP47, are the putative targets of miR-29 (Jha et al. 2011). Therefore, miR-29 may regulate ECM expression

in a coordinated fashion through inhibiting ECM production at both translational and posttranslational steps.

Downregulation of miR-29 members has been implicated in various fibrotic diseases including cardiac fibrosis, lung fibrosis, and liver fibrosis (Cushing et al. 2011). MiR-29 members appear to be negatively regulated by NF-κB and TGF-β pathways and downregulation of miR-29 seems to be a major mechanism for NF-κB- and TGF-β-mediated fibrotic activity (Roderburg et al. 2011).

MiR-29 represents a promising therapeutic option for the treatment of various fibrotic diseases including liver fibrosis. Success of this therapy is largely dependent on the development of a delivery system for efficient delivery of miR-29 to target cells. Alternatively, strategy can be developed to induce miR-29 expression in target cells. We recently showed that miR-29a expression in HSCs can be induced by ligands for farnesoid X receptor (FXR). FXR (NR1H4) is a member of the nuclear receptor superfamily that is highly expressed in liver, kidney, adrenals, and intestine (Anisfeld et al. 2005). FXR plays a key role in the homoeostasis of cholesterol and bile acids and FXR ligands have been developed for the treatment of cholestasis (Eloranta et al. 2008). Several studies including our own have identified a number of additional novel functions for FXR including antidiabetic, antihyperlipidemic, antihypertensive, and anti-inflammatory effects (He et al. 2006, Li et al. 2007, Zhang et al. 2008, Ge et al. 2011).

Recently, treatment with FXR ligands has been shown to prevent liver fibrosis in rodent models (Jiang et al. 2007, Wang et al. 2009b, Fuchs 2012). However, the mechanism of the FXR ligand-mediated antifibrotic effect remains incompletely understood. The study from Fiorucci et al. suggested that FXR/FXR ligands inhibit the fibrotic activity in HSCs through SHP-mediated suppression of NF-kB and/or TGF-b signaling pathways (Fiorucci et al. 2004).

Our recent study suggests that FXR-mediated induction of miR-29a may be a new mechanism for FXR/FXR ligands-mediated antifibrotic effect (Li et al. 2011a). FXR may directly induce miR-29a expression through binding to a putative FXR responsive element in the regulatory region of miR-29a gene as shown in our recent study (Li et al. 2011a). FXR may also induce miR-29a expression indirectly through blocking the NF-κB- and/or TGF-β-mediated suppression of miR-29a. Better understanding of the mechanism involved in the transcriptional upregulation of miR-29 gene expression may lead to the development of better strategy for the treatment of liver fibrosis through modulation of miR-29 expression in HSCs.

MiR132 expression has also been shown to be lost with transactivation of HSCs. MiR132 appeared to be critically involved in the regulation of methyl-CpG binding protein 2 (MeCP2) and downregulation of miR132 was associated with significant upregulation of MeCP2 in activated HSCs (Mann et al. 2011). This seemed to play an important role in the suppression of the expression of PPARγ, an important negative regulator of HSC transactivation. Reintroduction of miR132 into activated HSCs led to diminished MeCP2 protein expression and elevated levels of PPARγ transcript (Mann et al. 2011).

In addition to miR-29 and miR-132, a number of other miRNAs have been shown to be involved in the development of liver fibrosis. By using microarray, Zhu's group found that 16 miRNAs were upregulated and six miRNAs were downregulated in the fibrotic liver tissues from dimethylnitrosamine treated rats (Li et al. 2011b). Amongst them, rno-miR-34a, rno-miR-34b and rno-miR-34c were found to be the most upregulated, with a 30~130-fold increase in their expression levels over those of controls. Additionally, seven miRNAs were progressively downregulated as liver fibrosis progressed. Rno-miR-378, rno-miR-193 and rno-miR-878 were the three most downregulated, with an approximately two to eight-fold decrease in their

expression levels as compared with controls. One of the target genes of miR-34 family is ACSL1, which plays a central role in lipid and fatty acid metabolism in liver (Li et al. 2011b).

In another microarray study, the expression levels of 11 miRNAs were consistently upregulated in CCl_4-treated mice compared to the control mice, including mmulet- 7e, miR-125-5p, 199a-5p, 199b, 199b*, 200a, 200b, 31, 34a, 497, and 802. Overexpression of miR-199a, miR-199a*, miR-200a and miR-200b in LX-2 cells resulted in a significant induction of several fibrosis-related genes compared with a control miRNA (Murakami et al. 2011). TGFβ-induced factor (TGIF) and SMAD specific E3 ubiquitin protein ligase 2 (SMURF2), both of which are negative regulators for TGF-β signaling pathway, are candidate targets of miR-199a* and miR-200b, respectively, as determined by the Targetscan algorithm (Murakami et al. 2011). The study by Guo et al. showed that overexpression of miR-16 and miR-15b inhibited the proliferation of HSCs and induced apoptosis of these cells by downregulating the mitochondrial-associated antiapoptotic protein Bcl-2, leading to the activation of caspases 3, 8, and 9 (Guo et al. 2009). Ji's group showed that inhibition of miR-27a and miR-27b was capable of reversing the activated HSCs to quiescent state, with restored cytoplasmic lipid droplets and decreased cell proliferation (Ji et al. 2009).

MiR-122, as a liver specific miRNA, also plays an important role in the development of liver fibrosis. Our group has demonstrated that miR-122 expression is significantly downregulated in mouse fibrotic liver (unpublished data). Prolyl 4-hydroxylase, alpha polypeptide I (P4HA1) is one of the target genes of miR-122. Through downregulation of P4HA1, miR-122 overexpression may modulate post-translational modification of several collagen genes, which may lead to inhibition of collagen maturation and suppression of collagen production.

Studies have shown that liver fibrosis is associated with liver cancer. Major risk factors for hepatocellular carcinoma include HBV or HCV infection, alcoholic liver disease, and nonalcoholic fatty liver disease. Most of these risk factors can also cause the formation and progression of cirrhosis, which is present in 80 to 90% of patients with hepatocellular carcinoma (El-Serag 2011). It was reported that the 5-year cumulative risk for the development of hepatocellular carcinoma in patients with cirrhosis ranges between 5% and 30%, depending on the cause (with the highest risk among those infected with HCV), region or ethnic group (17% in the United States and 30% in Japan), and stage of cirrhosis (with the highest risk among patients with decompensated disease) (Fattovich et al. 2004). Therefore, the aim of the second part of my dissertation work is to develop effective treatment strategies for cancer therapy. We focus on the development of new strategies that enhance the performance of micellar and liposomal formulations as these carriers have been widely used for the delivery of various types of anticancer agents.

1.2 POLYMERIC MICELLES AS NANOCARRIERS FOR CANCER TARGETED DRUG DELIVERY

Polymeric micelles represent an effective delivery system for poorly water-soluble anticancer drugs. With small size (10-100 nm) and hydrophilic shell of PEG, polymeric micelles exhibit prolonged circulation time in the blood and enhanced tumor accumulation. In this chapter, the importance of rational design was highlighted by summarizing the recent progress on the development of micellar formulations. Emphasis is placed on the new strategies to enhance the drug/carrier interaction for improved drug loading capacity. In addition, the micelle-forming

drug-polymer conjugates are also discussed which have both drug-loading function and antitumor activity.

1.2.1 Introduction

Chemotherapeutic agents are typically water-insoluble, and their therapeutic outcome is compromised by the short circulation time and systemic toxicity. During the past century, tremendous efforts have been made to circumvent these limitations and improve the therapeutic benefit of anticancer therapeutics. This was originated from the concept of "magic bullet" that was proposed by Paul Ehrlich, recipient of the Nobel Prize for Physiology or Medicine in 1908, which suggests the benefit of targeted delivery of drug to the diseased cells. In the past decades, nanocarriers have emerged as an attractive research field in cancer therapy, including liposomes, micelles and nanoparticles made of various materials. Polymeric micelles are extensively studied carriers for the delivery of poorly water-soluble drugs. By enhancing the aqueous solubility and prolonging the half-life of chemotherapeutic agents, the anticancer agents can passively accumulate in tumor site through the leaky vasculature by the enhanced permeability and retention (EPR) effect (Gao et al. 2002, Nie et al. 2007). Compared with other drug carriers, micelles have the advantages of being small in size (10-100nm), which is critical for passive targeting to solid tumors, particularly the poorly vascularized ones (Davis et al. 2008).

Based on the type of intermolecular forces driving the micelle formation, block copolymer micelles can be divided into several categories including hydrophobically assembled amphiphilic micelles, polyion-complex micelles, and micelles stemming from metal complexation (Gaucher et al. 2005). The hydrophobically assembled micelles usually consist of

amphiphilic macromolecules that have distinct hydrophobic and hydrophilic domains, and the commonly used block segments of copolymers have been summarized (Sutton et al. 2007). Upon exposure to aqueous medium, the amphiphilic molecules are spontaneously self-assembled into supramolecular core/shell structures, and water-insoluble drugs can be loaded into the hydrophobic cores.

Micelles have demonstrated a variety of shapes such as spheres, rods, vesicles, tubules and lamellae depending on the relative length of hydrophobic/hydrophilic blocks as well as solvent environment (Yu et al. 1998, Shen et al. 1999, Choucair et al. 2003). Morphology of micelles has significant impact on the pharmacokinetic properties of micelles. For example, worm-like filomicelles have shown ten times longer circulation time compared with the spherical counterpart made of similar material (Geng et al. 2007).

The most commonly used hydrophilic segment of micelles for drug delivery is poly (ethylene glycol) (PEG), with a molecular weight of 2-15 kD. PEG is highly water-soluble, non-toxic and neutrally charged. PEG forms a hydrophilic corona on the surface of micelles which minimizes the nonspecific interaction with blood components and prolongs the circulation time. Besides PEG, other polymers including poly(N-vinyl pyrrolidone) (PVP) (Benahmed et al. 2001) and poly(N-isopropyl acrylamide) (pNIPAM) (Chung et al. 1998) have also been used as hydrophilic portion of micelles.

Most polymeric systems involve the use of polymers as the hydrophobic domain including polyesters such as poly(lactic acid) (PLA) and polyamides such as poly (L-lysine) (PLL) and poly (beta-amino ester). Biocompatibility and biodegradability are two important prerequisites in designing these micellar carriers for clinical application. Polyesters and polyamides undergo enzyme-catalyzed hydrolysis in vivo and thus are considered

biodegradable. Several polymer micelle systems that have been studied clinically (Kim et al. 2010b). For example, Genexol-PM, a polymeric micelle formulation of paclitaxel, was evaluated in a phase I study in patients with advanced malignancies with emphasis on pharmacokinetics evaluation (Kim et al. 2004). Phase II clinical trial of Genexol-PM was performed in patients with metastatic breast cancer (Lee et al. 2008) and advanced non-small-cell lung cancer (Kim et al. 2007). Some other micellar formulations also have their phase I clinical trial completed, including paclitaxel-incorporated micellar formulation, NK105 (Hamaguchi et al. 2007), pluronic polymer-bound doxorubicin (SP1049C) (Danson et al. 2004) and NK911, a micelle-encapsulated doxorubicin (Matsumura et al. 2004).

Another type of polymeric micelles that have been investigated involve the use of lipids as the hydrophobic core. For example, Torchilin's group has synthesized several PEG-diacyllipid conjugates, in which the hydrophobic segments are lipids of various acyl chains such as phosphatidylethanolamine (PEG-PE) (Trubetskoy et al. 1995). Due to the strong hydrophobic interactions between the double acyl chains (Lukyanov et al. 2004), the PEG-PE conjugates can form stable micelles with very low CMC value ($\sim 10^{-5}$ M) (Musacchio et al. 2009). These micelles can solubilize many types of poorly water-soluble drugs including paclitaxel (Gao et al. 2002), tamoxifen (Gao et al. 2002), porphyrin (Gao et al. 2002), camptothecin (Mu et al. 2005a), and vitamin K3 (Wang et al. 2004). The PEG-PE micelles exhibit favorable stability, longevity in blood and tumor accumulation via the EPR effect (Lukyanov et al. 2002, Lukyanov et al. 2004). In contrast to liposomes (Parr et al. 1997), the small size of micelles enables them to effectively penetrate the vasculature of tumors, even for those with very low cutoff size (Weissig et al. 1998).

Recently, Lam and colleagues have developed a series of micellar systems composed of PEG-cholic acid (CA) conjugates (Xiao et al. 2009). A conjugate of eight CA molecules with one PEG5000 chain (PEG_{5K}-CA_8) was shown to load paclitaxel with high loading capacity (7.3 mg paclitaxel/mL) and a size of 20-60 nm (Xiao et al. 2009). These paclitaxel-loaded PEG_{5K}-CA_8 micelles achieved improved anti-tumor effect and showed less toxicity in murine models of ovarian cancer compared to Taxol® and Abraxane® at equivalent paclitaxel doses (Xiao et al. 2009). Phase I clinical trial of paclitaxel-loaded PEG5K-CA_8 micelles demonstrated the superior anticancer efficacy and tolerance (Xiao et al. 2011). In addition, compared to PEG_{5K}-CA_8 micelles, a similar micellar carrier PEG_{2K}-CA_4 was demonstrated to have higher doxorubicin loading capacity and more sustained drug release profile (Xiao et al. 2011).

The last decade has seen significant progress in the development of various micellar systems for targeted delivery of anticancer agents (Liu et al. 2006, Sutton et al. 2007, Torchilin 2007). However, much improvement is still needed for the existing systems with respect to drug loading capacity and formulation stability. Despite the structural differences among the reported micellar systems, most of them mainly rely on hydrophobic/hydrophobic interaction for drug incorporation into the hydrophobic cores. Such mechanism, while working well for some highly lipophilic drugs, may not provide sufficient drug/carrier interaction to effectively load other drugs. Various strategies have been proposed to introduce additional drug-interactive domains into the micellar system to improve the overall carrier/drug interaction. In addition, progress has been made in developing dual-functional carriers that demonstrate both delivery function and antitumor activity. The following two sections will summarize some of the works from our lab and other labs in developing improved micellar systems for anticancer agents.

1.2.2 MICELLES WITH BUILT-IN DRUG-INTERACTIVE DOMAIN AS IMPROVED DELIVERY SYSTEMS FOR ANTICANCER AGENTS

The drug loading capacity of polymeric micelles is critically dependent on the compatibility between the drug and the micelle core (Latere Dwan'Isa et al. 2007). A series of studies have demonstrated that the drug loading capacity of micelles can be greatly enhanced by optimizing chemical structures of the inner core segment for stronger drug-carrier interaction. A typical example of the strategy for enhanced compatibility between drug and block copolymer is the development of hydrotropic polymers. Hydrotropy refers to a phenomenon that the aqueous solubility of a poorly soluble compound is significantly enhanced by the presence of large amounts of a second solute, named hydrotrope (Coffman et al. 1996). The hydrotropes aggregate only above a certain concentration, which is known as the minimal hydrotrope concentration (MHC) (Bauduin et al. 2005). Various studies have been carried out to elucidate the process of hydrotropic solubilization. Although the exact mechanism is not fully clarified, it may involve multiple non-covalent interactions including hydrophobic interaction, hydrogen bonding (Kim et al. 2010a) as well as parallel stacking effect (Ooya et al. 2006, Cui 2010).

Most of the hydrotropes include an aromatic ring substituted by heteroatoms. The aromatic rings are basically hydrophobic, which can stack with each other or with the benzene rings in drug molecules (Landauer et al. 1952). In addition, the polar groups may interact with drugs via hydrogen bonding (Charman et al. 1993). For example, nicotinamide, a typical hydrotrope, has been shown to form complex with various hydrophobic drugs and enhance their water solubility (Rasool et al. 1991). It has a pyridine ring that promotes the π-π stacking with drug molecules through its planarity (Sanghvi et al. 2007). In addition, self-association of nicotinamide was shown to play a major role in the hydrotropic solubilization of riboflavin

instead of complexation between the two species (Coffman et al. 1996). Another example is N,N-diethylnicotinamide, which was shown to be the most effective hydrotrope for solubilizing paclitaxel among more than 60 structures tested (Lee et al. 2003). One drawback of hydrotropic solubilization is that high concentration of hydrotrope is usually required, which may cause various side effects. This is due to the high MHC of usual hydrotropes of about 1 M, compared to the critical micelle concentration (CMC) of typical micelles at 10^{-2}-10^{-3} M (da Silva et al. 1999). To overcome this barrier, hydrotropic polymers have been developed which can dramatically enhance the local concentration of hydrotropes. Park's group has synthesized PEG block co-polymers with hydrotropes linked with the hydrophobic domain of polymeric micelles, which appeared to be a versatile strategy to enhance the water solubility of various hydrophobic drugs of different structures (Huh et al. 2005, Kim et al. 2011). The key factors that affect the performance of hydrotropic polymers include the polymer backbone, type and orientation of hydrotropic moieties and the spacer groups connecting the backbone and hydrotropes. The review by Ooya et al. provides a comprehensive summary of the studies regarding the structure-activity relationship of hydrotropic polymers (Ooya et al. 2006).

Besides hydrotropic effect, additional non-covalent interactions have been employed to improve drug loading in polymeric micelles. For example, modification of poly(ethylene glycol)-poly(beta-benzyl L-aspartate) (PEG-PBLA) block copolymer with benzyl ester on the PBLA chain enhanced the loading efficiency and stability of camptothecin-loaded micelles (Opanasopit et al. 2004). Incorporation of hydrogen-bonding urea-functional groups into block copolymers led to decreased CMC and improved stability of doxorubicin-loaded micelles (Kim et al. 2010c). Similarly, the stability of micelles was enhanced with increased number of acid/urea groups in the micelles, which was due to improved hydrogen-bonding between the

carrier molecules and acid-amine ionic interaction between the drug and carrier (Yang et al. 2012a). In addition, the loading of indomethacin and ibuprofen into polymeric micelles was dramatically improved by the acid-base interaction between hydrophobic segments of micelles and guest molecules containing carboxylic acid groups (Giacomelli et al. 2007). Furthermore, Kataoka's group has shown that the encapsulation of cisplatin into polymeric micelles was facilitated by metal-ligand coordination (Yokoyama et al. 1996, Nishiyama et al. 2001). Inclusion of aromatic end groups (e.g. benzoyl and naphthoyl) has also been shown to improve the loading of paclitaxel into mPEG750-b-oligo(epsilon-caprolactone)$_5$-based oligomeric micelles (Carstens et al. 2008).

We have recently demonstrated that the introduction of Fmoc as a "drug-interactive domain" can also significantly improve the drug-loading capacity of both emulsion and lipid-core micellar system (Gao et al. 2013). A series of PEGylated lipopeptide surfactants were designed and constructed to solubilize a synthetic antioxidant, JP4-039. Several ε-Boc-lysine derivatives with various protective groups at α-NH_2 position were tested for their ability to solubilize JP4-039, among which the α-Fmoc-ε-Boc lysine was shown to be the most potent one (Gao et al. 2013). Incorporation of this drug-interactive motif Fmoc into drug-loaded emulsion led to significant increase in the formulation stability. We then designed another polymer-based micelle system, in which the Fmoc motifs were located at the interfacial region of lipopeptide surfactants with PEG_{5K} as the headgroup and two oleoyl chains as the core-forming segment (Zhang et al. 2014). The PEG_{5K}-(Fmoc-OA)$_2$ exhibited lower CMC value and significantly improved loading capacity for paclitaxel compared with an analogue without Fmoc motifs. The paclitaxel-loaded PEG_{5K}-(Fmoc-OA)$_2$ micelles showed increased anticancer effect over Taxol in vitro and in vivo. In addition, 7 other drugs were effectively loaded into PEG_{5K}-(Fmoc-OA)$_2$

micelles, which suggests the utility and versatility of this platform for a broad range of drugs with different structures (Zhang et al. 2014). Although the exact mechanism of carrier-drug interaction is not fully understood, the hydrophobic interaction and π- π stacking effect possibly contribute to the compatibility between the drug and carrier.

1.2.3 PEG-DRUG CONJUGATES AS DUAL-FUNCTION CARRIERS FOR CANCER TARGETED DELIVERY

1.2.3.1 Rationale of Combination Therapy Using Polymer-Drug Conjugates as Carriers

As discussed above, improved drug loading capacity, stability and tumor-specific distribution can be achieved by various strategies. However, most of the polymeric materials for drug delivery are "inert" and lack of therapeutic activity. In addition, the use of large amounts of carrier materials may impose safety concerns (Croy et al. 2006). Since Ringsdorf (Ringsdorf 1975) proposed the concept of "polymeric prodrug" in 1975, the utility of polymer-drug conjugates in clinical therapy has been well demonstrated. Interestingly, the conjugate of hydrophobic drug with hydrophilic polymers might be self-assembled into micelles, which can be potentially useful for the loading of another therapeutic molecule. Drug encapsulation with a biologically active carrier is an attractive strategy as it represents a unique form of combination. Combination therapy with multiple agents working at several signaling pathways at the same time could not only lead to maximized anticancer effect but also help to overcome the drug resistance (Broxterman et al. 2005). For example, the combination of PGA-paclitaxel conjugate with cisplatin (Verschraegen et al. 2009) or carboplatin (Langer et al. 2008) has shown improved therapeutic benefits or reduced toxicity in Phase I clinical trial. In addition, the anticancer effect of N-(2-hydroxypropyl)methacrylamide (HPMA) copolymer-doxorubicin

conjugate in combination with HPMA copolymer-mesochlorin e6 was shown to be more efficacious than either conjugate alone (Shiah et al. 2001).

In contrast to the common combination regimen, drug-loading with bioactive carriers ensures the simultaneous arrival of multiple therapeutic agents at the same targeting site, and thus represents a promising strategy for better therapeutic outcome. These dual-function carriers not only deliver the drug to tumor site but also are biologically effective, which either enhances the therapeutic effect (Mi et al. 2011) or reduce the toxicity caused by the incorporated drug (Dong et al. 2005).

However, micellar systems based on drug-polymer conjugates are rarely used for the physical incorporation of another hydrophobic molecule. The following section summarizes some of the recent works from us and others, which demonstrate that such a strategy is not only feasible but also effective.

1.2.3.2 PEG-Vitamin E Conjugates as Dual-Function Carriers for Cancer Targeted Delivery

D-α-tocopheryl polyethylene glycol (PEG) 1000 succinate (TPGS) is a PEG derivatized natural Vitamin E which has been approved by FDA as a safe pharmaceutical adjuvant for drug formulation. In recent years the application of TPGS in drug formulations has been extensively studied, such as emulsifier in Poly (lactic-co-glycolic acid) (PLGA) nanoparticles (Mu et al. 2002), solubilizer and permeation enhancer (Yu et al. 1999), TPGS-based liposomes (Muthu et al. 2011), copolymers (Zhang et al. 2006) and nanocrystal (Liu et al. 2010). By inhibiting the function of P-glycoprotein (P-gp), TPGS also helps to overcome the multidrug resistance (Dintaman et al. 1999) and enhance the oral bioavailability of anticancer drugs (Varma et al.

2005). In addition, TPGS-doxorubicin conjugate was developed as a prodrug for enhanced therapeutic effect (Cao et al. 2008).

TPGS forms micelles in aqueous solution, which were used for the dispersion of functional nanostructures such as carbon nanotubes (Yan et al. 2007, Xu et al. 2010), fullerenes (Yan et al. 2007) and iron oxide (Chandrasekharan et al. 2011). However, with a relatively high critical micelle concentration (CMC) value of 0.2 mg/mL (Zhang et al. 2012), TPGS micelles are not stable and easily dissociated upon dilution by plasma after intravenous injection. Therefore, TPGS is usually used together with other excipients to form mixed micelles. For example, PEG-phosphatidylethanolamine (PEG-PE) was mixed with TPGS at a molar ratio of 2:1 for the loading of camptothecin (CPT), which increased the CPT solubility by at least 50% compared to PEG-PE micelles without TPGS (Mu et al. 2005b). Similarly, mixed micelles of 1,2-distearoyl-sn-glycero-3-phosphoethanolamine-N-[methoxy(polyethylene glycol)-1000] (DSPE-PEG) with TPGS were prepared to encapsulate an anticancer agent, 17-allyamino-17-demethoxygeldanamycin (17-AAG) (Chandran et al. 2010), resulting in controlled drug release and improved cytotoxicity compared with the free drug. In addition, TPGS also forms mixed micelles with Pluronic P105 (Gao et al. 2008), Pluronic P123 (Zhao et al. 2011) and Pluronic F127/poly(butyl cyanoacrylate) (PBCA) (Wang et al. 2009a). Compared with free drug or micelles without TPGS, those micelles showed improved solubility of hydrophobic anticancer drugs and increased cytotoxicity against MCF-7, MCF-7/ADR and HepG2 cell lines.

To further facilitate the use of TPGS as a micellar formulation, several strategies have been developed to decrease its CMC. Feng's group has conjugated one tocopheryl succinate molecule with a PEG_{2K} chain to generate $TPGS_{2K}$ for the delivery of docetaxel, which showed much lower CMC value compared with traditional TPGS (Mi et al. 2011). This improvement

has enabled the formation of stable drug-loaded TPGS micelles without the help of other polymers or lipids. Another benefit of longer PEG chain is to further decrease the nonspecific uptake of $TPGS_{2K}$ micelles by RES. The study by Wang et al showed that a conjugate of PEG_{2K} with two Vitamin E molecules exhibited further reduced CMC of 1.14 μg/mL (Wang et al. 2012a), compared to that of $TPGS_{2K}$ (21.9 μg/mL) and TPGS (200 μg/mL) (Mi et al. 2011). Importantly, PEG_{2K}-Vitamin E_2 well retained the intrinsic activity of TPGS in inhibiting the activity of P-gp. Doxorubicin-loaded $TPGS_{2K}$ micelles showed greater cytotoxicity and tumor inhibitory effect than doxorubicin formulated in conventional TPGS (Wang et al. 2012a). In light of this information, we have recently developed four PEG-Vitamin E conjugates that differ in PEG molecular weight (PEG_{2K} vs PEG_{5K}) and the molar ratio of PEG/Vitamin E (1/1 vs 1/2), and their paclitaxel loading capacity was subsequently compared (Lu et al. 2013a). Our data have shown that among all the four conjugates, PEG_{5K} conjugate with two Vitamin E molecules (PEG_{5K}-VE_2) showed the lowest CMC value, highest loading capacity and stability. All the four conjugates retained the P-gp inhibition activity of TPGS. Delivery of paclitaxel via PEG_{5K}-VE_2 led to significantly improved antitumor activity compared with the commercial formulation Taxol® and other paclitaxel micellar formulations.

1.2.3.3 PEG-Derivatized Embelin as a Nanocarrier for the Delivery of Paclitaxel

Embelin is an alkyl-substituted hydroxyl benzoquinone natural product discovered from the Japanese Ardisia Herb (Herba Ardisiae Japonicae) (Nikolovska-Coleska et al. 2004). Embelin was shown to possess a broad spectrum of biological activities including anti-diabetic (Bhandari et al. 2007), anti-inflammatory (Chitra et al. 1994) and hepato-protective effects (Singh et al. 2009). In addition, embelin exhibits antitumor activity in many types of cancers such as breast (Li et al. 2013c), colon (Dai et al. 2009), prostate (Danquah et al. 2009) and pancreatic cancer

(Mori et al. 2007). Through computational structure based computer screening, Wang et al (Nikolovska-Coleska et al. 2004) discovered that embelin is a potent inhibitor of X-linked inhibitor of apoptosis protein (XIAP), which partially explained its anticancer mechanism. XIAP is over-expressed in various types of cancer cells (Tamm et al. 2000), particularly in drug-resistant cancer cells (Berezovskaya et al. 2005), while it plays a minimal role in normal cells. Inhibition of XIAP has been demonstrated as an effective approach to selectively inhibiting the growth of cancer cells (Vogler et al. 2009). Embelin also inhibits NF-κB activation, which mediates the down-regulation of several genes including surviving, XIAP, IAP1/2, TRAF1, cFLIP, Bcl-2 and Bcl-xL (Ahn et al. 2007).

Bearing a long lipophilic chain, embelin is extremely hydrophobic and water-insoluble. In an attempt to explore the PEG modification as an approach to increase its water solubility, we have found that PEG-derivatized embelin forms micelles in aqueous solution (Huang et al. 2012). This is not a surprise considering the structural similarity between embelin with Vitamin E. Interestingly, the antitumor activity of embelin was well retained after coupling with PEG chain (Huang et al. 2012). In addition, the PEG-embelin micelles are highly efficient in solubilizing various types of anticancer agent such as paclitaxel (Huang et al. 2012, Lu et al. 2013b). Furthermore, PEG-embelin, at nanomolar range, showed synergistic effect with paclitaxel in several cancer cell lines tested (Huang et al. 2012). In vitro and in vivo studies have shown that the conjugate with two embelin molecules linked with one PEG chain is significantly more effective for loading paclitaxel than the conjugate with a 1:1 molar ratio of PEG and embelin. In addition, the PEG-embelin conjugates with longer PEG chain (PEG_{5K}) were shown to be more advantageous compared with the counterparts with shorter PEG chain ($PEG_{3.5K}$) (Huang et al. 2012, Lu et al. 2013b). Near infrared fluorescence (NIRF) imaging of

PC-3 xenograft-bearing mice showed that PEG_{5K}-EB_2 micelles were selectively accumulated at tumor site with minimal distribution in major organs including liver and spleen (Lu et al. 2013b). Delivery of paclitaxel via PEG_{5K}-embelin$_2$ micelles leads to superior antitumor activity compared to Taxol in murine models of breast and prostate cancers (Lu et al. 2013b).

1.2.3.4 PEG-Farnesylthiosalicylate (PEG-FTS) Conjugate Micelles for the Delivery of Paclitaxel

S-trans, trans-farnesylthiosalicylic acid (Salirasib, or FTS) is a synthetic antagonist of Ras protein. By disrupting the anchorage of Ras on cell membrane (Weisz et al. 1999), FTS is designed to inhibit Ras-dependent growth of cancer cells. Approximately 20 to 30% of human tumors express permanently active oncogenic Ras (Grewal et al. 2011), and the mutationally activated Ras was most commonly found in adenocarcinomas of the pancreas (90%), colon (50%), lung (30%), thyroid tumors (50%), and myeloid leukemia (30%) (Bos 1989, Downward 2003). Accordingly, FTS exhibited potent antitumor effect in various tumors such as pancreatic cancer (Weisz et al. 1999), colon cancer (Halaschek-Wiener et al. 2000), melanoma (Jansen et al. 1999) and neurofibromatosis (Barkan et al. 2006). In addition, Ras inhibitors demonstrated synergistic effect with other chemotherapeutics, which validated their application in combination therapy (Blum et al. 2005). For example, treatment of the resistant SW480 cells with FTS dramatically enhanced the sensitivity to gemcitabine and led to improved inhibition of tumor growth in vivo (Gana-Weisz et al. 2002).

Similar to Vitamin E and embelin, FTS is also a hydrophobic small molecule with a long hydrophobic chain and a functional group (-COOH) that can be readily used for further modification. The biological activity and chemical structure of FTS has prompted us to design the PEG-derivatized FTS conjugate as another dual-function micellar drug carrier (Zhang et al.

2013). A labile ester linkage was used to facilitate the release of FTS and disassembly of the drug-loaded micelles following intracellular delivery to tumor cells. Our data have shown that the PEG-FTS_2 readily forms micelles in aqueous solution with a CMC of 0.68 μM. Paclitaxel can be efficiently loaded into those micelles, which are spherical in morphology with a uniform size of 20-30 nm. Ras protein down-regulation and cytotoxicity of PEG-FTS_2 were comparable to free FTS as shown in 4T1.2 and HCT-116 cancer cell lines. The antitumor activity of paclitaxel-loaded PEG-FTS_2 micelles was shown to be significantly higher than that of Taxol in a syngeneic murine breast cancer model (Zhang et al. 2013).

1.2.3.5 Other Drug-Polymer Conjugate Micelles for the Delivery of a Hydrophobic Chemotherapeutics

Several other micellar systems have been studied, which are based on polymer-drug conjugates such as polymer-curcumin and polymer-adriamycin conjugates. Curcumin is a natural polyphenol compound with promising anti-cancer application (Aggarwal et al. 2003, Wilken et al. 2011). It was reported that curcumin blocks NF-κB pathway (Shishodia et al. 2005) and in turn, induces apoptosis and inhibits the function of protein kinase C, epidermal growth factor receptor tyrosine kinase, and HER-2 (Sharma et al. 2005, Aggarwal et al. 2006). Curcumin has shown antitumor activity against various types of cancers including those of breast (Holy 2002), colon (Jiang et al. 1996), prostate (Holy 2004, Deeb et al. 2007), kidney (Woo et al. 2003), liver (Yoysungnoen et al. 2006), lymphoid and myeloid tissues (Anuchapreeda et al. 2006), and melanoma (Odot et al. 2004). In spite of all the anticancer activities, the potential application of curcumin is hindered by its poor water solubility and limited bioavailability. Furthermore, high drug dose is required for a desired therapeutic outcome due to its relatively low potency.

Therefore, nanosized delivery systems with high loading capacity and tumor-specific distribution represent an attractive strategy to address these issues.

In an attempt to increase the solubility of curcumin, various formulations have been developed such as cyclodextrin (Yallapu et al. 2010), nanoparticles (Anand et al. 2010), microparticles (Shahani et al. 2011) and nano-sized complex (Zhang et al. 2011a). Polymer-curcumin conjugates were also synthesized as polymeric prodrugs. For example, Safavy et al. synthesized two conjugates including curcumin-PEG_{750} and curcumin-$PEG_{3.5K}$ (Safavy et al. 2007). Both conjugates exhibited enhanced water solubility and cytotoxicity against several human cancer cell lines in comparison with free curcumin (Safavy et al. 2007). To further increase the drug content in the nanoparticles, Tang et al. synthesized a curcumin prodrug by attaching it with two short oligo (ethylene glycol) (Curc-OEG) chains. Beta-thioester bond was applied which can be selectively cleaved intracellularly by glutathione and esterase to release the drug (Tang et al. 2010). With a curcumin loading content of 25.3 wt%, the Curc-OEG conjugate formed stable nanoparticles in aqueous solution and exhibited dramatic anticancer effect in vitro and in vivo without causing significant toxicity (Tang et al. 2010). Curcumin-polymer conjugates were also synthesized with hyaluronic acid (Manju et al. 2011a) and polyvinylpyrrolidone (Manju et al. 2011b). Most recently, Yang et al. (Yang et al. 2012b) demonstrated that the covalent curcumin-polymer conjugates can be further used to physically encapsulate additional curcumin. Curcumin was loaded into the polymeric micelles, which were synthesized by attaching multiple curcumin molecules to the hydrophobic poly (lactic acid) (PLA) backbone of PEG-PLA copolymer. Such micelles exhibited 10 times lower CMC value and dramatically enhanced curcumin loading capacity (~5 folds) compared to traditional mPEG-PLA micelles (Yang et al. 2012b).

Yokoyama et al. has reported that adriamycin (ADR)-conjugated polyethylene glycol–poly(aspartic acid) block copolymers (PEG-P[Asp(ADR)]) form micelles in aqueous solution and exhibited dramatic antitumor activity in vivo (Yokoyama et al. 1991, Yokoyama et al. 1992, Yokoyama et al. 1993). However, the ratio of chemically/physically entrapped adriamycin was not analyzed, and certain amounts of adriamycin derivatives were incorporated in the micelles as impurities, which may cause side effects (Yokoyama et al. 1994). The micelle preparation method was then improved which enabled the determination of this ratio and reduced the amounts of impurities (Yokoyama et al. 1994, Yokoyama et al. 1998). In addition, Yang et al. (Yang et al. 2012c) developed a dual-drug system in which doxorubicin was chemically linked to the PLA end of polyethylene glycol-b-poly lactic acid (PEG-b-PLA). This conjugate was mixed with RGD-PEG-b-PLA, PEG-b-PLA and an antivascular agent combretastatin A4 to prepare the micelles. This dual-drug system significantly enhanced cellular uptake of the drug by B16-F10 cells and human umbilical vein endothelial cells, and achieved significant antitumor effect with increased lifespan of tumor bearing mice.

In summary, pharmacological evaluation and drug formulation are two of the critical aspects in drug development process. This project has two specific aims: (1) to develop a novel therapeutic agent for disease treatment; and (2) to improve the efficacy of existing therapeutics via novel formulation strategies.

2.0 ROLES OF MIR-29A IN THE ANTIFIBROTIC EFFECT OF FXR IN HEPATIC STELLATE CELLS

2.1 BACKGROUND

Liver fibrosis is a chronic disorder that is characterized by an alteration of the balance between fibrogenesis and fibrolysis, resulting in accumulation of excessive amounts of extracellular matrix (ECM) and distortion of the normal liver architecture (Jiao et al. 2009). The activation and transformation of quiescent hepatic stellate cells (HSCs) into myofibroblast-like cells constitute a major mechanism for the increased production of ECM in the liver (Parsons et al. 2007, Friedman 2008). The mechanism of HSC activation is not completely understood and involves the alterations of a number of intracellular pathways such as TGF-β and PDGF signaling (Parsons et al. 2007, Friedman 2008). Several studies have shown that nuclear receptors such as peroxisome proliferators-activated receptor gamma (PPAR-γ) and pregnane-X receptor (PXR) also play an important role in the modulation of HSC activation and their biological functions (Miyahara et al. 2000, Galli et al. 2002, Marek et al. 2005).

FXR (farnesoid X receptor, NR1H4) is a member of the nuclear receptor superfamily that is highly expressed in liver, kidney, adrenals, and intestine (Forman et al. 1995). FXR plays a key role in the homeostasis of cholesterol and bile acids (BAs) by regulating the expression of genes involved in the synthesis and transport of BAs (Chiang 2002, Bertolotti et al. 2008). In addition to the potential of its ligands in the treatment of cholestasis (Claudel et al. 2002), FXR has been shown to be expressed in HSCs and negatively regulate the activation of HSCs and the associated overproduction of ECM in rodent models of liver fibrosis (Fiorucci et al. 2004, Fiorucci et al. 2005a, Fiorucci et al. 2005b). A study by Fiorucci et al. suggested that short heterodimer partner (SHP) played a role in the FXR-mediated antifibrotic effect. SHP is one of the FXR target genes and it effectively blocks the AP-1 signaling that is critically involved in ECM production (Fiorucci et al. 2004). However, the detailed mechanism that is involved in the antifibrotic effects of FXR remains incompletely understood.

MicroRNAs (miRNAs) are short non-coding RNA molecules that control gene expression via modulating the stability and/or the translational efficiency of target messenger RNAs (Lee et al. 1993, Ghildiyal et al. 2009). MiRNAs play a role in the control of a wide range of biological functions and processes such as development, differentiation, metabolism, carcinogenesis, immune response etc (Ghildiyal et al. 2009). MiRNAs are initially transcribed as long primary transcripts that undergo several processing steps to form the mature 22-nt miRNA:miRNA* duplex. The complementary strand miRNA* is typically degraded, while the mature single-stranded form is incorporated into the RNA-induced silencing complex (RISC). Most of miRNA binding sequences are found in the 3′-UTR of the mRNAs (Ghildiyal et al. 2009). However, increasing evidence suggests that miRNAs can also be targeted to both coding-regions and 5′-UTR of mRNAs (Forman et al. 2008). Several studies showed that

miRNAs were involved in the activation of HSCs: a number of miRNAs species are upregulated while many others are downregulated during the process (Guo et al. 2009, Ji et al. 2009, Venugopal et al. 2010). A recent study by Roderburg and colleagues showed that all three members (a, b, and c) of the miR-29 family were significantly downregulated in mouse liver with CCl_4 and common bile ligation induced liver fibrosis (Roderburg et al. 2011). Downregulation of miR-29a/b/c was also shown in activated HSCs in vitro. A likely role of miR-29 members in liver fibrosis is suggested by: a) overexpression of miR-29 in mouse HSCs led to downregulation of the expression of several ECM genes; and b) treatment with TGF-β or LPS-mediated activation of NF-κB signaling led to downregulation of the expression of miR-29a/b/c (Roderburg et al. 2011). The clinical significance is further supported by the observation that serum levels of miR-29a in patients with cirrhosis are inversely correlated with the stages of the disease (Roderburg et al. 2011). The critical role of miR-29 in fibrotic diseases was also demonstrated in animal models of pulmonary fibrosis (Cushing et al. 2011) and renal fibrosis (Wang et al. 2012d). However, it is unknown if miRNAs are also involved in the antifibrotic effect of FXR in HSCs.

In this study, we showed that activation of FXR by a synthetic ligand, GW4064, led to significant upregulation of the expression of miR-29a in mouse, rat, and human HSCs. Functional and reporter assays suggested that miR-29a is a potent mediator that negatively regulates the expression of several ECM genes. Furthermore, a functional FXR response element (FXRE) was found in the miR-29a promoter. Our study unveils a new mechanism by which FXR negatively regulates the expression of ECM in HSCs.

2.2 METHODS

2.2.1 Reagents and Chemicals

GW4064 (3-[2-[2-Chloro-4-[[3-(2,6-dichlorophenyl)-5-(1-methylethyl)-4-isoxazolyl]methoxy]phenyl]ethenyl]benzoic acid) was synthesized following a published protocol (Maloney et al. 2000). MiR-29a mimic and non-specific control miRNA mimic were purchased from ABI (Applied Biosystems, Foster City, CA). All products for cell culture were purchased from Invitrogen (Carlsbad, CA). pCMX, pCMX-FXR, and pCMV-βgal were described previously (Umesono et al. 1991). pCMX-vpFXR (a gift from Drs Enrique Saez and Ronald Evans at the Salk Institute) was generated by fusing the VP16 activation domain from the herpes simplex virus to the N terminus of the FXR (Downes et al. 2003).

2.2.2 Animals and HSC Isolation

Retired male Sprague-Dawley rats and C57BL/6 mice were from Charles River Laboratories. FXR-/- mice (Sinal et al. 2000) were purchased from Jackson Laboratories and bred in the Central Animal Facility of University of Pittsburgh. HSCs were isolated via in situ proteinase/collagenase perfusion followed by density gradient centrifugation as described (Thirunavukkarasu et al. 2005). Primary cells were more than 95% pure. Cells were grown on standard tissue culture plastic dishes in DMEM with 10% fetal bovine serum and antibiotics. HSCs were used following activation via culturing for 7 days. All studies conform to the Guide for the Care and Use of Laboratory Animals published by the US National Institutes of Health (NIH Publication No. 85-23, revised 1996).

LX-2, an immortalized human hepatic stellate cell line, was kindly provided by Dr. Scott L. Friedman (Mount Sinai School of Medicine, New York, NY, USA) (Xu et al. 2005). The cells were maintained in DMEM with 10% fetal bovine serum and antibiotics.

2.2.3 Real Time RT-PCR

Total RNA was extracted from cells with TRIzol reagent (Invitrogen) and the first-strand cDNA was synthesized by use of SuperScript III reverse transcriptase (Invitrogen). Real-time PCR analysis of rat, mouse, and human fibrosis-related genes and miR-29 precursor was performed by use of SYBR Green-based assays with the ABI 7300 Real-Time PCR System (Applied Biosystems, Foster City, CA) (Li et al. 2008a). Transcript abundance, normalized to β-actin expression, was expressed as fold increase over a calibrated sample.

For detection of mature miRNA, total RNA was reversely transcribed into cDNA using miScript Reverse Transcriptase Kit (Qiagen) according to the manufacturer's protocol. cDNA samples (2 μl) were used for real-time PCR in a total volume of 25 μl using miScript SYBR Green PCR Kit (Qiagen) and miRNA specific primers (Qiagen) on a qPCR machine (Applied Biosystems, Foster City, CA). The sequences of primers for all of the RT-PCR analysis were shown in Appendix A.

2.2.4 Western Blot Analysis

Protein extraction and Western blot analysis were performed as described (Li et al. 2008a). FXR antibody (sc-13063) and collagen 1A1 (COL1A1) antibody (sc-25974) were purchased from

Santa Cruz Biotechnology. Horseradish peroxidase–labeled goat anti-rabbit IgG and the ECL chemiluminescence kit were purchased from Amersham Biosciences (Piscataway, NJ).

2.2.5 Plasmid Construction

A fragment spanning 1.98 kb of 5′-flanking sequence of the human miR-29a gene was PCR-amplified from human genomic DNA using primers 5′-cgacgcgtgtgggtaagggagagggaag-3′ and 5′-cgacgcgttgctgactgatgagaggaaa-3′ and cloned into Mlu1 of pGL3-basic vector (Promega). A mutated construct that lacks a putative IR-1 (miR-29a/IR-1) binding site was similarly generated via cloning a fragment spanning 1.87 kb of 5′-flanking sequence of the miR-29a gene that was amplified using primers 5′- cgacgcgtctggtgttcgcagctttcac-3′ and 5′-cgacgcgttgctgactgatgagaggaaa-3′. A TK-Luc construct that contains three copies of miR-29a/IR-1 sequence was generated by annealing the oligonucleotides 5′-agcttcttggaggtcacagacctcgaggtcacagacctcgaggtcacagacctcgttg- 3′ and 5′-caacgaggtctgagacctcgaggtctgagacctcgaggtctgagacctccaaga-3′ followed by ligation into HindIII/BamHI-digested TK-Luc. For functional analysis of miR-29a, 3′-UTR segments containing the miR-29a-binding sequences or without binding sequences for COL1A1, collagen 3A1 (COL3A1), and elastin-1 (ELN1) genes were PCR amplified from human genomic DNA utilizing the corresponding forward and reverse primers (Appendix A). The PCR product was then subcloned into the SacI-MluI site downstream of the stop codon in the pMIR-REPORT Firefly Luciferase reporter vector (Ambion).

2.2.6 Transfection Assays

Normal monkey kidney fibroblast cells (CV-1 line) were grown to 60–70% confluence in 48-well plates. Cells were transiently transfected using Lipofectamine2000 (Invitrogen) with pGL3-miR-29a in the presence or absence of pCMX-vpFXR or pCMX-FXR. pCMX was added to ensure identical amounts of DNA in each well. Transfection efficiency was monitored by co-transfection of pCMV-βgal plasmid. Twenty-four h later, cells were treated with GW4064 or DMSO vehicle. Cell extracts were prepared 24 h after GW4064 treatment and the luciferase and β-galactosidase assays were performed as described (He et al. 2006) and luciferase activity was normalized against β-galactosidase activity. Transfection experiments were performed on at least three occasions and in each case were done in triplicate. Data were represented as fold induction over reporter gene alone. In a separate study, CV-1 cells were transfected with pMIR-COL1A1-3'-UTR, pMIR-COL3A1- 3'-UTR, or pMIR-ELN1-3'-UTR in the presence of miR-29a mimic or non-specific control miRNA mimic. The reporter expression was then similarly examined as described above 24 h following transfection.

2.2.7 Electrophoretic Mobility Shift Assay (EMSA)

FXR and retinoid X receptor (RXR) proteins were generated in vitro by coupled in vitro transcription/translation (TNT system, Promega) with pCMX-FXR and pCMX-RXR plasmids. The DNA probe miR-29a/IR1 (5'- gaagaggtcacagacctctgg -3') was derived from a region in the human miR-29a promoter that contains a putative FXR response element. It was labeled with [γ-^{32}P]-ATP by using the Klenow fragment of DNA polymerase. DNA-binding reactions were carried out as follows: aliquots of in vitro translation mixture were incubated in 20 μL binding

buffer (10 mM Hepes, pH 7.9, 10 mM EGTA, 10 mM EDTA, 0.25 mM DTT, and 10% glycerol) containing 2 μg polydI: dC (Sigma) and 6–20 x 10^3 cpm of DNA probe at room temperature for 20 min. For supershift assays, 0.2 μg rabbit anti-FXR IgG was added and the samples were incubated for another 10 min. The binding mixture was then applied onto a 5% polyacrylamide gel (0.5 x Tris-Borate-EDTA buffer) for electrophoresis. The gels were dried and exposed at –80°C for autoradiography.

2.2.8 Chromatin Immunoprecipitation (ChIP) Assay

ChIP assay was performed using a ChIP assay kit (Millipore, Massachusetts, USA) according to the instructions of the manufacture. Soluble chromatin was prepared from LX-2 cells treated with 1 μM GW4064 for 24 hours. Chromatin was immunoprecipitated with antibodies (2 μg) directed against FXR (sc-13063). Final DNA extractions were PCR amplified using primer pairs that cover an IR-1 consensus sequence in the miRNA-29a promoter as follows: forward, 5'-GTGGGTAAGGGAGAGGGAAG-3'; antisense, 5'-ACATTGCCTTCTCCCCAAAG-3'.

2.2.9 Statistical Analysis

All data are expressed as means ± standard deviation unless otherwise stated. Comparisons between two groups were made with unpaired Student's t-test. Comparisons between three or more groups were made with analysis of variance followed by Tukey-Kramer post hoc analysis. In all cases, $P < 0.05$ was considered statistically significant.

2.3 RESULTS

2.3.1 Treatment of rat HSCs with GW4064 led to significant inhibition of the mRNA expression of several ECM genes

Using 6-ECDCA as a specific ligand, Fiorucci and colleagues (Fiorucci et al. 2004) have previously shown that activation of FXR leads to a significant inhibition of collagen 1A1 (COL1A1) expression in both primary rat HSCs and an immortalized human hepatic stellate cell line HSC-T6. In this experiment, we examined if GW4064 could similarly inhibit the expression of COL1A1 in rat HSCs. GW4064 is also a synthetic ligand that is highly specific for FXR and has been widely used in studying FXR-mediated gene regulation in vitro and in vivo (Maloney et al. 2000, Li et al. 2009a). Treatment with GW4064 was conducted at the concentration of 1 μM for 24 h, which shows optimal sensitivity and specificity based on our previous experience. Figure 2 shows that GW4064 treatment resulted in a significant downregulation of the expression of COL1A1 mRNA in rat HSCs. GW4064 also significantly inhibited the expression of several other fibrosis-related genes including COL1A2, COL3A1, COL4A1, COL5A1, elastin 1 (ELN 1), and fibrillin 1 (FBN 1) (Figure 2). Inhibition of ECM protein expression by GW4064 was also confirmed as shown in Western analysis of COL1A1 expression (Figure 3).

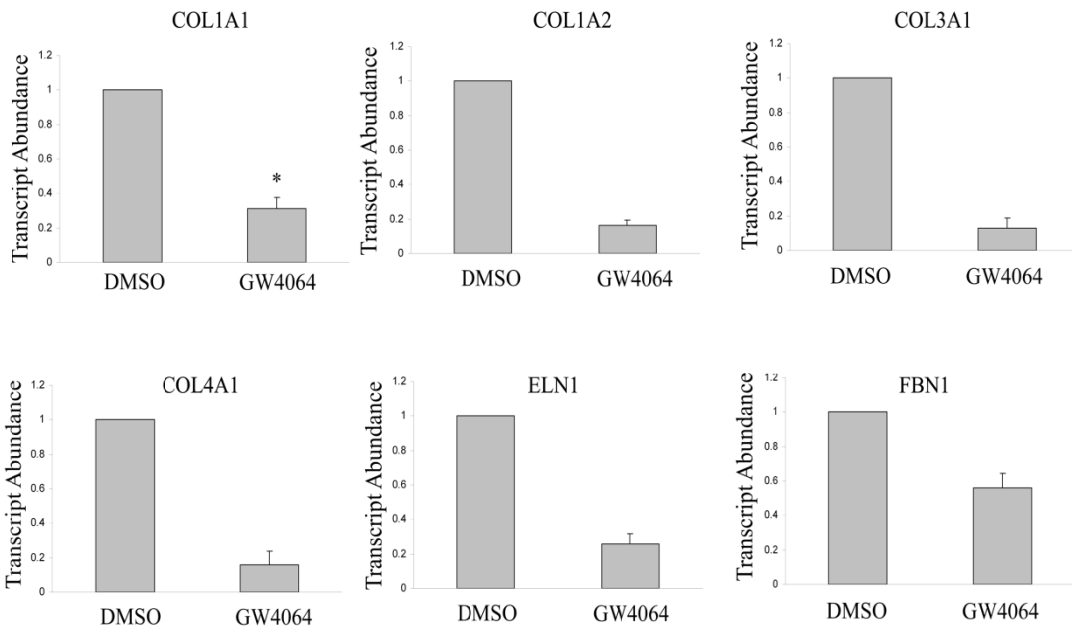

Figure 2 GW4064 treatment led to downregulation of the mRNA expression of ECM genes in rat HSCs.

Rat HSCs were isolated as described under Materials and Methods and cultured for 7 days to allow transactivation. HSCs were then treated with GW4064 (1μM) or DMSO vehicle. The mRNA expression levels of several ECM genes were determined by real-time RT-PCR 24 h after the treatment. n = 3; *, $P < 0.05$ (versus DMSO).

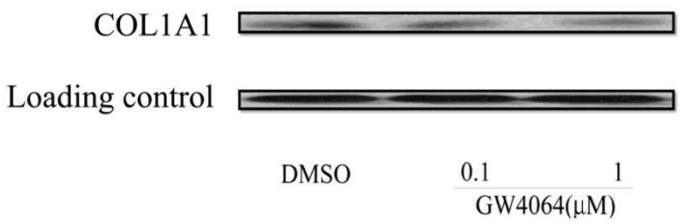

Figure 3 GW4064 treatment led to downregulation of COL1A1 protein expression in rat HSCs.

Rat HSCs were isolated as described in Materials & Methods and cultured for 7 days to allow transactivation. HSCs were then treated with GW4064 or DMSO vehicle. The expression level of COL1A1 was determined by Western blot 24 h following the treatment. Shown in the figure were representative data from three independent experiments.

2.3.2 GW4064 treatment led to upregulation of miR-29a in rat and mouse HSCs

Following the demonstration of the inhibition of the mRNA expression of several ECM genes by GW4064, we went on to explore the potential mechanism involved. We hypothesized that a miRNA might be involved based on the fact that a cluster of ECM-related genes were affected by GW4064 treatment. Multiple algorithms were used to screen for miRNAs that may be involved in the regulation of ECM including Microcosm Targets, TargetScan, and PITA (Lewis et al. 2003, Xin et al. 2009, Dong et al. 2010). Members of miR-29 family including miR-29a, miR-29b, and miR-29c were identified by all three programs to be the best candidates as ECM-targeting miRNAs. As an initial step to study a potential role of miR-29a in GW4064-mediated effects, we examined if the expression of miR-29a is regulated by GW4064 in HSCs. Figure 4A shows that GW4064 treatment resulted in a significant increase in the expression of miR-29a gene as assessed by real-time RT-PCR analysis of miR-29a precursor. A similar induction of miR-29a expression by GW4064 was also observed in LX-2 cells (an immortalized human hepatic stellate cell line) (Figure 4B) and HSCs isolated from wild-type mice (Figure 4C). However, no induction of miR-29a was observed in HSCs prepared from FXR-/- mice (Figure 4D), suggesting that induction of miR-29a by GW4064 was mediated by FXR.

Interestingly, GW4064 treatment had no effect on the expression of miR-29b in both rat and mouse HSCs (Figure 5). Induction of miR-29a in mouse liver was also observed following oral delivery of GW4064 (Figure 6).

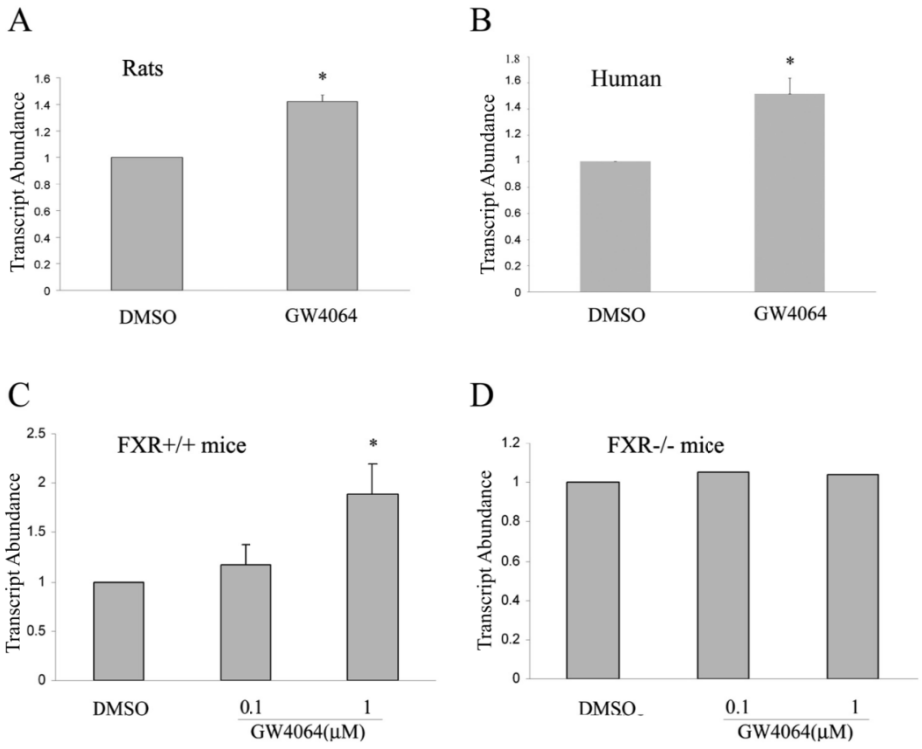

Figure 4 GW4064 treatment led to up-regulation of miR-29a expression in HSCs.

Rat HSCs (A) or LX2 cells (B) were treated with GW4064 or DMSO vehicle. The expression level of miR-29a was determined by real-time RT-PCR 24 h after the treatment. The effect of GW4064 on miR-29a expression was similarly examined in HSCs isolated from wild-type mice (C) or FXR (-/-) mice (D). n = 3; *, $P < 0.05$ (versus DMSO).

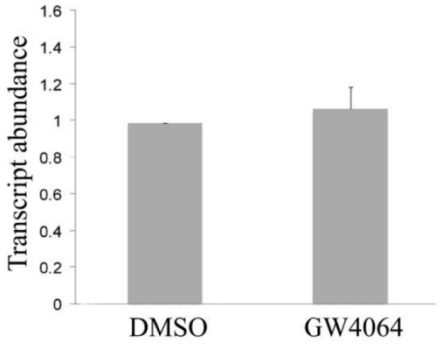

Figure 5 miR-29b expression is not altered in rat HSCs treated with GW4064.

Rat HSCs were isolated as described in Materials and Methods and cultured for 7 days to allow transactivation. HSCs were then treated with GW4064 or DMSO vehicle. The expression level of miR-29b was determined by real-time RT-PCR 24 h following the treatment. N = 3. $P > 0.05$ (vs. DMSO).

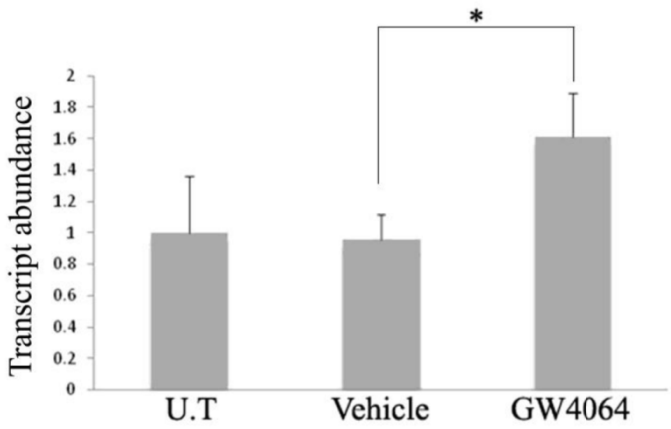

Figure 6 miR-29a expression is induced in mouse liver by FXR ligand treatment.

Mice were treated for 7 days with vehicle or the synthetic FXR agonist GW4064 (100 mg/kg). The expression level of miR-29a was determined by real-time RT-PCR. N = 3. *P <0.05 (vs. vehicle).

2.3.3 MiR-29a negatively regulated the expression of ECM in HSCs

Following demonstration of induction of miR-29a by GW4064 we then examined the effect of miR-29a overexpression on the expression of several ECM genes in HSCs to further establish a role of miR-29a in the GW4064/FXR-mediated antifibrotic effect. HSCs were transfected with a miR-29a mimic, a control sequence or a miR-29a inhibitor and the mRNA expression of several ECM genes was examined 24 h later. As shown in Figure 7, overexpression of miR-29a mimic in HSCs resulted in a significant inhibition of the mRNA expression of all six ECM genes examined. Higher levels of ECM mRNAs were observed in HSCs treated with miR-29a inhibitor compared to cells treated with control sequence. This might be due to the inhibition of endogenous miR-29a that is involved in the control of the basal levels of ECM expression.

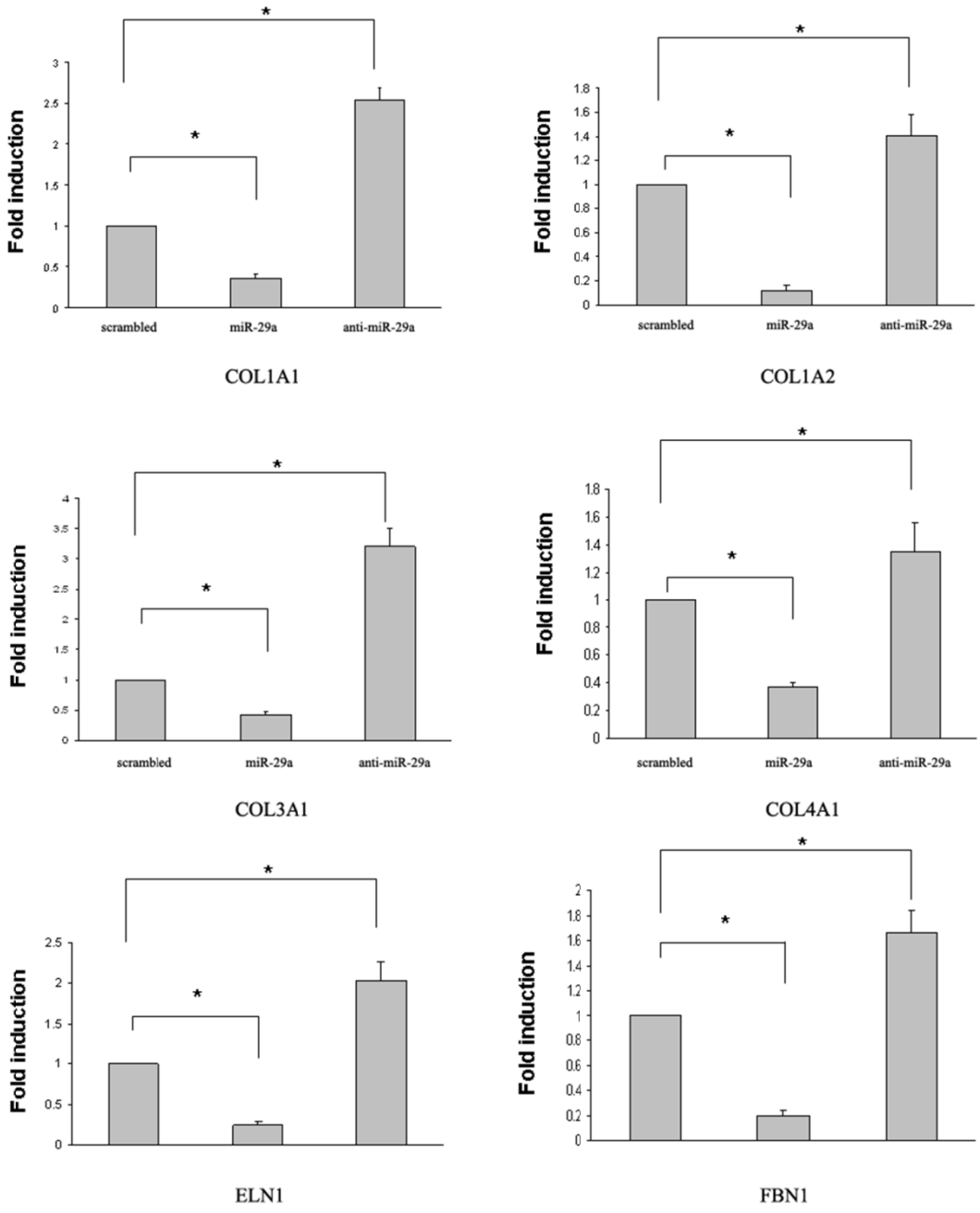

Figure 7 Overexpression of miR-29a resulted in down-regulation of the mRNA expression of ECM genes in rat HSCs.

HSCs were transfected with miR-29a mimic, nonspecific control miRNA mimic, or miR-29a inhibitor (25 pmol/well in 6-well plates by 10 μl of Lipofectamine) for 24 h. The mRNA expression levels of several ECM genes were then determined by real-time RT-PCR. n = 3; *, $P < 0.05$ (versus control miRNA).

The effect of miR-29a appears to be target sequence-specific as it showed no effect on the expression of FXR and SHP expression at both mRNA and protein level over a wide range of concentration (Figure 8-9). MiR-29a treatment had no effect either on GW4064-mediated induction of SHP expression, suggesting that the function of FXR was well-retained in miR-29a-treated HSCs (Figure 10). In contrast, miR-29a inhibited the expression of COL1A1 at both mRNA and protein levels in a dose-dependent manner (Figure 8-9).

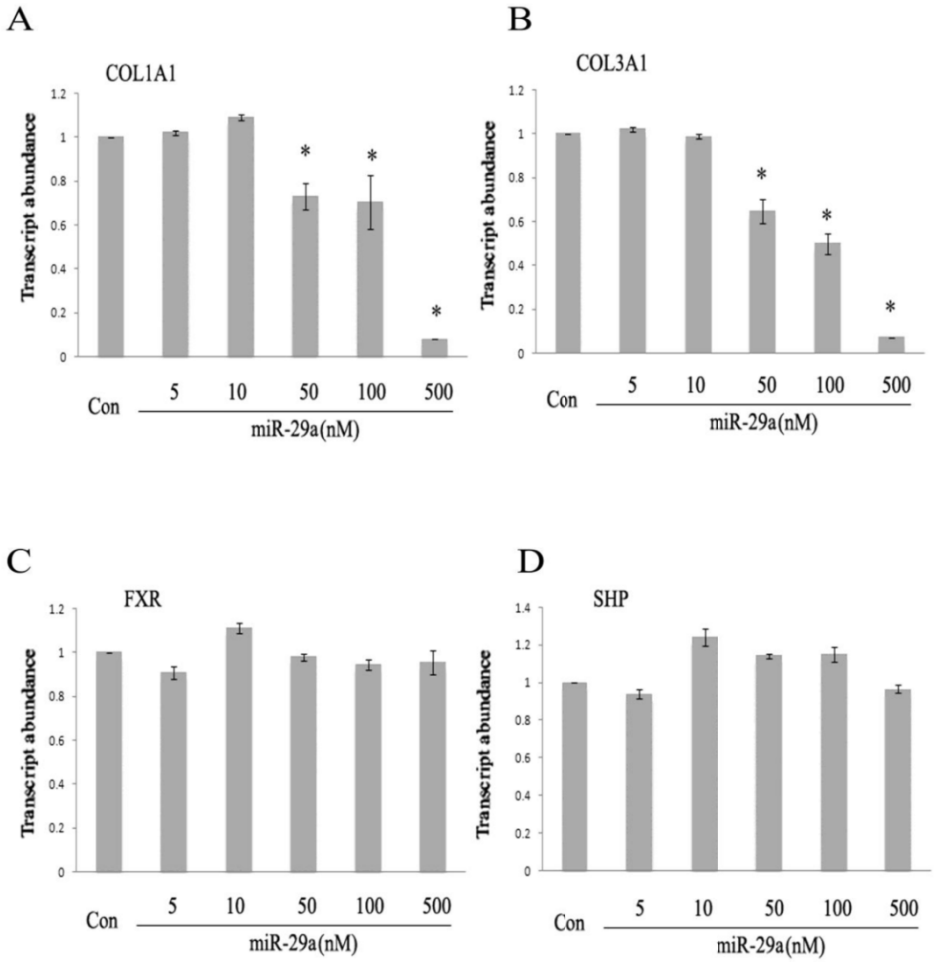

Figure 8 Overexpression of miR-29a resulted in downregulation of the mRNA expression of ECM genes in rat HSCs in a dose dependent manner without affecting the mRNA expression of SHP or FXR.

HSCs were transfected with different concentrations of miR-29a mimic (5~500 nM) or non-specific control miRNA mimic (500 nM) for 24 h. The mRNA expression levels of COL1A1, COL3A1, FXR and SHP were then determined respectively by real-time RT-PCR. N = 3. $P < 0.05$ (vs. control miRNA).

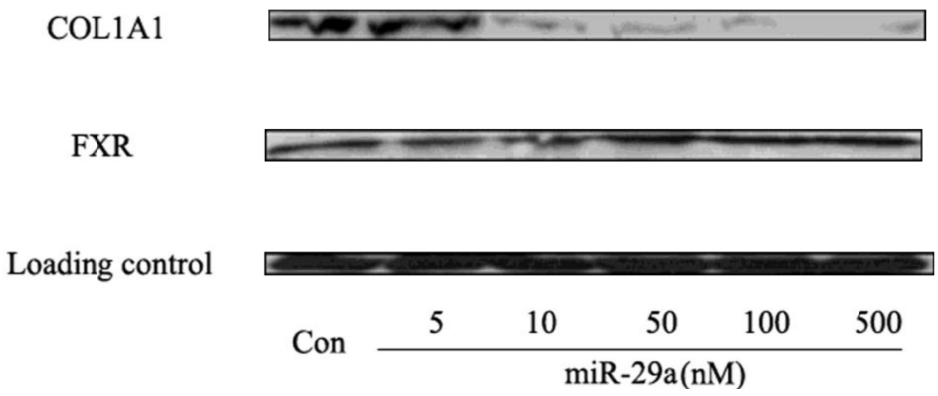

Figure 9 Overexpression of miR-29a resulted in downregulation of the expression of COL1A1 protein in rat HSCs in a dose dependent manner without affecting the protein expression of FXR.

Rat HSCs were transfected with different concentrations of miR-29a mimic (5~500 nM) or non-specific control miRNA mimic (500 nM) for 24 h. Protein expression levels of COL1A1 and FXR were determined by Western blot. Shown in the figure were representative data from three independent experiments.

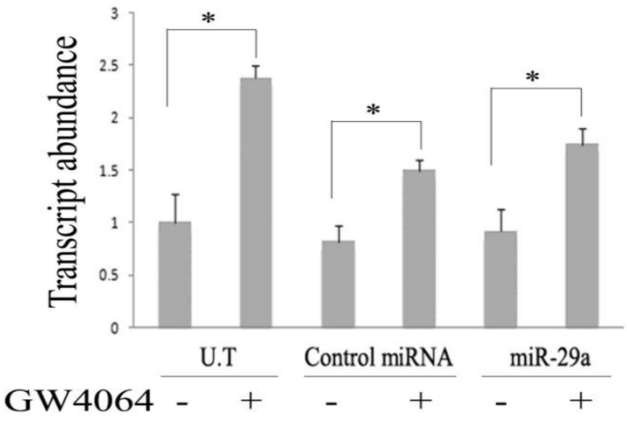

Figure 10 Overexpression of miR-29a does not affect FXR-mediated SHP induction following GW4064 treatment.

HSCs were transfected with miR-29a mimic or nonspecific control miRNA mimic (50 nM) for 24 h followed by treatment with GW4064 or DMSO vehicle for another 24 h. The mRNA expression level of SHP was then determined by real-time RT-PCR. N = 3. $P < 0.05$ (vs. control miRNA).

To further establish a role of miR-29a in the regulation of ECM expression we examined the effect of miR-29a on the expression of several reporter constructs that contain the respective 3'-UTRs from COL1A1, COL3A1 and ELN1 genes. All of the three 3'-UTRs contain a putative miR-29a target sequence as analyzed by TargetScan algorithm. As shown in Figure 11A, transfection of cells with miR-29a mimic significantly inhibited the expression of the reporter construct with an intact COL1A1 3'-UTR. Such inhibitory effect was completely lost for a mutant reporter construct lacking the miR-29a target sequence. These results suggest that the presence of the miRNA target site in the COL1A1 3'-UTR of the reporter construct is necessary for the inhibition by miR-29a. Similar results were observed with the construct with a 3'-UTR from either COL3A1 or ELN1 gene (Figure 11B-C).

2.3.4 Human miR-29a is a likely target gene of FXR

Upregulation of miR-29a expression by GW4064 suggests that activation of FXR modulates miR-29a expression at the transcriptional level. We then hypothesized that activation of FXR enhances miR-29a expression via exerting its stimulatory activity on miR-29a promoter. To test this hypothesis, we constructed a luciferase reporter expression plasmid (pGL3-miR-29a) that is driven by a 1.98 kb sequence of human miR-29a promoter. To examine promoter activation, CV-1 cells were co-transfected with pGL3-miR-29a and pCMX-FXR expression vector, followed by GW4064 treatment. CV-1 cells instead of HSCs were used for transfection due to low transfection efficiency in the HSCs. As shown in Figure 12, treatment with GW4064 resulted in a significant increase in the transcriptional activity of the miR-29a promoter. To further elucidate a role of FXR in regulating miR-29a promoter activity, we then co-transfected pGL3-miR-29a with an expression plasmid encoding a constitutively activated FXR, vpFXR.

vpFXR was generated by fusing the VP16 activation domain to the N terminus of FXR cDNA (Downes et al. 2003). Figure 12 shows that co-expression of vpFXR in CV-1 cells significantly enhanced the miR-29a promoter activity, clearly demonstrating that a genetic activation of FXR enhances miR-29a promoter activity.

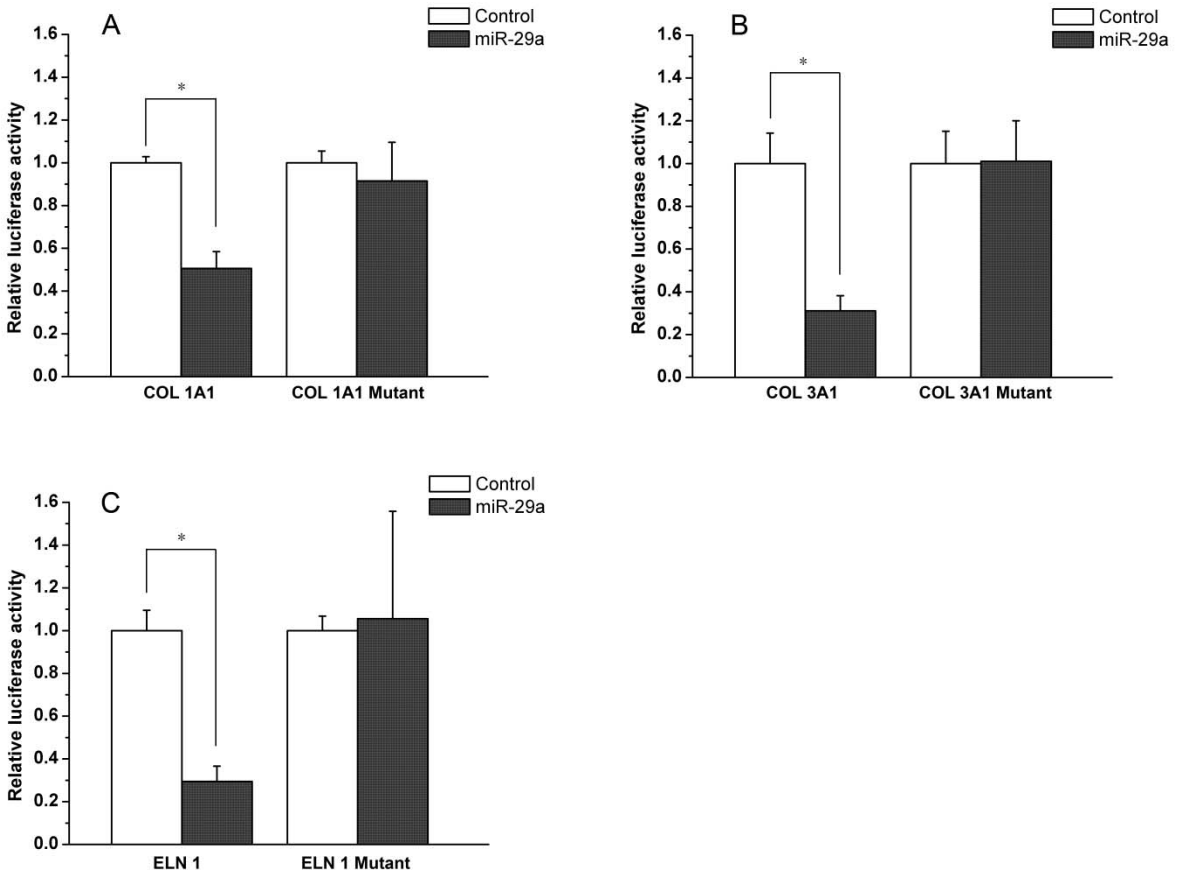

Figure 11 miR-29a regulates the expression of ECM genes through targeting at the 3'-UTR of their mRNAs. CV-1 cells were transfected with a luciferase construct with Col1A1-3'-UTR (A), Col3A1-3'-UTR (B) or ELN-3'-UTR (C) in the presence of miR-29a mimic or nonspecific control miRNA mimic. Luciferase assay was performed 24 h after the transfection. Data shown in the panels represent mean (S.D.) from triplicate assays. n = 3; *, $P < 0.05$ (versus control miRNA).

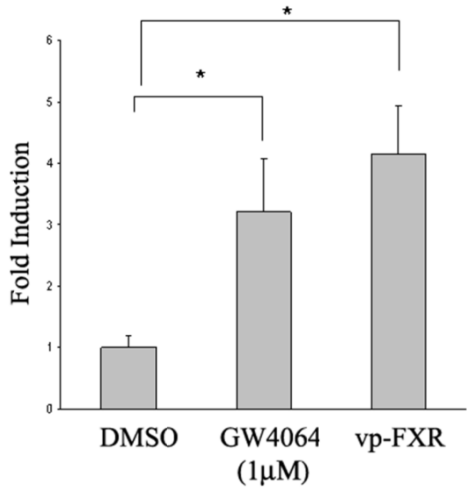

Figure 12 FXR enhances the transcriptional activity of the miR-29a gene promoter.

A luciferase reporter driven by a human miR-29a promoter of 1984 base pairs was used to study the miR-29a promoter activity. CV-1 cells were transiently transfected with pGL3-miR-29a in the presence or absence of pCMX-FXR. Five hours later, the transfection medium was replaced with complete medium and cells were incubated for 20 h. Cells were then cultured in the presence of GW4064 or vehicle DMSO for 24 h. Luciferase assay was then performed. Data shown in the panels represent mean (S.D.) from triplicate assays. To examine the effect of genetic activation of FXR on miR-29a promoter activity, CV-1 cells were transfected with pGL3-miR-29a in the presence or absence of pCMX-vpFXR. Luciferase assays were then examined as described above. n = 3; *, $P < 0.05$ (versus DMSO).

To search for FXR responsive elements (FXREs) that may mediate miR-29a induction by GW4064, the 2 kb miR-29a promoter sequence was subjected to in silico analysis with a Webbased algorithm (NUBIScan). One imperfect inverted repeat spaced by one nucleotide (IR1) site was identified, and its sequences and location are shown in Figure 13A. To determine whether miR-29a/IR1 is necessary and sufficient in mediating FXR transactivation, a heterologous tk-luciferase reporter gene that contain three copies of miR-29a/IR1 element was generated and tested for FXR transactivation in CV-1 cells. As shown in Figure 13B, the synthetic tk reporter gene was activated by FXR in the presence of its agonist GW4064. To

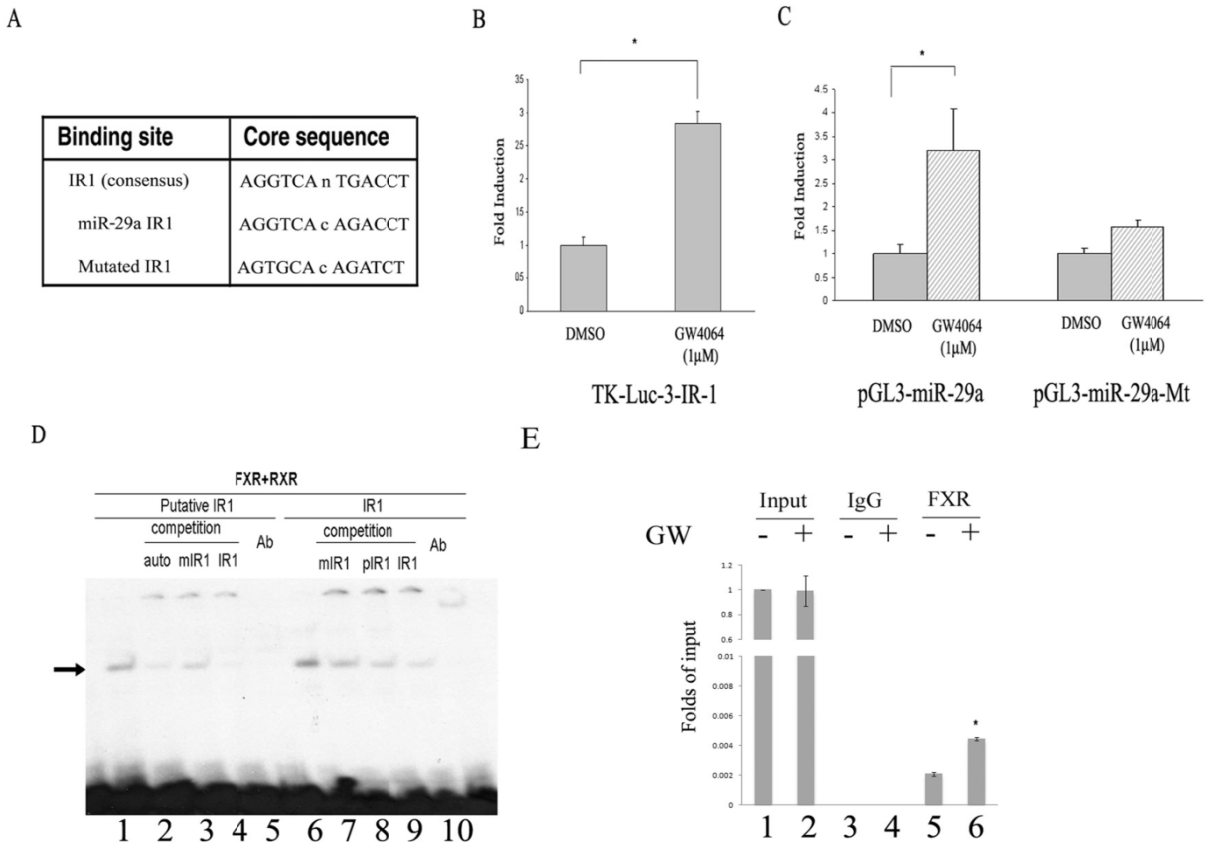

Figure 13 Analysis of putative FXREs in human miR-29a promoter.

A, identification of a putative FXRE in human miR-29a promoter through an in silico analysis with a Web-based algorithm (NUBIScan). B, miR-29a/IR-1 mediates FXR transactivation of a heterologous tk-luciferase reporter gene. n =3; *, $P < 0.05$ (versus DMSO). C, mutation of miR-29a/IR-1 on the miR-29a promoter eliminates activation by FXR. n = 3; *, $P < 0.05$ (versus DMSO). D, electrophoretic mobility shift assay analysis of the binding of FXR/RXR to miR-29a/IR-1 in human miR-29a promoter. Double-stranded oligonucleotides (-1924/-1936) were end-labeled with [γ-^{32}P]ATP using T4 polynucleotide kinase. The labeled probe was incubated with in vitro-translated RXR/FXR for 20 min. The reactions were analyzed by electrophoresis in a nondenaturing 5% polyacrylamide gel followed by autoradiography. In some studies, the samples were preincubated with anti-FXR antibody before gel electrophoresis. E, ChIP analysis of the binding of FXR to miR-29a/IR-1 in human miR-29a promoter in LX-2 cells. Soluble chromatin was prepared from LX2 cells treated with 1 μM GW4064 or DMSO for 24 h. Chromatin was immunoprecipitated with antibodies directed against FXR. The extracted DNA was PCR amplified using primer pairs that cover an IR-1 consensus sequence in the miRNA-29a promoter.

further determine whether this IR1 sequence is responsible for FXR-mediated transactivation of miR-29a promoter, we generated a mutant pGL3-miR-29a in which this putative FXR binding site was eliminated. The wild-type and mutated plasmids were then similarly transfected into the CV-1 cells, and their transfection efficiency was compared. Figure 13C shows that the FXR-mediated activation of miR-29a promoter was substantially diminished when the miR-29a/IR1 site was eliminated. The above studies strongly suggested a likely role of miR-29a/IR1 element in FXR-mediated transactivation of human miR-29a promoter.

Figure 13D shows the result of an EMSA with a 20 bp oligonucleotide that contains the putative FXRE (lanes 1 ~ 5). A typical IR1/FXRE oligonucleotide was also included as a positive control (lanes 6 ~ 10) because FXR is known to bind to IR1 with high specificity and affinity. Interaction of the oligonucleotide with in vitro translated FXR/RXR yielded a DNA/protein band of expected mobility (lane 1). This binding was specific, as it was inhibited by addition of excess unlabelled (cold) miR-29a/IR1 (lane 2) or IR1/FXRE (lane 4) but not a mutated miR-29a/IR1 (lane 3). Addition of antibody against FXR to the reaction mixture resulted in the disappearance of the radiolabeled band (lane 5) (Figure 13D). This supershifting confirms the identity of the protein that interacts with the DNA as being FXR.

To further demonstrate the binding of FXR to miR-29a/IR1, chromatin immunoprecipitation (ChIP) assay was then performed. In this experiment, LX-2 cells were treated with vehicle (DMSO) or GW4064 for 24 h before ChIP analysis using an anti-FXR antibody or the control mouse IgG. As shown in Figure 13E, treatment of LX-2 cells with GW4064 led to a significant increase in the recruitment of FXR to miR-29a/IR1. Together these results suggested that miR- 29a is a direct transcriptional target of FXR.

2.4 DISCUSSION

We have demonstrated in this study that miR-29a was significantly upregulated in HSCs following treatment with GW4064, a synthetic FXR-specific agonist. Overexpression of miR-29a in HSCs resulted in a significant inhibition of the mRNA expression of a number of ECM genes including collagens, elastin and fibrillin. MiR-29a also significantly inhibited the expression of a reporter expression plasmid that contains a full-length 3'-UTR from COL1A1, COL3A1 or ELN1 gene. These results are consistent with the notion that miR-29a may be critically involved in the FXR-mediated inhibition of ECM expression in HSCs.

Induction of miR-29a in HSCs is likely to be mediated by FXR as: a) GW4064 is highly specific for FXR and is often used as a "chemical tool" to show that BA target genes are regulated in a FXR-specific manner (Maloney et al. 2000); and b) the induction of miR-29a was abolished in FXR-/- mouse HSCs. We have also identified an imperfect IR1 as a FXRE that appears to be involved in GW4064-mediated upregulation of miR-29a in HSCs. IR1 is a typical FXRE that has been implicated in the regulation of a number of FXR target genes. Thus, miR-29a is a likely target gene of FXR.

Various biological functions have been reported for members of miR-29 family including miR-29a, b and c. These include modulations of self-renewal in hematopoietic progenitor cells (Han et al. 2010), regulations of WNT signaling in human osteoblasts (Kapinas et al. 2010), control of host-HIV-1 interactions (Nathans et al. 2009), and regulation of the expression of ECM in fibroblasts and stellate cells (Jiang et al. 2010) etc. Clearly, the biological functions of miRNAs are complex and may be tissue- or cell type-specific. A study from van Rooij et al. (van Rooij et al. 2008) has shown that dysregulation of miR-29 plays an important role in cardiac fibrosis following myocardial infarction. All three members of miR-29 family

were downregulated in the region of heart adjacent to the infarct. Systemic delivery of a cholesterol-conjugated miR-29b inhibitor led to increased expression of collagen in liver, kidney and heart, suggesting a role of miR-29 in regulating the expression of ECM in vivo (van Rooij et al. 2008). Recently, downregulation of miR-29 has also been shown in rodent models of liver fibrosis and in liver biopsies from patients with HCV infection (Kwiecinski et al. 2009, Pogribny et al. 2010). The role of miR-29 members in liver fibrosis was further demonstrated in a recent study by Roderburg et al. in which all members of miR-29 were significantly downregulated in mouse liver in both CCl_4 and common bile ligation models (Roderburg et al. 2011). They have further shown that TGF-β or NF-κB signaling negatively regulated the expression of miR-29, suggesting TGF-β↑→miR−29↓ or NF-κB↑→miR-29↓ as an important mechanism in the development of liver fibrosis (Roderburg et al. 2011). A similar role of TGF-β↑→miR−29↓ was also demonstrated in a mouse model of lung fibrosis (Cushing et al. 2011). These data, together with our observation that activation of FXR led to upregulation of miR-29a, strongly support an important role of miR-29 in the control of ECM expression under both physiological and pathophysiological conditions. They also suggest the potential of miR-29 as a novel therapeutics for the treatment of various fibrotic diseases including liver fibrosis.

It is likely that other mechanisms are involved in the antifibrotic effect of FXR/FXR ligands in addition to a direct activation of the miR-29a gene. A number of studies including our work have suggested that many nuclear receptors such as FXR and SHP inhibit various inflammatory signalings including NF-κB, AP-1, and TGF-β via competition for essential cofactors or recruitment of corepressors (He et al. 2006, Zhang et al. 2011b). Therefore, it is possible that treatment of HSCs with FXR ligands at quiescent stage may prevent the NF-κB- and/or TGF-β-mediated downregulation of miR-29 expression during their transactivation

process. Studies are currently ongoing in our laboratory to test this hypothesis. Alternatively, FXR and/or SHP may directly inhibit the expression of fibrosis-related genes through the interference of AP-1 and/or TGF-β signaling as suggested by Fiorucci et al. in their study (Fiorucci et al. 2004). Clearly, more studies are required in the future to better understand the contribution of each potential mechanism to the overall antifibrotic effect of FXR.

Animal models are indispensable in simulating the micro-environment composed of various cell types in the fibrotic liver. Two of the most commonly used models of experimental fibrosis are bile duct ligation (BDL) and iterative toxic damage (for example, elicited by CCl_4 intoxication). BDL results in a reproducible portal tract fibrosis over a short period of time (4-6 weeks in rats, 2-3 weeks in mice). However, it shows little resemblance to human fibrotic liver diseases (except for chronic biliary obstruction) and an altered metabolism of most drugs that are primarily secreted through the biliary tract or that undergo enterohepatic circulation. Liver fibrosis induced by carbon tetrachloride (CCl_4) results from repetitive (necrotic) hepatocyte death. It allows the study of acute liver injury, advanced fibrosis, and fibrosis reversal. The major disadvantages are the severe hepatocyte necrosis and its dependence on massive oxidative stress that is not found to such an extent in human chronic liver diseases (Popov et al. 2009). In addition, tissue bank serves as a tissue procurement resource which provides ethically-collected, highly-annotated tissue specimens for academic research. Liver specimens at difference fibrotic stages could be a useful resource to provide data that are more clinically relevant.

It should be noted that, despite a similar function in regulation of ECM expression, miR-29a, b and c may be differentially up- or down-regulated under different physiological or pathophysiological conditions. MiRNA-29a and miR-29b1 are clustered together and are located in chromosome 7 in humans, whereas the miR-29b2/miR-29c cluster is found on

chromosome 1. A study by (Pogribny et al. 2010) shows that miR-29c was downregulated in a mouse model of dietary nonalcoholic steatohepatitis. In contrast, in a rat model of common bile duct ligation and in liver biopsies from HCV patients, prominent downregulation of miR-29a and moderate downregulation of miR-29b were observed (Kwiecinski et al. 2009). We only observed a significant upregulation of miR-29a in both mouse and rat HSCs following GW4064 treatment, which is likely due to lack of functional FXR response element in the miR-29b2/miR-29c transcriptional unit. This is in contrast to downregulation of all members of miR-29 family in mouse models of liver fibrosis in the study by Roderburg et al., which may be due to the fact that the expression of both miRNA-29a/miR-29b1 and miR-29b2/miR-29c is negatively regulated by NF-κB and/or TGF-β signaling. This may reflect a complex mechanism in the regulation of miRNA expression.

In summary, we have shown for the first time that activation of FXR led to expression of miR-29a in HSCs, which may play an important role in FXR-mediated antifibrotic effect. Our study provides new insight into the mechanism by which FXR/FXR ligands control the expression of ECM in HSCs. It also suggests a miR-29a-based new therapy for the treatment of liver fibrosis.

3.0 MIR-29B INHIBITS COLLAGEN MATURATION IN HEPATIC STELLATE CELLS THROUGH DOWN-REGULATING THE EXPRESSION OF HSP47 AND LYSYL OXIDASE

3.1 BACKGROUND

Liver fibrosis is a wound-healing response characterized by an increased and altered deposition of extracellular matrix (ECM) components, particularly collagen type I and III (Olaso et al. 1998). In progressive fibrosis, the ECM accumulates gradually and disrupts the function of normal tissues, leading to liver dysfunction and ultimately end-stage organ failure. It has been demonstrated that liver fibrosis can be inhibited by suppressing the synthesis of ECM such as collagen.

The biosynthesis of collagen is a multi-step process. The regulation of this process involves many intracellular and extracellular factors such as HSP47 and LOX. HSP47 is an endoplasmic reticulum (ER)-resident molecular chaperone specific for collagen synthesis, and it plays an essential role in procollagen processing. After the synthesis of α-polypeptide chains, HSP47 assists in the correct folding and stabilization of triple-helical procollagen molecules (Nagata 1996). This process is crucial for subsequent secretion, cleavage and fibril formation of collagen (Ishida et al. 2006). The role of HSP47 on collagen maturation has been demonstrated

both in vitro and in vivo (Hosokawa et al. 1998, Nagai et al. 2000, Rocnik et al. 2002, Ishida et al. 2006).

Lysyl oxidase (LOX) is an extracellular enzyme that catalyzes the oxidative deamination of hydroxylysine and lysine residues in collagen and elastin. The resulting peptidyl aldehyde products spontaneously form covalent cross-links with unmodified lysine residues or with other peptidyl aldehyde residues. These cross-links are necessary for the formation of insoluble collagen and elastic fibers as well as mature functional extracellular matrix (Kagan et al. 1991). Abnormally increased lysyl oxidase enzyme activity can lead to excessive accumulation of insoluble collagen fibers and is directly associated with fibrotic diseases (Sommer et al. 1993, Kagan 2000).

MiRNAs are small non-coding RNAs that play a central role in gene regulation (He et al. 2004). MiRNAs repress the expression of target genes by interacting with their 3'-UTRs, causing mRNA degradation or translational repression. Accumulating data have demonstrated the critical role of miRNAs in fibrotic diseases. For example, miR-27a and 27b were shown to reverse the transactivation and inhibit the proliferation of HSCs by targeting the retinoid X receptor α . It was also shown that miR-15b and miR-16 can promote apoptosis by targeting Bcl-2 and the caspase signaling pathway (Guo et al. 2009). Lakner et al. showed that the expression of miR-19 was significantly down-regulated in activated HSCs (Lakner et al. 2012). Transfection of activated HSCs with miR-19b mimic negatively regulated TGF-β signaling components, as demonstrated by decreased TGF-β receptor II (TGF-βR II) and SMAD3 expression (Lakner et al. 2012). Among the reported miRNA species that were involved in liver fibrosis, miR-29 is emerging as a key suppressor of fibrotic changes (van Rooij et al. 2008, Roderburg et al. 2011). MiR-29 is significantly down-regulated during liver fibrosis in mice and

humans (Roderburg et al. 2011), and extensive interest has been focused on the mechanism by which miR-29b inhibits fibrosis. For example, Kwiecinski et al. have identified the profibrogenic growth factors PDGF-B, PDGF-C, IGF-I and VEGF-A as target genes of miR-29 (Kwiecinski et al. 2010). We and others recently showed that members of miR-29 family can down-regulate multiple genes coding for ECM proteins including collagens, fibrillins, and elastin (Luna et al. 2009, Li et al. 2011a, Sekiya et al. 2011). This regulation is achieved at post-transcriptional or translational level by targeting to their 3'-UTR.

In addition to altering the ECM expression at mRNA or translational level, microRNAs can also regulate the post-translational maturation of ECM by targeting relevant genes. For example, we have recently shown that miR-122 expression was significantly reduced in transactivated HSCs and in the livers of mice treated with CCl_4 (Li et al. 2013a). In addition, over-expression of miR-122 markedly attenuated the expression of prolyl 4-hydroxylase subunit alpha-1 (P4HA1), leading to decreased collagen maturation and ECM production (Li et al. 2012). However, a possible role of miR-29b in post-translational modifications of ECM remains unexplored. The purpose of this study was to determine whether miR-29b plays a role in ECM maturation through a post-translational mechanism. Our data showed that miR-29b was down-regulated during liver fibrosis and stellate cell activation, which was associated with an up-regulation of HSP47 and LOX expression. In contrast, a forced expression of miR-29b in cultured hepatic stellate cells inhibited the expression of HSP47 and LOX and led to defective regulation of ECM maturation. Our findings suggest that miR-29b is involved in the regulation of ECM maturation by targeting HSP47 and LOX.

3.2 METHODS

3.2.1 Ethics Statement

All procedures in the animals and cell culture studies were reviewed and approved by Institutional Animal Care and Use Committee of the University of Pittsburgh. The animals were housed and maintained in compliance with standards established in the Animal Welfare Act and the Guide for the Care and Use of Laboratory Animals (IACUC#: 1103914).

3.2.2 Animals and cell culture

Primary rat HSCs were isolated from retired male Sprague-Dawley rats (Charles River Laboratories. Wilmington, MA) (Thirunavukkarasu et al. 2005). HSCs were used 3 days after isolation as quiescent cells, and 7-14 days after isolation as activated cells. The purity of our primary rat HSCs was >95% (Thirunavukkarasu et al. 2005). The immortalized human hepatic stellate cell line LX-2 was kindly provided by Dr. Scott L. Friedman (Mount Sinai School of Medicine, New York, NY, USA) (Xu et al. 2005). Unless otherwise stated, all of the cells were maintained in Dulbecco's modified Eagle's medium (DMEM) containing 4.5 mg/mL glucose, supplemented with 10% fetal bovine serum, 100 U/mL penicillin, and 100 g/mL streptomycin at 37°C in 5% CO_2. All products for cell culture were purchased from Invitrogen (Carlsbad, CA). To establish an animal model of liver fibrosis, carbon tetrachloride (CCl_4; Merck; 0.6 mL/kg of body weight) was injected to CD-1 mice (Charles River Laboratories, Wilmington, MA) intraperitoneally twice a week for six weeks (Li et al. 2012). Common bile duct ligation

(CBDL) was performed on rats according to the literature (Roderburg et al. 2011). Sham-operated rats served as controls. HSCs were isolated 3 weeks following CBDL.

3.2.3 RNA isolation and qRT-PCR

Total RNA was extracted from cells and tissues with TRIzol reagent, and the first-strand cDNA was synthesized using SuperScript III reverse transcriptase according to manufacturer's instructions (Invitrogen, San Diego, CA). The qRT-PCR was performed using SYBR Green-based assays with the ABI Prism 7300 Real-Time PCR System (Applied Biosystems, Foster City, CA) (Li et al. 2011a). The analysis of miR-29b expression was performed according to our previous protocol (Li et al. 2012). Briefly, total RNA enriched with miRNAs was isolated from HSCs using the mirVana miRNA isolation kit (Applied Biosystems. Foster City, CA), followed by stem-loop real-time RT-PCR (SLqRT-PCR). The primers for qRT-PCR were obtained from MWG Biotech, and their sequences are listed in Appendix A.The relative transcript abundance was analyzed as previously reported (Li et al. 2011a) and calculated from three independent experiments.

3.2.4 Western Blot Analysis

Forty-eight h after transfection with 50 nM of control miRNA or miR-29b, the whole-cell lysates of LX-2 cells were prepared as described previously (Li et al. 2011a). Equal amounts of protein (30 μg) were separated by 10% SDS-polyacrylamide gel and transferred to PVDF membrane (Millipore, Billerica, MA). The membranes were blocked in phosphate-buffered saline with 0.05% Tween 20 (TPBS) containing 5% skim milk and incubated with specific

primary antibody (rabbit anti-HSP47 IgG, rabbit anti- β-actin IgG or goat-anti-LOX IgG, Santa Cruz Biotechnology) overnight, followed by incubation with secondary antibody (horseradish peroxidase-conjugated goat anti-rabbit IgG or horseradish peroxidase-conjugated donkey anti-goat IgG, Jackson ImmunoResearch Laboratories, West Grove, PA) for 1 h. ECL chemiluminescence kit (Amersham Biosciences, Piscataway, NJ) was used to detect the signals from HSP47 and β-actin, and the LOX signal was detected with the SuperSignal West Femto Chemiluminescent Substrate (Thermo Fisher Scientific)..

3.2.5 Plasmid Constructs

The wild-type 3'-UTR of HSP47 and LOX genes were PCR amplified from human genomic DNA using the primers listed in Appendix A. The mutant 3'-UTR of HSP47 without putative miR-29b-binding sequence was also amplified. To clone the mutant 3'-UTR of LOX without the putative miR-29b binding sites, two fragments of LOX 3'-UTR were amplified separately and joined by overlap extension PCR according to a published method (Ho et al. 1989). The PCR products of wild-type or mutant 3'-UTR for HSP47 were then cloned into the MluI-HindIII site downstream of the stop codon in the pMIR-REPORT Firefly Luciferase reporter vector (Ambion). The segments of wild-type or mutant 3'-UTR for LOX were cloned into the same vector at SacI-MluI site. The sequences of the generated constructs were confirmed by restriction digestion and sequencing.

3.2.6 Transfection and luciferase assays

LX-2 cells were grown in 96-well plates. Reporter plasmids and miRNAs (ABI, Applied Biosystems, Foster City, CA) were co-transfected into LX-2 cells using Lipofectamine2000 (Invitrogen, Carlsbad, CA) according to the manufacturer's instruction. To normalize the value of luciferase activity for transfection efficiency and cell viability after transfection, the pCMV-βgal plasmid was co-transfected (Umesono et al. 1991). Cells were washed and lysed 24h following transfection as described (He et al. 2006), and the luciferase activity and β-galactosidase activity were measured. Transfection experiments were repeated three times independently and in each case were done in triplicate. Data were presented as relative luciferase activity of control miRNA.

3.2.7 Electron Microscopy

For the TEM study, LX-2 cells were cultured in 10% fetal bovine serum /DMEM in the presence of ascorbic acid phosphate (136 μg/mL). The EM study was performed 3-5 days after the cell culture became confluent. Cultured cells were rinsed in PBS and fixed with cold 2.5% glutaraldehyde in 0.1 M PBS. The specimens were rinsed in PBS, post-fixed in 1% Osmium Tetroxide with 0.1% potassium ferricyanide, rinsed in PBS, dehydrated through a graded series of ethanol and embedded in Epon. Semi-thin (300 nm) sections were cut on a Reichart Ultracut, stained with 0.5% Toluidine Blue and examined under the light microscope. Ultrathin sections (65 nm) were stained with uranyl acetate and Reynold's lead citrate and examined on Jeol 1011 transmission electron microscope.

3.2.8 LOX Activity Assays

To measure the effect of miR-29b on extracellular LOX activity, LX-2 cells were transfected with control miRNA or miR-29b and cultured in complete medium until confluent at which time it was replaced by serum free, phenol red free DMEM. At 3 days post-confluence, the conditioned media were collected and concentrated using 10,000 molecular weight cut-off Amicon Ultra centrifugal filter units (Millipore) (Fogelgren et al. 2005). The LOX enzyme activity of concentrated media was measured using the Amplex Red fluorescence assay as previously described (Palamakumbura et al. 2002). Briefly, the samples were incubated with the reaction mixture at 37 °C for 1 h, which consisted of 50 mM sodium borate (pH 8.2), 1.2 M urea, 50 μM Amplex Red (Sigma-Aldrich), 0.1 units/mL horseradish peroxidase, and 10 mM 1,5-diaminopentane (cadaverine) substrate in the presence or absence of 500 μM β-Aminopropionitrile (BAPN, Acros Organics). After incubation, the fluorescence intensity of each sample was determined by a PerkinElmer LS 50B luminescence spectrometer (Waltham, MA) (λex = 560 nm; λem = 590 nm). The difference of fluorescent intensity value between the samples with or without BAPN was used to calculate the specific LOX activity. Data was normalized by total protein amount and expressed as the fold induction over control samples. All samples were assayed in triplicate.

3.2.9 Statistical Analysis

Unpaired Student's t-test was performed on data of qRT-PCR and luciferase assays. All data are reported as means ± standard deviations unless otherwise stated. $P < 0.05$ was considered statistically significant.

3.3 RESULTS

3.3.1 Expression level of HSP47 and LOX are upregulated in cellular and animal models of liver fibrosis, with down-regulation of miR-29b

We hypothesized that miR-29b is involved in the post-translational modification of ECM proteins in addition to its role in regulating ECM expression at mRNA and translational levels. Computational prediction by the algorithms Target scan and miRanda has identified HSP47 and LOX as potential target genes of miR-29. Therefore, we further hypothesized that miR-29b inhibits ECM maturation through targeting HSP47 and LOX. To test this hypothesis, we first examined the expression level of HSP47, LOX and miR-29b in the CCl_4-induced model of liver fibrosis. I.P. injection of CCl_4 to mice for 6 weeks resulted in significant upregulation of HSP47 and LOX mRNA in liver tissue (Figure 14A-B). Similarly, the protein expression of HSP47 and LOX in the liver of CCl_4 treated mice was significantly increased compared with vehicle-treated group (Figure 14C). This is consistent with the reported data that the expression of HSP47 (Masuda et al. 1994) and LOX (Furui et al. 1995) was markedly induced during the progression of CCl_4-induced liver fibrosis in rats. The expression of miR-29b in mice liver tissue was measured by SLqRT-PCR technique. The results showed that there was a significant decrease in the expression of miR-29b in the fibrotic liver (Figure 14D).

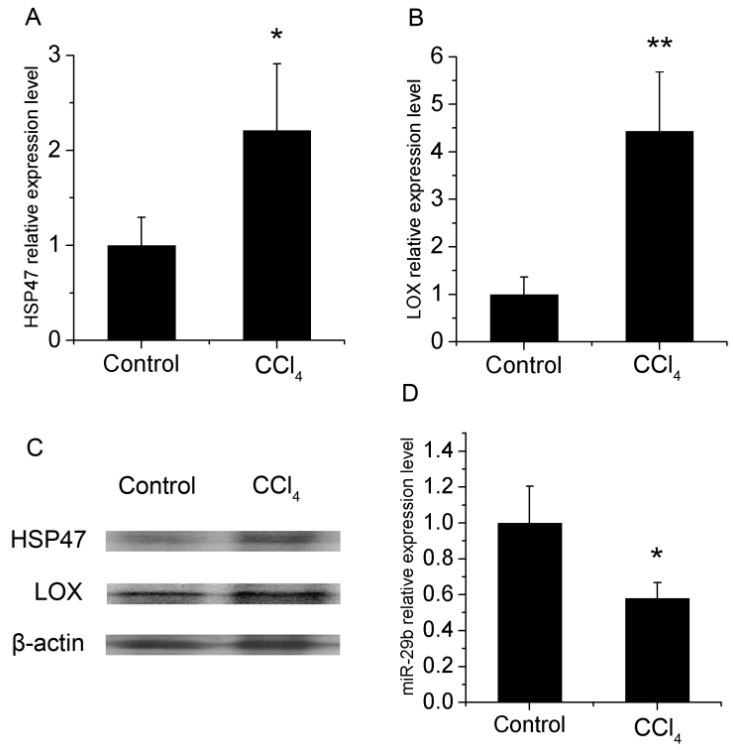

Figure 14 Altered expression of HSP47, LOX and miR-29b in mouse liver following CCl_4 treatment.

CD-1 mice were treated with corn oil or CCl4 for 6 weeks as described in the Materials and methods. Liver tissues were harvested and Quantitative PCR was conducted to detect the mRNA expression levels of HSP47 (A) and LOX (B). (C) Western blots were conducted to detect the protein expression levels of HSP47 and LOX. (D) Expression of miR-29b was decreased in the liver of mice treated with CCl4. *P < 0.05, **P < 0.01.

Since HSCs are the major source of ECM and become activated during liver fibrosis, we have also examined the gene expression in primary-cultured rat HSCs. Data showed that the expression of HSP47 and LOX in culture-activated HSCs was dramatically increased at both mRNA (Figure 15A-B) and protein levels (Figure 15C) compared with that in quiescent cells. The over-expression of HSP47 and LOX in activated HSCs was accompanied by the reduced expression of miR-29b (Figure 15D). In an independent model of liver fibrosis induced by bile

duct ligation, the in vivo activated HSCs isolated from bile duct ligated rats showed higher level of HSP47 and LOX expression than HSCs from normal rats (Figure 15E-F).

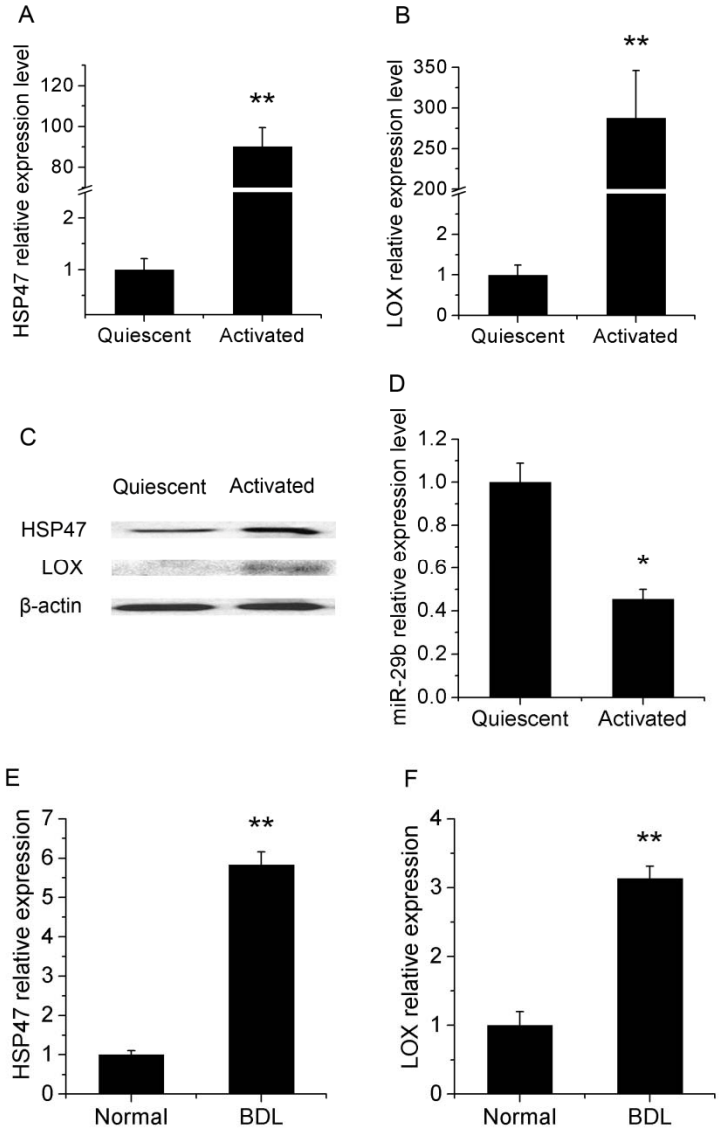

Figure 15 Altered expression of HSP47, LOX and miR-29b in rat HSCs during culture-induced activation. Quiescent and activated HSCs of rat were isolated and harvested as described in the Materials and methods. Quantitative PCR was conducted to detect the mRNA expression levels of HSP47 (A) and LOX (B). (C) Western blots were conducted to detect the protein expression levels of HSP47 and LOX. (D) Expression of miR-29b was decreased in the activated HSCs. Expression of HSP47 (E) and LOX (F) mRNA in HSCs was up-regulated at 3 weeks following CBDL-induced liver fibrosis of rats.*$P < 0.05$, **$P < 0.01$.

3.3.2 Transfection of LX-2 cells with miR-29b led to a significant inhibition of HSP47 and LOX expression

LX-2 is an immortalized human hepatic stellate cell line that exhibits typical features of primary HSCs such as over-expression of α-SMA and responsiveness to transforming growth factor-β (TGF-β) (Xu et al. 2005). TGF-β signaling is known to play an important role in stimulating stellate cell activation and ECM synthesis (Gressner et al. 1993, Gressner 1995). To define a role of TGF-β signaling in regulating the expression of HSP47, LOX, and miR-29b during HSC transactivation, the mRNA expression levels of these genes were examined in LX-2 cells with or without TGF-β1 treatment. Figure 16A-B showed that the expression of Col1A1 and Col3A1 was significantly up-regulated following TGF-β treatment, which was consistent with the known effect of TGF-β on collagen expression (Li et al. 2012). TGF-β-treatment also led to significant increases in the mRNA expression levels of HSP47 and LOX in LX-2 cells (Figure 16C-D). Again, these changes were associated with a decrease in the expression level of miR-29b (Figure 16E). These results strongly suggest a role of TGF-β signaling in regulating the expression of HSP47, LOX, and miR-29b during HSC transactivation.

3.3.3 miR-29b down-regulated gene expression by targeting the putative binding sequence on the 3'-UTRs of HSP47 and LOX

The above studies clearly show an inverse correlation between miR-29b and HSP47/LOX gene expression in both fibrotic liver and transactivated HSCs. To evaluate the contribution of decreased miR-29b expression to the increased expression of HSP47 and LOX

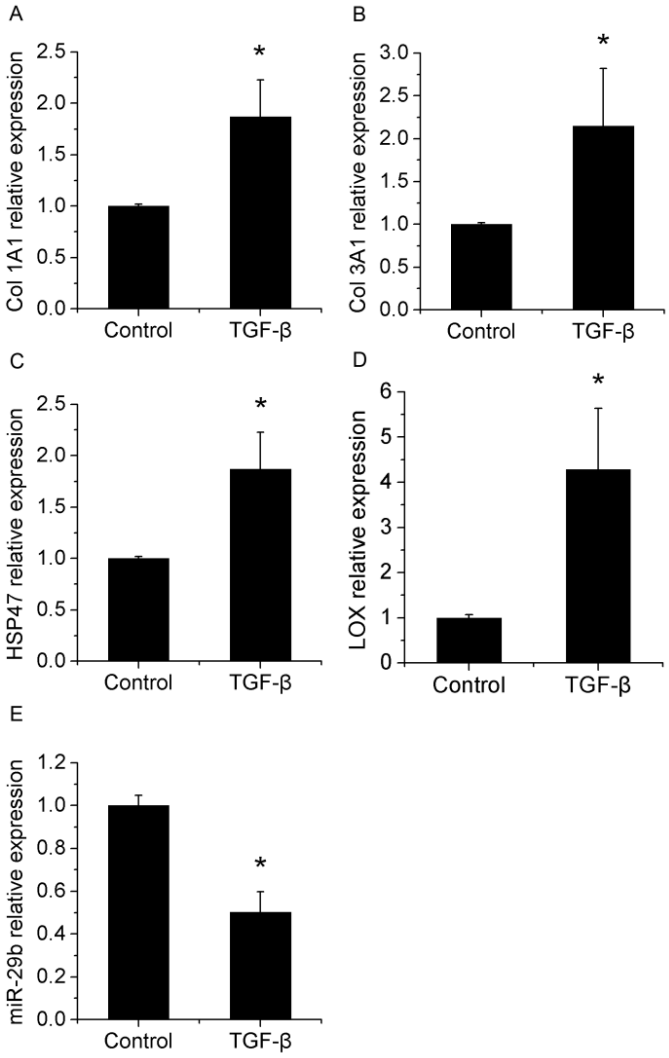

Figure 16 TGF-β treatment induced HSP47 and LOX mRNA expression and suppressed miR-29b expression in LX-2 cells.

LX-2 cells were treated with TGF-β (5ng/ml) as described in the Materials and methods and harvested at 24h after treatment. Quantitative PCR was conducted to detect the mRNA expression levels of Col1A1 (A), Col 3A1 (B), HSP47 (C) and LOX (D). (E) Expression of miR-29b was decreased in the activated HSCs. *P < 0.05.

during fibrotic changes, we investigated the effect of forced expression of miR-29b on the HSP47 and LOX expression level in LX-2 cells. LX-2 cells were transfected with miR-29b or control sequence and the mRNA expression of HSP47 and LOX was examined 24 h later by

real-time RT-PCR. The data showed that transfection of LX-2 cells with miR-29b led to a significant inhibition of HSP47 and LOX expression at both mRNA (Figure 17A-B) and protein (Figure 17C) levels.

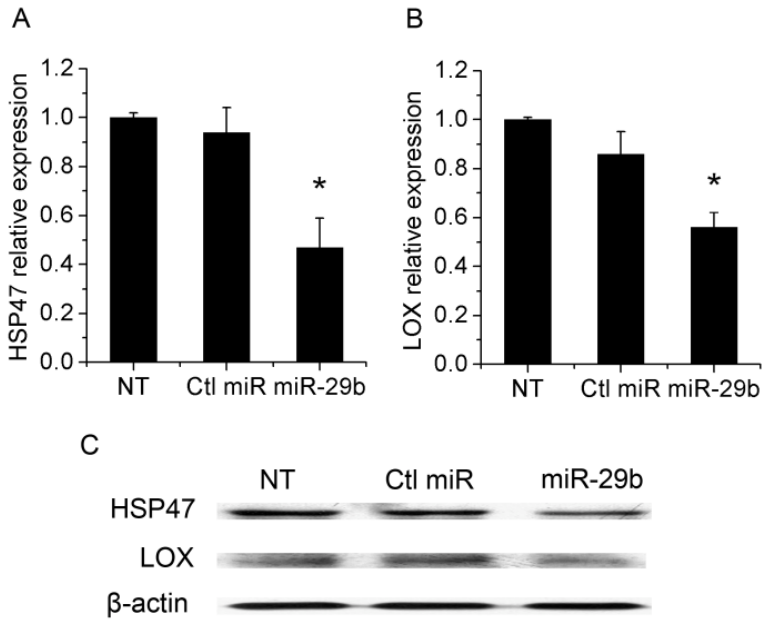

Figure 17 Transfected miR-29b decreased the expression of HSP47 and LOX and mRNA and protein levels. Cells were transfected with either non-specific control miRNA or miR-29b at a final concentration of 50 nM. The mRNA expression levels of HSP47 (A) and LOX (B) were analyzed by qRT-PCR at 24 h post-transfection. Data represent quantification of four independent experiments, *$p < 0.05$ (vs. control miRNA). (C) Western blots were conducted to detect the HSP47 and LOX expression at 48 h post-transfection.

To confirm whether HSP47 and LOX are direct targets of miR-29b, the 3'-UTR of HSP47 or LOX gene containing the putative target sites (wild-type HSP47 3'-UTR and wild-type LOX 3'-UTR, Figure 18A) was subcloned into a luciferase reporter vector. A control reporter plasmid was similarly constructed in which the putative target sites were deleted (mutant HSP47 3'-UTR and mutant LOX 3'-UTR, Figure 18A). Each plasmid construct was co-transfected with miR-29b or control miRNA into LX-2 cells, followed by measurement of

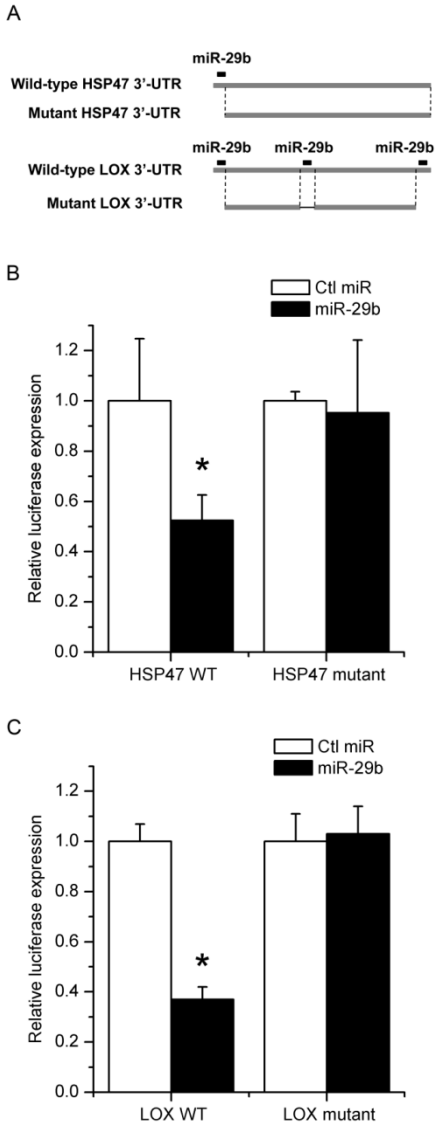

Figure 18 MiR-29b directly targets the 3'-UTR of HSP47 and LOX mRNAs.

(A) Scheme of wild-type and mutant 3'-UTRs of human HSP47 and LOX. Wild type 3'-UTRs include the putative binding sites highlighted. Deletion mutant eliminates the putative binding sites. (B) LX-2 cells were transfected with a luciferase construct with HSP47-3'-UTR in the presence of 50 nM miR-29b or non-specific control miRNA. Luciferase assay was performed 24 h post-transfection. Transient transfection of miR-29b in LX-2 cells decreased the luciferase activity of the wild-type HSP47-3'-UTR construct, whereas no change in the luciferase activity of mutant HSP47-3'-UTR construct was seen. (C) Same experiment with LOX 3'-UTR luciferase vectors as in (B), miR concentration=10nM. Luciferase activity was normalized against the control groups. Data shown in the panels represent means± (SD) of the fold increase over the control. N = 3. *P < 0.05 (vs. control miRNA).

luciferase activity. As shown in Figure 18B, miR-29b significantly inhibited the luciferase activity of the wild-type HSP47-3'-UTR construct. In contrast, such an inhibitory effect was essentially abolished when the putative miR-29b target sequence is deleted from the reporter construct (Figure 18B). Similar results were observed with the plasmid construct containing the 3'-UTR of LOX gene (Figure 18C). These data suggest that miR-29b down-regulated the expression of HSP47 and LOX via targeting the putative binding sequence on the respective 3'-UTR of HSP47 and LOX mRNA. Taken together, all of the data above suggest a causal effect of decreased miR-29b expression on the upregulation of HSP47 and LOX during fibrotic changes.

3.3.4 The functions of HSP47 and LOX in LX-2 cells were inhibited by transfection with miR-29b

To investigate the physiological significance of the inhibitory effect of miR-29b on LOX expression, we transfected LX-2 cells with miR-29b and examined its effect on LOX enzymatic activity. Since LOX is a secreted enzyme, the conditioned medium was collected after transfection to determine the enzyme activity of LOX in extracellular environment. Figure 19A shows that LOX activity was significantly decreased by miR-29b compared with control miRNA. As a positive control, the known LOX inhibitor BAPN also showed inhibition on LOX activity (Figure 19B).

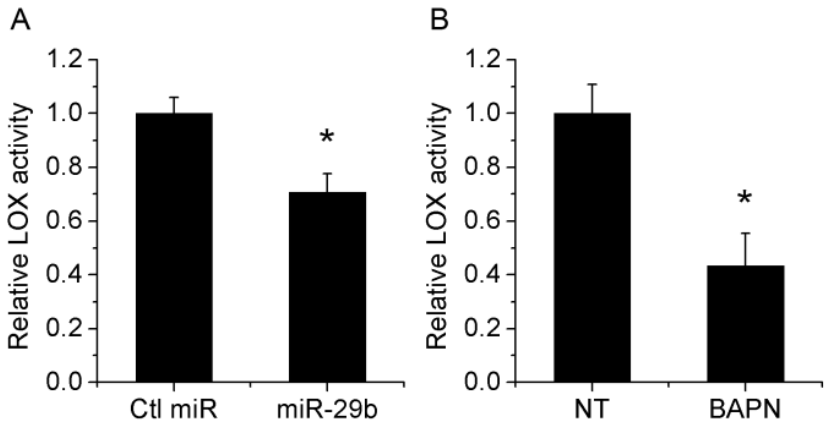

Figure 19 Extracellular LOX activity of LX-2 cells transfected with miR-29b.

(A) Extracellular LOX enzyme activity was significantly reduced in the 72 h supernatant of miR-29b transfected LX-2 cells than that of control miRNA transfected cells. (B) LOX activity in the conditioned media was significantly inhibited by 100μM BAPN. Data represent mean ± SD, n = 3. *P < 0.05.

After demonstrating the inhibitory effect of miR-29b on HSP47 and LOX expression, we further investigated the role of miR-29b in the post-translational maturation of ECM. LX-2 cells were transfected with miR-29b and the morphology of extracellular fibrils was examined by electron microscopy. The extracellular fibrils from control miRNA treated cells were organized as expected (Figure 20A-C). This is in contrast with those from miR-29b transfected cells, which were relatively thin and sparse, and frequently contained more branches (Figure 20D-F). This difference became more dramatic at day 5 post-confluence compared to day 3 and day 4. These observations are consistent with the reported data generated from HSP47-/- embryonic fibroblasts (Ishida et al, 2006) or BAPN-treated osteoblasts (Hong et al, 2004). These results suggest that miR-29b over-expression can lead to defects of extracellular fibrils, with the potential contribution from HSP47 and LOX inhibition.

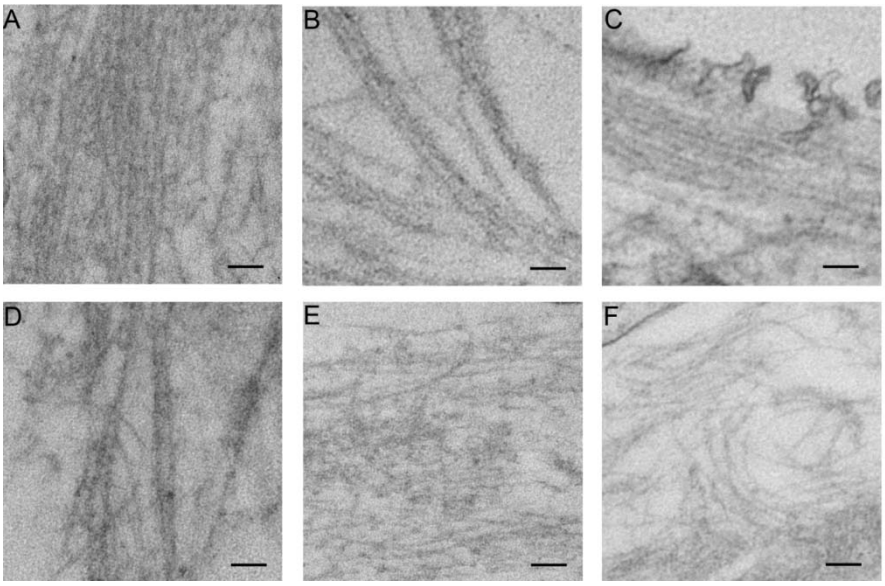

Figure 20 Effect of miR-29b on the morphology of extracellular fibrils secreted from LX-2 cells.

LX-2 cells were transfected with control miRNA (A-C) or miR-29b (D-F). The extracellular fibrils were observed by Transmission Electron Microscopy at 3 d (A and D), 4 d (B and E) and 5 d (C and F) after the cells became confluent. Bar, 100 nm.

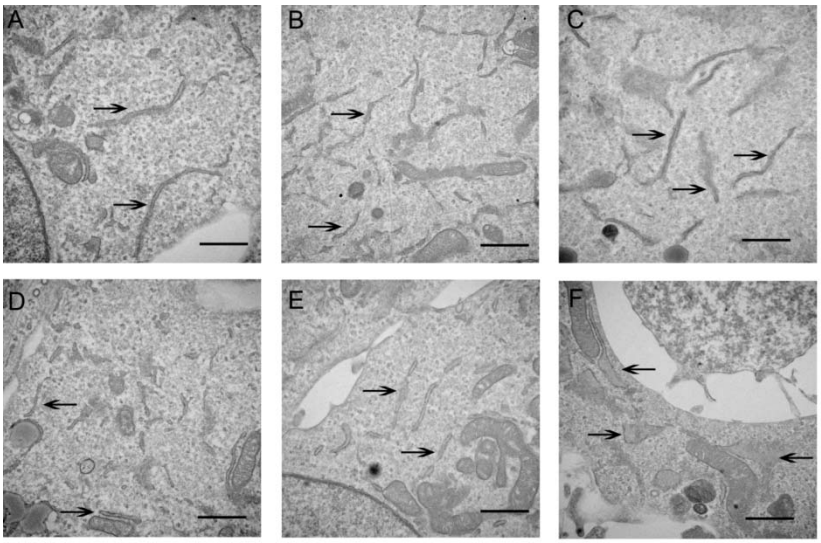

Figure 21 Dilation of the ER following miR-29b tranfection examined by transmission electron microscopy.

LX-2 cells were transfected with control miRNA (A-C) or miR-29b (D-F) and samples were harvested at 3 d (A and D), 4 d (B and E) and 5 d (C and F) post-confluence. Arrows indicate the ER. Bar, 1 μm.

Besides the change of ECM morphology, we also noticed dramatic ER dilation in miR-29b-treated LX-2 cells compared with control miRNA-treated cells (Figure 21A-F), and this difference was most dramatic at day 5 post-confluence (Figure 21C and 21F). This observation is in agreement with the notion that miR-29b can decrease HSP47 expression, leading to the accumulation of misfolded collagen in the ER lumen.

3.4 DISCUSSION

Various miRNAs have been reported to regulate the synthesis of ECM proteins. We and others have previously demonstrated that miR-29 significantly down-regulates expression of several ECM genes including collagen (Li et al. 2011a, Sekiya et al. 2011), fibronectin (Sekiya et al. 2011) and lamininγ1 (Sengupta et al. 2008). In addition, it has been reported that miR-17 (Shan et al. 2009) and miR-199 (Lee et al. 2009) down-regulate fibronectin expression. In addition, Col 1A2 and laminin γ1 have been validated as direct targets of let-7g (Ji et al. 2010) and miR-124 (Cao et al. 2007), respectively. In this study we reported a novel mechanism by which miR-29b inhibits the ECM synthesis at post-translational level. Specifically, we showed that miR-29b inhibited the post-translational maturation of ECM by targeting HSP47 and LOX.

Through bioinformatic analysis by Targetscan and miRanda, we identified putative miR-29b binding sites on the 3'-UTR of two genes, HSP47 and LOX, which are critically involved in the post-translational modification of ECM. Our data showed that both mRNA and protein expression of HSP47 and LOX in liver tissue was highly up-regulated in CCl_4-induced fibrosis, and their expression level in rat HSCs was also increased during cell transactivation in vitro and in vivo. The up-regulation of HSP47 and LOX was consistently associated with a dramatic

down-regulation of miR-29b expression in all studies, which strongly supports a correlation between miR-29b and those two genes. This inverse correlation was further confirmed in TGF-β treated LX-2 cells. Transfection of LX-2 cells with miR-29b led to reduced expression of HSP47 and LOX at both mRNA and protein levels. In addition, the predicted miR-29b targeting sites at the 3'-UTR of HSP47 and LOX were validated by luciferase reporter assay, indicating that HSP47 and LOX are direct targets of miR-29b. Furthermore, over-expression of miR-29b in LX-2 cells can lead to abnormal morphology of ECM fibrils according to TEM images, suggesting a significant role of miR-29b in post-translational maturation of ECM. Taken together, our data strongly support the role of miR-29b in inhibiting the ECM maturation via targeting HSP47 and LOX.

In view of the critical role of HSP47 and LOX in stabilizing collagen fibrils, both have been investigated as molecular targets in developing new therapies for the treatment of fibrotic diseases including liver fibrosis. HSP47 is a collagen-specific chaperone that is essential for the maturation of collagen, which is the dominant ECM constituent in the fibrotic tissue (Guo et al. 2004). The absence of HSP47 in collagen-producing cells can lead to several consequences. Firstly, HSP47 knockout can cause deficiency of collagen maturation and increase the susceptibility of collagen triple helices to protease digestion (Ishida et al. 2006). Secondly, HSP47-/- cells showed significantly reduced collagen secretion rate and highly accumulation of insoluble aggregate of collagen in the ER, which induced ER stress and apoptosis of collagen-producing cells through the up-regulation of CHOP (Marutani et al. 2004). Both accelerated collagen degradation and induction of apoptosis of ECM-producing cells help to inhibit the ECM accumulation. Thus, HSP47 inhibitors have been explored for the treatment of fibrotic diseases. Pirfenidone, a small-molecule drug with well-established anti-fibrotic efficacy,

significantly inhibited the TGF-β1-stimulated expression of HSP47 in lung fibroblasts (Nakayama et al. 2008) and A549 cells (Hisatomi et al. 2012). In addition, suppression of HSP47 by specific siRNA significantly reduced the accumulation of collagens and delayed the progression of fibrotic diseases in experimental animal models (Wang et al. 2008b, Xia et al. 2008). Another study has shown that vitamin A-modified liposomal formulation carrying siRNA against mRNA encoding rat gp46, a homolog of HSP47, decreased collagen deposition in fibrotic rat liver (Sato et al. 2008). Likewise, miR-29b-mediated down-regulation of HSP47 likely contributed to the production of sparse and branched extracellular fibrils by miR-29b-transfected cells (Figure 20D-F). We have further shown a dramatic dilation of the ER in miR-29b-treated LX-2 cells (Figure 21D-F), which is probably caused by accumulation of misfolded collagen aggregates in the ER. The dilation of ER in miR-29b over-expressing cells provides another functional evidence for the down-regulation of HSP47 by miR-29b in LX-2 cells.

The lysyl oxidase family consists of five members: lysyl oxidase (LOX) and lysyl oxidase-like 1–4 (LOXL1-LOXL4). All members share conserved C-terminal catalytic domains that contribute to the enzyme activity in catalyzing the cross-linking of collagen and elastin molecules (Kagan et al. 2011). The protein expression and activity LOX and LOXL were shown to be up-regulated in various fibrotic diseases including liver fibrosis (Siegel et al. 1978, Kim et al. 1999) and atrial fibrillation (Adam et al. 2011). β-Aminopropionitrile (BAPN) is a potent irreversible inhibitor of LOX that specifically inhibits all LOX isoenzymes except LOXL2 (Payne et al. 2007). BAPN has been studied for its antifibrotic efficacy in animal models of liver fibrosis (Kagan 2000) and lung fibrosis (Riley et al. 1982). Treatment of rats with BAPN inhibited the early increases in liver stiffness, which is important for initiating the early stages of fibrosis (Georges et al. 2007). There was also a significant decrease in the α-SMA positive

area in the liver section of CCl_4/BAPN treated rats compared with the CCl_4 group (Georges et al. 2007). Interestingly, LOX inhibition by BAPN can also reduce the mRNA expression of elastin (Jackson et al. 1991). Our observations further validate miR-29b as an antifibrotic therapeutics through inhibition of HSP47 and LOX.

A unique feature of miRNA-mediated gene regulation is that individual miRNA can regulate hundreds of genes at the same time (Satoh et al. 2011). For example, SPARC (Zhu et al. 2012), BMP-1 (Luna et al. 2009) and fibronectin (Kadler et al. 2008) have been reported as target genes of miR-29b, and those molecules may also contribute to the altered fibril formation besides HSP47 and LOX. This property of miRNAs allows them to coordinate complex programs of gene expression to achieve similar consequences. Recently, Chou et al. (Chou et al. 2013) reported that miR-29b can inhibit tumor metastasis by targeting LOX, LOXL2 and LOXL4 in breast cancer cells. This observation indicates the implication of miR-29b and LOX in the regulation of tumor microenvironment besides ECM synthesis. More studies are needed to better understand the regulation of each factor by miR-29 and their respective contribution to the altered ECM biosynthesis under various pathological conditions. Nevertheless, our observations strongly support a role of miR-29b in the regulation of ECM maturation during liver fibrosis.

In conclusion, we have shown for the first time that miR-29b plays a role in collagen maturation. These data, together with other published works, suggest complex mechanisms by which miR-29 regulates ECM biosynthesis at multiple steps. Our data further indicates that miR-29 may become a promising therapeutic for the treatment of liver fibrosis.

4.0 FMOC-CONJUGATED PEG-VITAMIN E2 MICELLES FOR TUMOR-TARGETED DELIVERY OF PACLITAXEL: ENHANCED DRUG-CARRIER INTERACTION AND LOADING CAPACITY

4.1 BACKGROUND

Paclitaxel (PTX) is a potent anticancer agent acting through the stabilization of microtubules (Horwitz 1994). However, the clinical benefit of PTX is limited by its poor water solubility. The widely-used clinical formulation Taxol® contains alcohol and Cremophor EL which can cause irritation and hyperactivity reactions (Soga et al. 2005). Therefore, substantial efforts have been made to develop alternative formulations to improve the solubility of PTX. Polymeric micelles have attracted significant attention due to their unique advantages for the intravenous delivery of paclitaxel and other hydrophobic drugs. The small size (10-100nm) of micelles and hydrophilic corona shells of PEG are critical for the long blood circulation time and effective passive targeting to tumor tissues through enhanced permeability and retention (EPR) effect (Gao et al. 2002), leading to enhanced antitumor efficacy and decreased toxicity. Several micelle formulations of PTX have been developed and hold great promise for clinical application, such as NK105 (PTX-loaded polyethylene glycol-(L-aspartic acid) micelles) (Kato et al. 2012) and Genexol-PM (a PTX incorporated PEG-PLA micelle system) (Kim et al. 2007).

D-alpha-tocopheryl polyethylene glycol (PEG)-1000 succinate (TPGS) is a PEG derivative of Vitamin E that has been used as an excipient in various drug formulations (Yu et al. 1999, Win et al. 2006, Cao et al. 2008, Muthu et al. 2011). TPGS has intrinsic P-gp inhibitory effect which helps to overcome multidrug resistance (Dintaman et al. 1999, Collnot et al. 2010). TPGS is self-assembled into micelles in aqueous solution, however, the high critical micelle concentration (CMC) decreases the stability of micelles in physiological environment (Mi et al. 2011). By increasing the PEG length and including one additional VE chain, the PEG_{2K}-VE_2 micelles achieved lower CMC value, higher loading capacity for doxorubicin and enhanced anticancer effect compared with PEG_{2K}-VE and traditional TPGS (Wang et al. 2012a). We recently synthesized and compared four PEG-Vitamin E conjugates that differ in PEG molecular weight (2K vs. 5K) and the number of Vitamin E molecules (1 vs. 2) (Lu et al. 2013a). PEG_{5K}-Vitamin E_2 (PEG-VE_2) was shown to be the most stable and effective micellar formulation of PTX. The tumor growth inhibitory effect of PTX-loaded PEG_{5K}-VE_2 was significantly improved in comparison to Taxol formulation or other three PTX micellar formulations in vivo (Lu et al. 2013a). Nevertheless, the drug loading capacity of PTX-loaded PEG_{5K}-VE_2 micelles was still inadequate, which warranted further studies.

We have recently shown that incorporation of a drug-interactive domain into a lipid surfactant can improve both drug-loading capacity and formulation stability. This concept was experimentally tested when we were formulating JP4-039, a mitochondria-targeted antioxidant. We have synthesized a series of PEG-lipopeptides that have a PEG hydrophilic headgroup, one or several oleoyl chains, and amino acids derivatized with various functional motifs at the interfacial region. Among several functional groups tested, 9-Fluorenylmethoxycarbony (α-Fmoc) was identified to be the most effective drug-interactive motif that not only enhances the

JP4-039 loading capacity but also improves the stability of JP4-039-loaded emulsion and micellar formulations (Gao et al. 2013). The improved drug/carrier interaction can be attributed to the hydrophobic/hydrophobic interaction, hydrogen bonding, and π–π stacking between the Fmoc-containing carrier and JP4-039 (Gao et al. 2013).

We hypothesize that inclusion of Fmoc moiety shall similarly improve the drug loading capacity of PEG_{5K}-VE_2 micelles for PTX. In the current work, we synthesized a novel amphiphilic polymer, PEG_{5K}-(Fmoc)-VE_2 (PEG-FVE_2) by introducing an Fmoc motif into PEG_{5K}-VE_2 conjugate. To evaluate the ability of PEG-FVE_2 micelles for loading PTX, the drug loading capacity of those micelles was investigated. The interaction between Fmoc moiety and PTX molecule was analyzed by measuring the change of Fmoc fluorescence intensity with different drug: carrier ratios. Cytotoxicity of blank micelles and PTX-loaded micelles was studied against free PTX using various tumor cell lines. Finally, the therapeutic efficacy and toxicity of PTX-loaded micelles were investigated using a syngeneic mouse model of breast cancer (4T1.2).

4.2 METHODS

4.2.1 Materials

PTX (98%) was purchased from AK Scientific Inc. (CA, USA). Dulbecco's phosphate buffered saline (DPBS) was purchased from Lonza (MD, USA). Methoxy-PEG5,000-OH, dimethyl sulfoxide (DMSO), 3-(4,5-dimethylthiazol-2-yl)-2,5- diphenyl tetrazolium bromide (MTT), Triton X-100, Dulbecco's Modified Eagle's Medium (DMEM), succinate anhydride, Boc-lys-

(Boc)-OH and Fmoc-lys-(Boc)-OH were all purchased from Sigma-Aldrich (MO, USA). Fetal bovine serum (FBS) and penicillin-streptomycin solution were from Invitrogen (NY, USA). D-alpha-tocopheryl was purchased from Tokyo Chemical Industry (OR, USA). N,N'-Dicyclohexylcarbodiimide (DCC) was purchased from Alfa Aesar (MA, USA). 4-Dimethylaminopyridine (DMAP) was purchased from Calbiochem-Novabiochem Corporation (CA, USA). All solvents used in this study were HPLC grade.

4.2.2 Synthesis of PEG_{5K}-Fmoc-VE_2 (PEG-FVE_2)

PEG-FVE_2 was synthesized via solution phase condensation reactions from MeO-PEG-OH with a molecular weight of 5,000 Da. Fmoc-lys-(Boc)-OH (4 eq.) was coupled onto the terminal -OH of PEG using DCC (4 eq.) and DMAP (0.2 eq.) as coupling reagents in DCM for overnight. Fmoc-lys-(Boc) PEG ester was precipitated and washed three times with cold ethanol and ether, respectively. Then, Boc groups were removed by the treatment with 50% trifluoroacetic acid in DCM, and the Fmoc-lysyl PEG ester was precipitated and washed three times with cold ethanol and ether, respectively. Boc-lys-(Boc)-OH (2 eq.) was coupled onto the terminal -NH_2 of Fmoc-lysyl PEG ester using DCC (2 eq.) and DMAP (0.1 eq.) as coupling reagents in DCM for overnight. The di-Boc PEG ester was precipitated and washed three times with cold ethanol and ether, respectively. Then, Boc groups were removed by the treatment with 50% trifluoroacetic acid in DCM, and the di-NH_2 PEG ester was precipitated and washed three times with cold ethanol and ether, respectively. The resulting white powder precipitate was dried under vacuum. Vitamin E succinate (4 eq.) was coupled to the deprotected amino groups of lysine with the assistance of DCC (4 eq.) and DMAP (0.2 eq.). The resulting PEG-FVE_2 was precipitated and

washed three times with cold ethanol and ether, respectively. The final product was subsequently dialyzed against water and lyophilized to yield white powder.

4.2.3 Preparation and characterization of PEG-FVE_2 micelles

Drug-free or PTX-loaded PEG-FVE_2 micelles were prepared according to published procedures (Lu et al. 2013a). Briefly, PTX solution (10 mM in chloroform) was mixed with PEG-FVE_2 (10 mM in chloroform) at various molar ratios. The chloroform was removed by nitrogen flow and a thin dry film of drug/carrier mixture was formed. High vacuum was then applied to remove any traces of remaining solvent. DPBS was added into each vial to hydrate the film. The samples were then probe-sonicated for 2 min at 3 watts. The blank micelles were similarly prepared except that PTX was not added.

The size of micelles was measured by dynamic light scattering (DLS) method using a Malvern Zetasizer (Nano ZS; Malvern instruments Ltd, Worcestershire, UK). The PTX concentration was kept at 1 mg/mL for DLS measurements. To observe the morphology of PEG-FVE_2 micelles, the aqueous micelle formulation was deposited onto copper grids with Formvar and stained with 1% uranyl acetate. Imaging was performed at room temperature using transmission electron microscopy (TEM) (JEM-1011, JEOL, Japan) (Lu et al. 2013a). To measure the PTX loading efficiency, unincorporated free PTX was removed by filtering through a syringe filter with pore size of 0.22 μm (Lu et al. 2013b). The amount of PTX loaded into micelles was analyzed by HPLC according to a published method (Lu et al. 2013b). The drug loading capacity (DLC) and drug loading efficiency (DLE) were calculated according to the following formula (Lu et al. 2013b):

DLC (%) = [weight of drug used/(weight of polymer + drug used)] ×100%

DLE (%) = (weight of loaded drug/weight of input drug) ×100%.

4.2.4 CMC measurement

The CMC of PEG-FVE_2 was determined by employing pyrene as a fluorescence probe as described previously (Lu et al. 2013b). Briefly, aliquots of 50 μL pyrene solution (4.8×10^{-6} M) were mixed with various amount of PEG-FVE_2 in chloroform. The chloroform was then removed by nitrogen flow and high vacuum to form a thin film in the vials. Each sample was hydrated with 400 μL DPBS to give a final pyrene concentration of 6×10^{-7} M with PEG-FVE_2 concentrations ranging from 6×10^{-5} to 0.25 mg/mL. The samples were kept shaking at 37 ℃ for 24 h to reach equilibrium, followed by fluorescence measurement at the wavelength of em/ex= 334 nm/390 nm using Synergy H1 Hybrid Multi-Mode Microplate Reader (Winooski, VT). The fluorescence intensity was plotted against PEG-FVE_2 concentration. The CMC was determined from the threshold concentration, where the fluorescence intensity begins to increase dramatically.

4.2.5 Fluorescence measurement of blank and PTX-loaded micelles

Micelle formulations with or without PTX were prepared in 500 μL of water as described (Zhang et al. 2014). The fluorescence intensity was measured with a Synergy H1 Hybrid reader (BioTek). The emission spectra were recorded ranging from 300-400 nm with a fixed excitation at 270 nm.

4.2.6 Hemolytic effect of micelles

Rat blood was collected via cardiac puncture with heparin as the anticoagulant. The blood sample was centrifuged at 1500 rpm for 10 min at 4 ℃ to collect the red blood cells (RBCs). The RBCs were washed with 30 mL ice-cold DPBS for three times and diluted to 2% w/v with ice-cold DPBS. One mL of diluted RBC suspension was mixed with blank PEG-VE_2 or PEG-FVE_2 micelles to obtain final polymer concentrations of 0.2 or 1.0 mg/mL. The mixture was incubated at 37 ℃ with constant shaking for 4 h and then centrifuged at 1500 rpm for 10 min at 4 ℃. One hundred μL of supernatant from each sample was transferred into a 96-well plate. The absorbance at 540 nm was measured using a PerkinElmer LS 50B luminescence spectrometer (Waltham, MA) at the wavelength of 540 nm to determine the release of hemoglobin from RBCs. Triton X-100 (2%) and DPBS were also incubated with RBCs as positive and negative controls, respectively. The percent of hemoglobin release was calculated as $(OD_{sample}-OD_{negative\ control})/(OD_{positive\ control}-OD_{negative\ control}) \times 100\%$ (Lu et al. 2013b).

4.2.7 Cell culture

Huh-7 is a human hepatocellular carcinoma cell line and Hepa 1-6 is a mouse hepatoma cell line. 4T1.2 is a mouse metastatic breast cancer cell line. MCF-7 is a human breast cancer cell line. All cell lines were cultured in DMEM containing 10% FBS and 1% penicillin-streptomycin at 37 ℃ in a humidified incubator with 5% CO_2.

4.2.8 In vitro cytotoxicity study

The PTX-loaded PEG-FVE_2 micelles were examined for their cytotoxicity against four cancer cell lines using PTX-loaded PEG-VE_2 micelles, Taxol® formulation and PTX dissolved in DMSO as control groups. The 4T1.2 cells were seeded in 96-well plates at a density of 1000 cells per well. After incubation for 24 h, the cells were treated with various formulations at the indicated PTX concentrations for 72 h, followed by MTT assay as described previously (Lu et al. 2013b). Briefly, 20 μL of 3-(4,5-dimethylthiazol-2-yl)-2,5-diphenyltetrazoliumbromide (MTT) in DPBS (5 mg/mL) was added to each well and the cells were further incubated for 4 h. The medium was then removed and 150 μL DMSO was added into each well to solubilize the MTT formazan. The absorbance at 570 nm was detected by PerkinElmer LS 50B luminescence spectrometer (Waltham, MA). Data were shown as the percentages of cell viability calculated from triplicate wells using the formula: $[(OD_{treat} - OD_{blank})/(OD_{untreat} - OD_{blank}) \times 100\%]$. The cytotoxicity with Huh-7, Hepa 1-6 and MCF-7 cells was similarly performed except that the cells were seeded at a density of 5000 cells per well.

4.2.9 Animals

Female BALB/c mice, 10-12 weeks and male Sprague-Dawley rats were purchased from Charles River Laboratories (Wilmington, MA). All animals were housed under pathogen-free conditions according to AAALAC guidelines. All animal-related experiments were performed in full compliance with institutional guidelines and approved by the Animal Use and Care Administrative Advisory Committee at the University of Pittsburgh.

4.2.10 In vivo anti-tumor therapeutic study

A syngeneic murine breast cancer model was used to evaluate the therapeutic efficacy of PTX-loaded PEG-FVE_2 micelles. 2 x 10^5 4T1.2 cells in 200 μL PBS were inoculated s.c. at the right flank of female BALB/c mice. Treatments were initiated when tumors in the mice reached a volume around 50 mm^3 and this day was designated as day 0. On day 0, mice were randomly divided into five groups (n=5) and treated with tail vein injection of saline (control), blank PEG-FVE_2 micelles, PTX-loaded PEG-VE_2 micelles (PEG-VE_2 : PTX=1:5, mol : mol), PTX-loaded PEG-FVE_2 micelles (PEG-FVE_2 : PTX=1:5, mol : mol) and Taxol® (all at 10mg PTX/kg). Blank PEG-FVE_2 micelles were given at the equivalent dosage of the carrier in the group of PTX-loaded micelles. The treatment was performed three times a week for 2 weeks. Tumor size was measured with digital caliper three times a week. Tumor volume was calculated by the formula: $(L \times W^2)/2$, where L is the longest and W is the shortest in tumor diameters (mm). Mice were sacrificed at the end of experiment. To compare between groups, relative tumor volume (RTV) was calculated at each measurement time point (where RTV equals the tumor volume at a given time point divided by the tumor volume prior to the first treatment). Mice were euthanized when tumor volume reached 2000 mm^3. To monitor potential toxicity, the body weight of each mouse was measured three times a week. In addition, serum levels of aspartate aminotransferase (AST) and alanine aminotransferase (ALT) were examined at the completion of the study.

4.2.11 Statistical analysis

Statistical analysis was performed by Student's t-test for two groups, and one-way ANOVA for multiple groups, followed by Newman-Keuls test if $P < 0.05$. All results were reported as the mean ± standard deviation (SD) unless otherwise indicated. A value of $P < 0.05$ was considered statistically significant.

4.3 RESULTS

4.3.1 Synthesis and biophysical characterization of PEG-FVE$_2$

PEG-FVE$_2$ polymer was synthesized by conjugating PEG$_{5K}$ with Vitamin E succinate using dendritic oligo-lysine as the scaffold. Fmoc-lys-(Boc) and Boc-lys-(Boc) were sequentially linked to PEG$_{5K}$ by condensation reaction, followed by conjugation with succinate VE. The synthetic scheme is shown in Figure 22. The structure of PEG-FVE$_2$ was confirmed by ^{1}H NMR (Figure 23A) and MALDI-TOF (Figure 23B). In Figure 23A, the peaks between 7.2 ppm and 8.5 ppm were assigned to the Fmoc group. The peak at 3.3 ppm corresponded to the –OCH$_3$ on the end of mPEG, the intense peaks at 3.5 ppm could be assigned to the methane protons of the polyethylene glycol. The proton peaks below 3.0 ppm were assigned to the Vitamin E succinate. MALDI-TOF indicated that the molecular weight of PEG-FVE$_2$ was around 6500 (Figure 23B), which is in agreement with the calculated molecular weight of 6502.

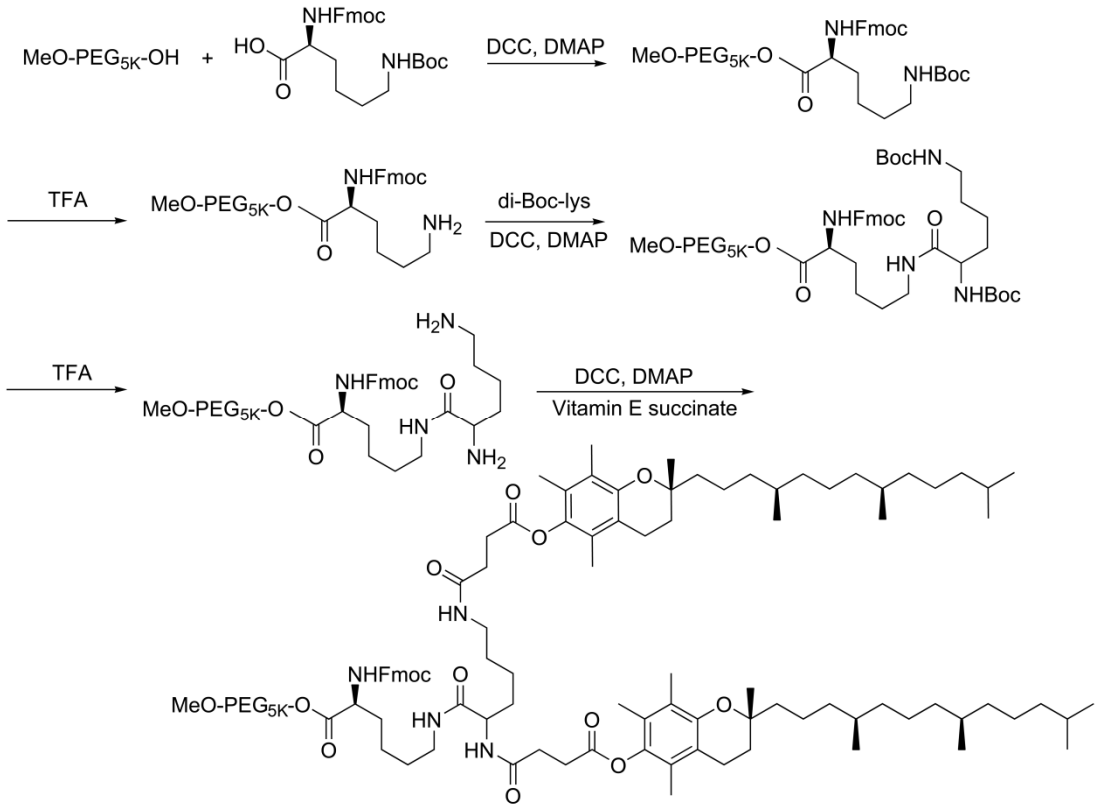

Figure 22 Synthesis scheme of PEG-FVE$_2$ conjugate.

The sizes of PTX-loaded PEG-FVE$_2$ micelles at different carrier: drug molar ratios were determined by DLS analysis. The sizes of blank and drug-loaded micelles were both around 60 nm (Table 2). PTX could be loaded into PEG-FVE$_2$ micelles at a carrier: drug molar ratio as low as 0.5:1. This is in contrast to PEG-VE$_2$ micelles for which a minimal carrier: drug molar ratio of 2.5:1 was required to solubilize PTX (Lu et al. 2013a). In addition, the drug loading efficiency as determined by HPLC was also improved by increasing the carrier: drug ratios. More than 95% of the input PTX was incorporated into the micelles at a carrier: drug molar ratio of 1:1 and above (Table 2).

The morphology of PEG-FVE$_2$ micelles was examined by TEM (Figure 24A-C). In aqueous solution, PEG-FVE$_2$ self-assembled and formed a mixture of worm-like and spherical

structures in the absence of PTX (Figure 24A). Similar structures were observed for PTX-loaded PEG-FVE$_2$ micelles at various carrier: drug ratios (Figure 24B-C). This observation was in contrast to the PEG-VE$_2$ without Fmoc moiety which formed uniform spherical micelles (Figure 24D).

A

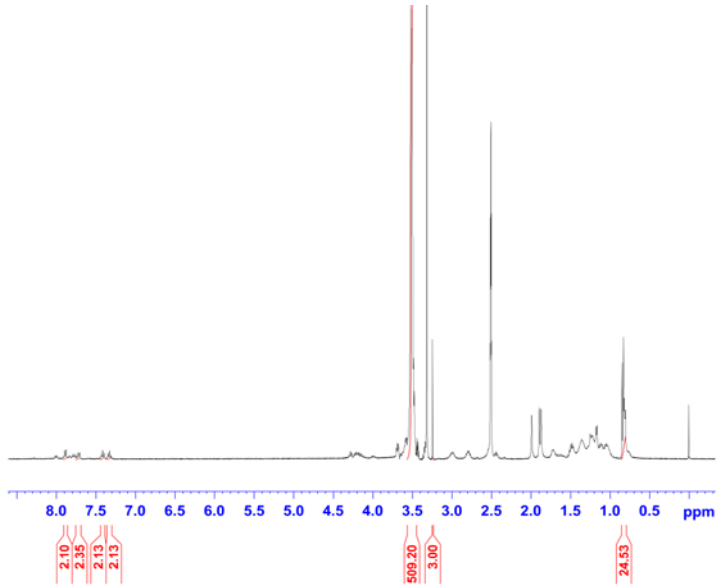

B

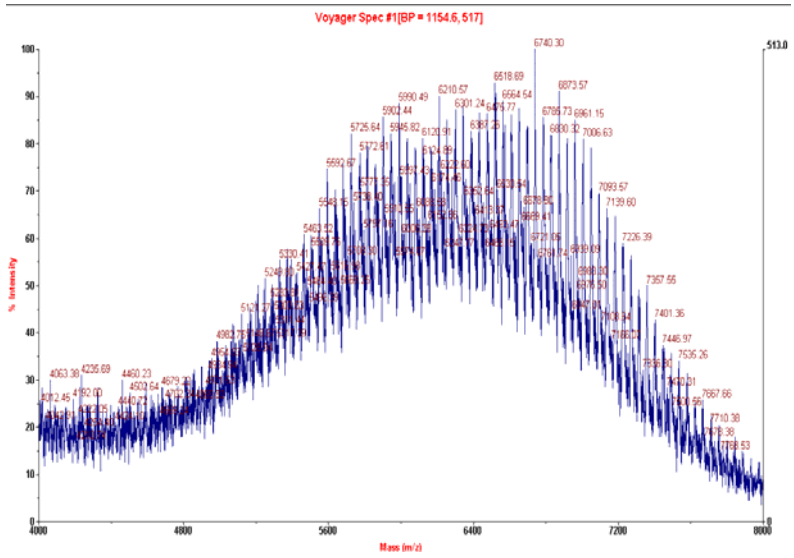

Figure 23 ^{1}H-NMR (A) in DMSO and Mass spectrum (B) of PEG-FVE$_2$

Table 2 Characteristics of blank and PTX-loaded PEG-FVE$_2$ micelles.

micelle	[a]molar ratio	[b]Size (nm)	[c]PDI	[d]DLC (%)	[e]DLE (%)
PEG-FVE$_2$	-	60.12±2.99	0.208	-	-
PEG-FVE$_2$:PTX	0.5:1	55.32±1.84	0.256	20.8	87.0
	1:1	61.60±3.55	0.213	11.6	96.0
	2.5:1	68.64±2.90	0.224	5.0	95.4
	5:1	70.06±6.84	0.226	2.6	98.9

[a]The PTX concentration was 1mg/mL in all the drug-loaded samples above.
[b]Data represents the mean ± standard deviation (n=3)
[c]PDI: Polydispersity index.
[d]DLC: drug loading capacity
[e]DLE: drug loading efficiency

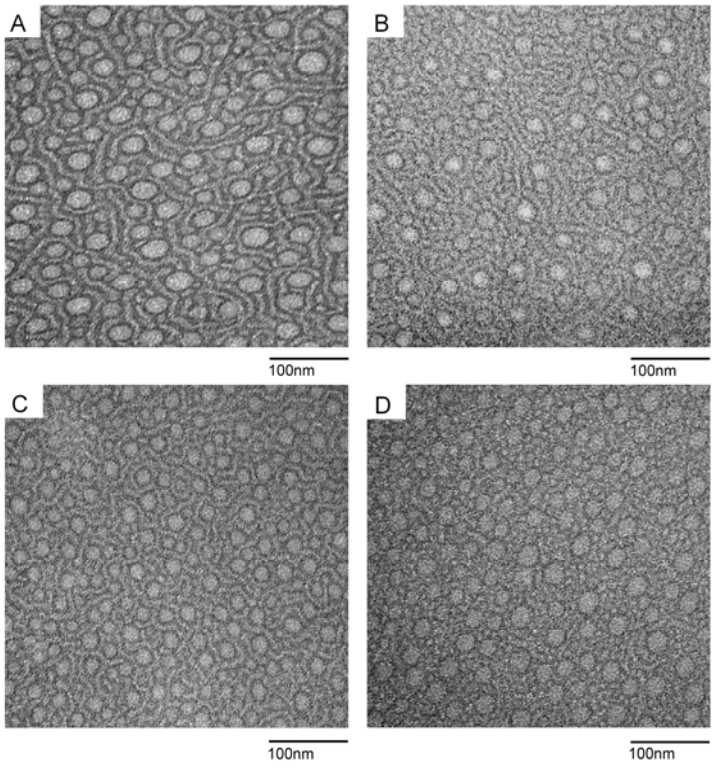

Figure 24 Typical TEM images of blank PEG-FVE$_2$ micelles (A), PTX-loaded PEG-FVE$_2$ micelles (B-C) and blank PEG-VE$_2$ micelles (D).

The PEG-FVE$_2$: PTX molar ratio was 1 : 1 (B) or 3 : 1(C). PTX concentration was kept at 1mg/mL. Bar = 100 nm.

The CMC of PEG-FVE_2 polymer was measured with pyrene as the fluorescent probe. A series of pyrene-loaded PEG-FVE_2 micelles were prepared with a fixed concentration of pyrene and different concentrations of polymer. When the concentration of a polymer reaches its CMC, the micellization is marked by an abrupt increase in fluorescence intensity of pyrene at the wavelength of 390 nm (Sezgin et al. 2007). Based on this principle, the fluorescence intensity was recorded and plotted against the logarithmic concentration of the PEG-FVE_2 polymer, and the CMC value was determined. Figure 25 shows that the CMC of PEG-FVE_2 micelles was 4 μg /ml, which was slightly higher than that of PEG-VE_2 (1.7 μg/ml) (Lu et al. 2013a), but still significantly lower than that of TPGS (0.2 mg/ml)(Mi et al. 2011).

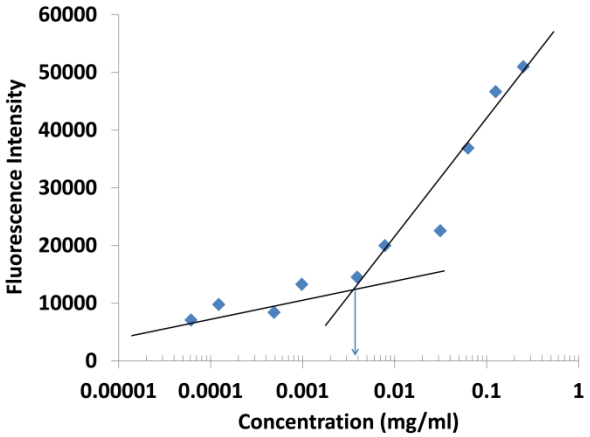

Figure 25 CMC determination of the PEG-FVE_2 micelles using pyrene as a hydrophobic fluorescence probe. The fluorescence intensity of pyrene was measured (Ex/Em = 334nm/ 390nm) and plotted against the logarithmic concentration of PEG-FVE2 micelles. The concentration of pyrene was kept at 6×10^{-7} mol/L. Values reported are the means ± SD, n=3.

4.3.2 Fluorescence quenching assay

The improved PTX loading capacity of PEG-FVE_2 over PEG-VE_2 suggests a role of Fmoc/PTX interaction in the formation of PTX-loaded PEG-FVE_2 micelles. To test this

hypothesis, we studied the Fmoc/PTX interaction via fluorescence quenching assay. We chose an excitation wavelength of 270 nm and examined the emission spectra of PEG-FVE_2, PEG-VE_2 and free PTX ranging from 300 nm to 400 nm. As shown in Figure 26A, there is a distinct fluorescence peak at the emission wavelength of 305 nm for PEG-FVE_2. This fluorescence appeared to be highly specific for Fmoc because minimal fluorescence intensity was detected for either PEG-VE_2 or free PTX (Figure 26A). We then prepared several PTX-loaded PEG-FVE_2 micelles with constant PEG-FVE_2 concentration but varying amounts of PTX, and similarly measured the fluorescence intensity. As shown in Figure 26B, the fluorescence intensity of Fmoc group at 305 nm was dramatically reduced with increased amount of PTX. We also conducted a similar experiment with several different mixed micelles that had a fixed concentration of PTX (0 or 0.1mg/mL) but varying amounts of PEG-FVE_2. As shown in Figure 26C, at each concentration of PEG-FVE_2, the Fmoc fluorescence intensity at 305 nm was dramatically reduced in the presence of PTX. Figure 26D summarizes the changes of fluorescence intensity at 305 nm from the above fluorescence studies. It is apparent that the carrier: drug molar ratio affected the degree of reduction in fluorescence, which became more dramatic with increased amount of PTX.

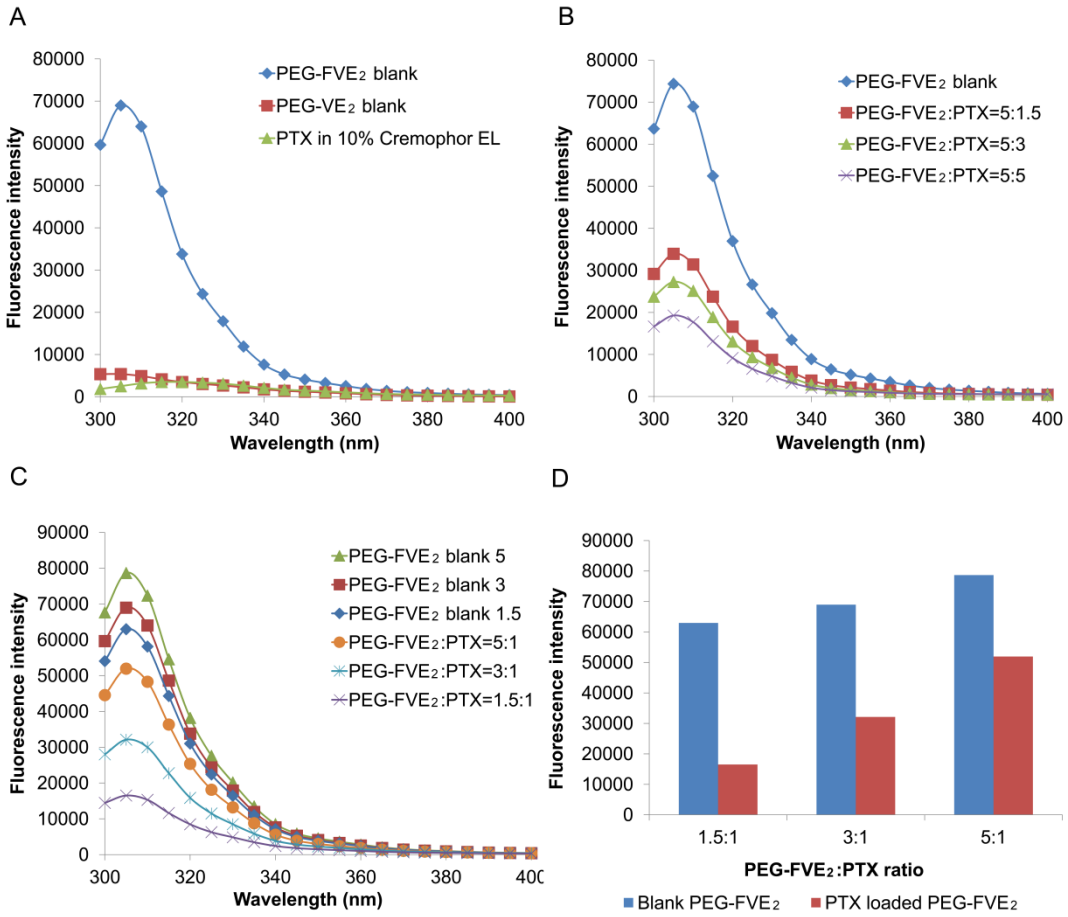

Figure 26 Change of Fmoc fluorescence intensity in PEG-FVE$_2$ loaded with various amount of PTX.

The fluorescence emission spectra at 300-400 nm were recorded with a fixed excitation wavelength of 270 nm (A-C). (B) Fluorescence spectra at different drug: carrier molar ratios with fixed concentration of PEG-FVE$_2$ at 3.81 mg/mL. (C) Fluorescence spectra at different drug: carrier molar ratios with fixed concentration of PTX at 0.1mg/mL. (D) Summary of changes in the fluorescence intensity of various formulations in (C) at 305nm.

4.3.3 Hemolytic effect of micelles

The PEG-FVE$_2$ polymer is amphiphilic and could solubilize lipids or insert into phospholipid membranes to induce membrane destabilization (Savic et al. 2003). Detrimental interaction between the polymeric materials and blood constituents such as red blood cells must be avoided for intravenous drug delivery. Therefore, the hemolytic effect of PEG-FVE$_2$ micelles was

evaluated as an indicator of the hematocompatibility. Polyethylenimine (PEI), a cationic polymer with potent cell surface activity, was included as the positive control. As shown in Figure 27, incubation of RBC with PEI caused significant hemolysis in a concentration-dependent manner. In contrast, with PEG-FVE_2, the percentage of hemolysis was less than 5 % at both 0.2 mg/ml and 1mg/ml, which is considered as non-hemolytic according to the Guiding Principles of Hemolysis Test [H]GPT4-1 (Li et al. 2009b). These data suggest that the PEG-FVE_2 polymer is hemocompatible and suitable for intravenous administration. It is possible that the hemolytic effects differ between species; therefore, human blood will be used to further evaluate the hemolytic effect of PEG-FVE_2 polymer in the future.

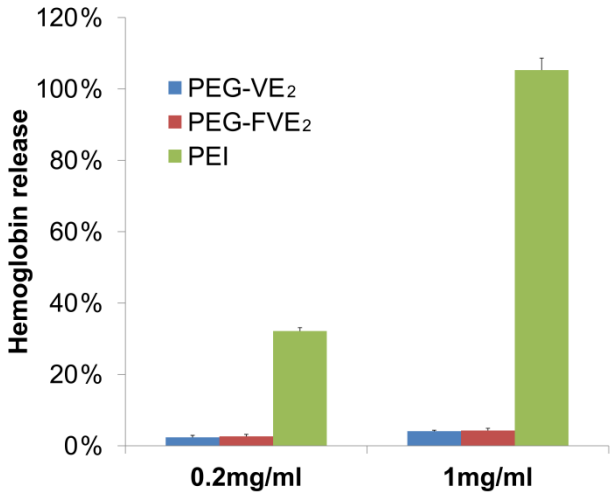

Figure 27 Hemolytic activity of PEG-FVE_2 compared to PEG-VE_2 and PEI.

The polymers (0.2 mg/mL or 1 mg/mL) were incubated with rat red blood cells (RBCs) for 4 h at 37 ℃ in an incubator shaker. The degree of RBCs lysis was determined by measuring the absorbance of solution at 540 nm after centrifuge. 2% Triton X-100 and DPBS were used as positive and negative control, respectively. Values are presented as means ± SD, n=3.

4.3.4 In vitro cytotoxicity of PTX-loaded micelles

The cytotoxicity of PTX-loaded PEG-FVE_2 micelles was investigated in breast cancer cell lines such as 4T1.2, MCF-7, and liver cancer cell lines including Hepa 1-6 and Huh-7 cells (Figure 28A-D). PTX-loaded PEG-VE_2 micelles, free PTX dissolved with DMSO, and Taxol were included as control formulations. PTX-loaded PEG-FVE_2 and PEG-VE_2 micelles showed comparable tumor cell killing effect in all of the cell lines tested (Figure 28A-D). In 4T1.2 cancer cells, both PTX-loaded PEG-VE_2 and PEG-FVE_2 micellar formulations were more cytotoxic than free PTX, but less active than Taxol formulation (Figure 28A). However, the two PTX micellar formulations showed higher level of cytotoxicity than both Taxol and free PTX towards MCF-7 cells (Figure 28B), Hepa 1-6 cells (Figure 28C) and Huh-7 cells (Figure 28D).

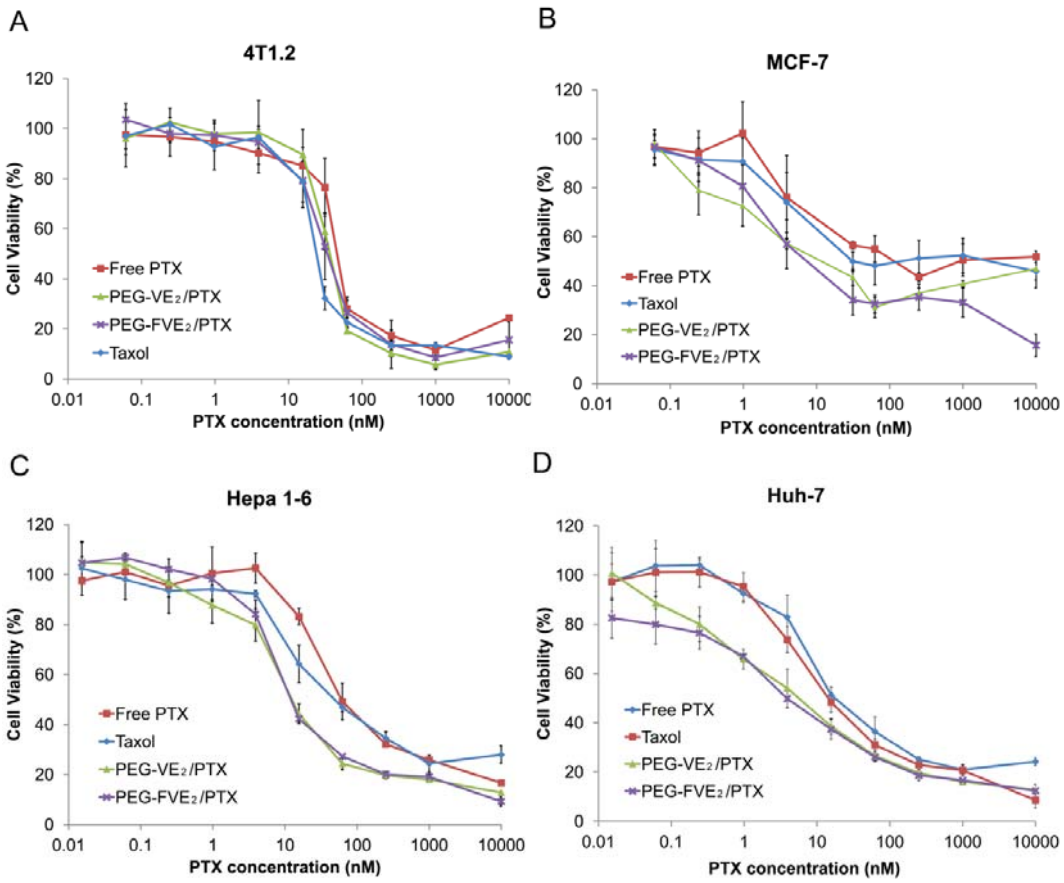

Figure 28 In vitro cytotoxicity of free PTX, PTX-loaded PEG-FVE$_2$ micelles, PTX-loaded PEG-VE$_2$ micelles and Taxol formulation against several cancer cell lines.

4T1.2 (A), MCF-7 (B), Hepa 1-6 (C) and Huh-7 (D) cells were treated with various formulations for 72 h followed by MTT assay. Data are reported as mean ± SD, n=3.

The IC_{50} of various formulations in the four tumor cell lines tested are summarized in Table 3. Carrier alone (PEG-FVE$_2$ or PEG-VE$_2$) showed minimal cytotoxicity at the concentrations used for PTX mixed micelles (Figure 29).

Table 3 The IC_{50} of various PTX formulations on 4T1.2, MCF-7, Hepa 1-6 and Huh-7 cell lines.

IC_{50} (nM)	Free PTX	Taxol	PEG-VE_2/PTX	PEG-FVE_2/PTX
4T1.2	40.4 ± 4.8	27.6 ± 3.8	35.0 ± 1.9	33.6 ± 2.2
MCF-7	98.5 ± 22.6	42.9 ± 27.0	12.3 ± 4.6	8.1 ± 2.3
Hepa 1-6	81.0 ± 12.8	54.3 ± 18.0	15.2 ± 0.9	16.5 ± 1.2
Huh-7	23.4 ± 7.0	16.8 ± 3.9	5.4 ± 2.0	4.7 ± 1.4

A

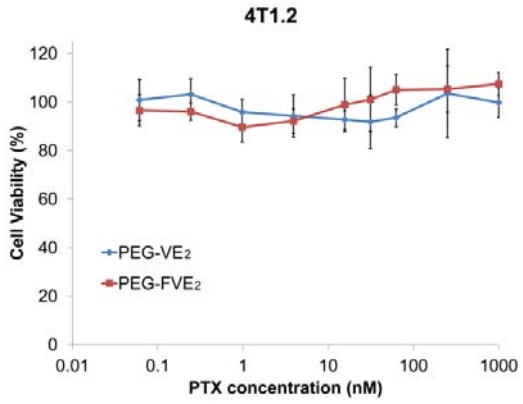

B

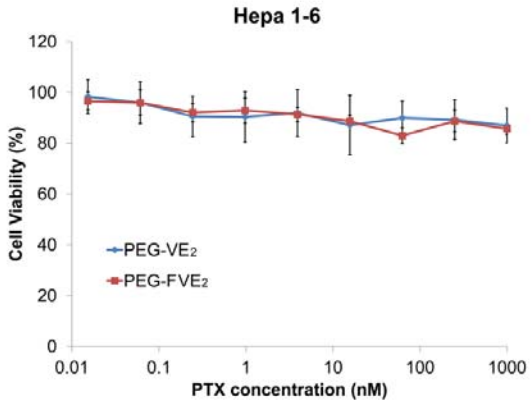

Figure 29 Cytotoxicity of blank PEG-FVE_2 and PEG-VE_2 to 4T1.2 (A) and Hepa 1-6 (B) cells

4.3.5 In vivo therapeutic study

The in vivo tumor growth inhibitory effect of PTX-loaded PEG-FVE_2 micelles was investigated in a syngeneic murine breast cancer model (4T1.2). As shown in Figure 30A, blank PEG-FVE_2 micelles showed minimal inhibitory effect on tumor growth compared with the control group treated with saline. Taxol exhibited moderate effect in inhibiting the tumor growth at the PTX dose of 10 mg/kg. In contrast, at the same PTX dose, a significant improvement in tumor

growth inhibition was achieved in the mice treated with PTX-loaded PEG-VE_2 micelles. Furthermore, the antitumor effect of PTX-loaded PEG-FVE_2 micelles was even higher than that of PTX-loaded PEG-VE_2 micelles

The toxicity of all of the formulations was evaluated by following their effects on animal behavior, body weight, as well as serum levels of AST and ALT. Mice treated with Taxol frequently showed transient apathy (Danhier et al. 2009) and decreased overall activity over 10 min post-injection. This is likely caused by Cremophor EL and ethanol in the Taxol formulation. In contrast, there was no noticeable change in activity of mice after injection of PTX-loaded PEG-FVE_2 micelles. No significant changes in body weight occurred in all of the groups (Figure 30B). In addition, serum levels of AST and ALT in the mice treated with PTX-loaded PEG-FVE_2 micelles were comparable to those in saline treated group (Figure 30C-D), suggesting the negligible toxicity of PTX-loaded PEG-FVE_2 in vivo.

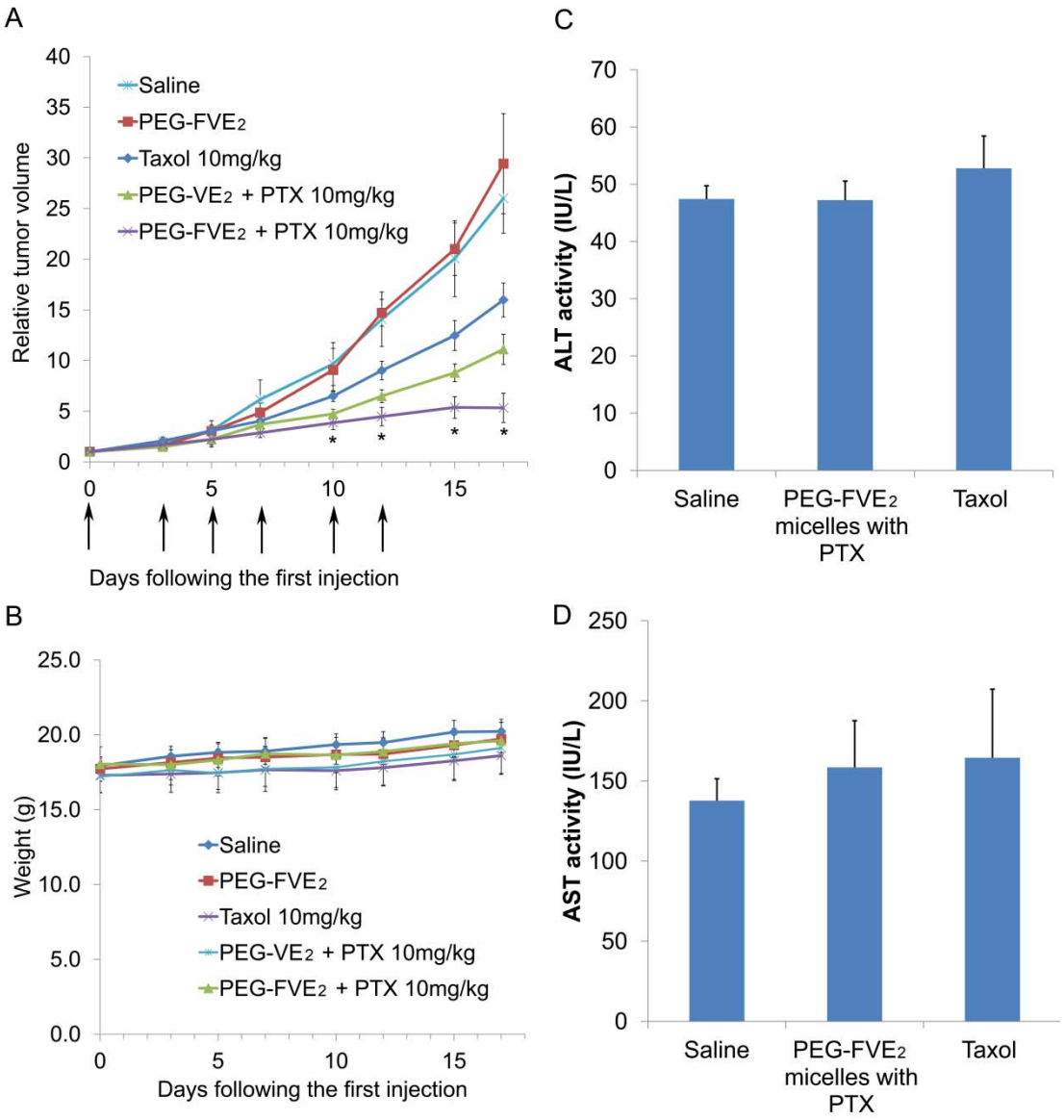

Figure 30 Antitumor activity and toxicity of PTX-loaded PEG-FVE$_2$ micelles in vivo.

(A) Enhanced antitumor activity of PTX formulated in PEG-FVE$_2$ micelles in vivo. Balb/c mice were inoculated s.c. with 4T1.2 cells (2 x 10^5 cells/mouse). After the tumor volume reach 50 mm^3, the mice received various treatments via tail vein injection three times a week for two weeks as indicated by arrows in the graph. Tumor volume was measured and plotted as relative tumor volume. (B) Change of body weights in mice receiving different treatments. The ALT (C) and AST (D) enzyme activity in serum was measured at the conclusion of experiment. Data are presented as mean ± SD. *$p<0.05$ versus Taxol treated mice. N=5.

4.4 DISCUSSION

We have previously shown that inclusion of drug-interactive Fmoc moiety into a lipopeptide surfactant can dramatically enhance its ability for loading JP4-039, a poorly water-soluble antioxidant (Gao et al. 2013). In this study, we applied this concept in the optimization of PEG-VE_2 polymeric material and synthesized a novel compound PEG-FVE_2. Here we demonstrated that PEG-FVE_2 is more effective for the loading of PTX compared with PEG-VE_2.

Drug solubility in amphiphilic di-block copolymer micelles is affected by the compatibility between the drug and the micelle core (Latere Dwan'Isa et al. 2007). Accumulating data have demonstrated that the drug loading capacity and stability of micelles can be greatly improved by tailoring the inner core segment of micelles for stronger drug-carrier interaction. Besides hydrophobic interaction, the compatibility between drug and carrier was shown to be improved by various additional non-covalent bonding. For example, hydrogen-bonding of micelles with doxorubicin significantly enhanced their loading capacity and stability (Kim et al. 2010c, Yang et al. 2012a). In addition, acid-base interaction between hydrophobic segments of micelles and guest molecules containing carboxylic acid groups also dramatically improved the loading of indomethacin and ibuprofen (Giacomelli et al. 2007). Furthermore, metal-ligand coordination facilitated the encapsulation of cisplatin into polymeric micelles (Yokoyama et al. 1996, Nishiyama et al. 2001). In particular, Park's group showed that inclusion of "hydrotropic motifs" into the hydrophobic domain of polymeric micelles represented a versatile strategy to enhance the compatibility of carrier with poorly water-soluble drugs (Huh et al. 2005, Kim et al. 2011). Similarly, inclusion of aromatic end groups into the hydrophobic chain of di-block copolymers improved the stable incorporation of camptothecin (Opanasopit et al. 2004) and PTX (Carstens et al. 2008, Gao et al. 2013). Data from this study

and another recent study (Zhang et al. 2014) suggest that incorporation of a drug-interactive motif (Fmoc) at the interfacial region represents an effective strategy in improving the performance of lipid-core micellar systems in loading hydrophobic drugs such as PTX.

Various mechanisms are likely to be involved in the carrier/drug interactions of PTX-loaded PEG-FVE_2 micelles, such as hydrophobic interaction with PTX, hydrogen bonding and the π- π stacking effect (Lu et al. 2013a). The enhanced PTX loading capacity was most likely due to excellent Fmoc-PTX compatibility, which results from the rigid aromatic structure of Fmoc moieties that may interact with those in PTX. This hypothesis was further supported by the change in Fmoc fluorescence intensity in the presence of PTX, which indicated the close proximity between Fmoc and PTX. The decrease of Fmoc fluorescence intensity likely results from the fluorescence quenching caused by intermolecular π-π interactions (Shirai et al. 1999). This information not only supports a role of Fmoc in the improved PTX loading capacity of PEG-FVE_2 micellar system, but also sheds new light on the design of novel polymeric nanocarriers for the delivery of other aromatic structure-containing drugs such as doxorubicin.

In contrast to the PEG-VE_2 micelles that form typical spherical structures, PEG-FVE_2 micelles showed predominantly elongated, worm-like morphology. This might be attributed to the strong inter-molecular interaction among the PEG-FVE_2 molecules mediated by Fmoc moieties. Fmoc is known to promote parallel interactions of individual short peptides carrying the same group, which often leads to the formation of elongated nanoassemblies (Gao et al. 2013). It was reported that drug carriers with worm-like shape, also known as filomicelles, have shown longer circulation time compared with spherical nanoparticles composed of the similar materials, leading to improved drug accumulation in tumors (Geng et al. 2007, Christian et al. 2009, Simone et al. 2009). Additional studies on the pharmacokinetic profile of PEG-FVE_2

micelles would help to better understand the contribution of micelle morphology to their circulation time and tumor accumulation.

MTT assay showed that the cytotoxicity of PTX-loaded PEG-FVE_2 and PEG-VE_2 micelles was more potent than that of free PTX solubilized in DMSO in all the cell lines tested. In Hepa 1-6 and Huh-7 cells, the cell killing effect of PTX-loaded PEG-FVE_2 and PEG-VE_2 micelles was even higher than that of Taxol formulation at the same PTX concentrations. This might be attributed to the increased cellular uptake of PTX into the cells due to the well-known p-gp inhibitory effect of Vitamin E derivatives (Dintaman et al. 1999, Lu et al. 2013a). The fact that the cytotoxicity of PTX-loaded PEG-FVE_2 micelles was similar or slightly higher than that of PTX-loaded PEG-VE_2 micelles suggests that the PEG-FVE_2 retained the function of PEG-VE_2 in enhancing the cellular uptake of drug-loaded micelles.

A highly metastatic murine breast cancer cell line 4T1.2 was selected to investigate the in vivo therapeutic efficacy of PTX-loaded PEG-FVE_2 micelles. PTX-loaded PEG-FVE_2 micelles demonstrated significantly higher tumor inhibitory effect compared with Taxol. The superior antitumor efficacy along with the minimal toxicity can be possibly attributed to a more effective EPR effect resulting from the PEG corona and the elongated shape of PEG-FVE_2 micelles (Geng et al. 2007), as well as enhanced intracellular uptake due to p-gp inhibition (Dintaman et al. 1999, Lu et al. 2013a). Further studies are currently ongoing in our lab to better understand the mechanism for the improved antitumor activity of PTX-loaded PEG-FVE_2 micelles.

To date there is no report about how PEG-FVE_2 conjugate is metabolized and eliminated in vivo. Theoretically, the ester bond can be cleaved, and the Fmoc group can be oxidized at certain positions, followed by conjugation with glucuronide or sulfate to become sufficiently

polar and readily excreted. In order to determine the metabolic fate of new chemical entities, the models most often used in vitro include: 1) metabolizing recombinant enzymes (e.g., CYP and UDP-glucuronosyltransferases); 2) subcellular fractions (e.g., microsomes, cytosols or S-9 fractions); and 3) cellular organelles (e.g., hepatocytes and liver slices) (Jia et al. 2007). Analysis of the metabolites from incubation supernatants is required and usually accomplished by HPLC with mass spectrometry (Ackley et al., 2004). Investigation about metabolic pathway of PEG-FVE_2 conjugate will be helpful to understand its potential biological effect on human body, which is required for FDA approval.

In summary, we have shown that PEG-FVE_2 possess higher loading capacity for PTX compared to PEG-VE_2. This effect could be attributed to the high compatibility and interaction between PTX and Fmoc moiety. We have further shown that PTX-loaded PEG-FVE_2 micelles led to significantly improved tumor inhibitory effect than Taxol with minimal toxicity in vivo. Our study suggests that incorporation of a drug-interactive motif (Fmoc) at the interfacial region represents an effective strategy to improve the performance of the micellar systems in loading poorly water-soluble drugs.

5.0 INCORPORATION OF A SELECTIVE SIGMA-2 RECEPTOR LIGAND ENHANCES UPTAKE OF LIPOSOMES BY MULTIPLE CANCER CELLS

Background: Sigma-2 receptor is an attractive target for tumor imaging and targeted therapy, since it is over-expressed on multiple types of solid tumors including prostate cancer, breast cancer and lung cancer. SV119 is a synthetic small molecule which binds to sigma-2 receptors with high affinity and specificity. In this study we investigated the utility of SV119 in mediating selective targeting of liposomal vectors to various types of cancer cells.

Methods: SV119 was covalently linked with polyethylene glycol-dioleyl amido aspartic acid conjugate (PEG-DOA) to generate a novel functional lipid, SV119-PEG-DOA. This lipid was utilized for the preparation of targeted liposomes to enhance their uptake by cancer cells. Liposomes with various SV119 density (0, 1, 3 and 5 mole%) were prepared and their cellular uptake was investigated with several tumor cell lines. In addition, doxorubicin (DOX) was loaded into targeted and unmodified liposomes, and the cytotoxic effect on DU-145 cells was evaluated by MTT assay.

Results: Liposomes with or without SV119-PEG-DOA both have mean diameter of approximately 90 nm and neutral charge. Incorporation of SV119-PEG-DOA significantly increased the cellular uptake of liposomes by DU-145, PC-3, A549, 201T and MCF-7 tumor cells, as shown by both fluorescence microscopy and by quantitative measurement of fluorescence intensity. In contrast, the uptake of liposomes by normal BEAS-2B cells was not

increased by SV119. In a time course study, the uptake of SV119-liposomes by DU-145 cells also was significantly higher at each time point compared with unmodified liposomes. Furthermore, DOX-loaded SV119-liposomes showed significantly higher cytotoxicity to DU-145 cells compared with DOX-loaded unmodified liposomes.

Conclusion: SV119-liposomes were developed for targeted drug delivery to cancer cells. The targeting efficiency and specificity of SV119 liposomes to cancer cells was demonstrated in vitro. The results of this study suggest that SV119-modified liposomes might be a promising drug carrier for tumor targeted delivery.

5.1 BACKGROUND

One major problem with conventional anticancer agents is the severe side effects on normal tissues and organs. To solve this issue, targeted drug delivery to solid tumors was developed as an effective strategy to improve therapeutic effect and minimize toxicity. Success of targeted drug delivery is affected by many factors, including the choice of a targeting ligand. Many types of ligands have been explored including antibodies, peptides, aptamers, and small molecule ligands (Wang et al. 2008a). Small molecule ligands have the advantages of minimal immunogenicity, excellent chemical stability and ease of synthesis (Wang et al. 2012b). Some examples of small molecule ligands that have been developed for tumor-targeting include ligands of folate receptor (Lee et al. 1995), prostate-specific membrane antigen (PSMA) (Moffatt et al. 2006), and integrin receptors (Zhang et al. 2010).

Recently there has been increased interest in exploring sigma receptor ligands for tumor imaging and targeted therapy. The exact biological functions of sigma receptors are not fully

defined yet. Sigma-1 receptors functionally regulate ion channels belonging to various molecular families and have been shown to be involved in neuronal plasticity and central nervous system diseases. Recent studies have shown that sigma-2 receptor shapes cancer cell electrical signature upon environmental conditions (Crottès et al. 2013). An interesting possibility is that sigma and/or sigma-1 receptors could mediate anti-cancer effects by modulating ion channels (Aydar et al. 2004). Sigma receptors are over-expressed in a variety of human tumors including non-small cell lung carcinoma (NSCLC), prostate cancer, melanoma, and breast cancer. Small molecule ligands of sigma receptors have been developed and demonstrated potential as tumor imaging agents (John et al. 1999, Cobos et al. 2008, Maurice et al. 2009). We and Dr. Huang's group reported that sigma receptor ligands such as anisamide effectively mediated selective delivery of liposomes containing doxorubicin (DOX) to prostate cancer cells in vitro and in vivo (John et al. 1993, Banerjee et al. 2004). Recently, extensive studies from Dr. Huang's group demonstrated targeted delivery of oligodeoxynucleotides and siRNA to lung cancer and melanoma using anisamide-decorated nanoparticles (Li et al. 2006b, Li et al. 2008b, Nakagawa et al. 2010). In addition, another sigma receptor ligand haloperidol was shown to improve by more than 10-fold the transfection of MCF-7 breast carcinoma cells compared with control (unmodified) liposomes (Mukherjee et al. 2005).

Both anisamide and haloperidol do not distinguish between sigma-1 and sigma-2 receptor subtypes with respect to binding. In this study we examine if sigma 2-selective ligands can be employed for targeted delivery of liposomal vectors. There are several potential advantages with sigma 2-selective ligands for tumor-targeted delivery. First, there is a higher density of sigma-2 versus sigma-1 receptors in tumor samples and in cultured tumor cells (Vilner et al. 1995, Wheeler et al. 2000). Second, ligand binding and photoaffinity labeling

studies have demonstrated lower expression of sigma-2 vs. sigma-1 receptors in normal tissues from the central nervous system, gastrointestinal tract, kidney, liver and heart (Matsumoto et al. 2007). Third, a correlation between sigma-2 receptor expression and tumor proliferation has been established both in vitro and in vivo (Mach et al. 1997, Colabufo et al. 2006), but such a correlation was not observed for the sigma-1 subtype.

SV119 is a small molecule ligand that binds to sigma-2 receptors with high affinity and specificity (Kashiwagi et al. 2007). The tumor-targeting efficiency of SV119 has been demonstrated by conjugating SV119 with apoptosis-inducing peptides, resulting in selective killing of tumor cells (Spitzer et al. 2012). In the present study, the potential of SV119 to direct selective delivery of liposomes to multiple tumor cell lines was explored. Liposomes are well-established drug carriers for intravenous delivery and several liposomal formulations have been approved for clinical applications (Di Paolo et al. 2008). Our results show that incorporation of a SV119 derivatized PEG-lipid significantly increased the cellular uptake of liposomes by several tumor cell lines but not by normal cells. In addition, DOX-loaded SV119-modified liposomes showed significantly higher cytotoxicity compared with unmodified liposomes loaded with DOX. These findings suggest that SV119-liposomes may have potential for targeting the delivery of anticancer agents to tumors that over-express sigma-2 receptors.

5.2 METHODS

5.2.1 Materials

L-α-phosphatidylcholine (Soy PC), DSPE-PEG(2000)-OCH_3 and 1,2-dioleoyl-sn-glycero-3-phosphoethanolamine-N-(lissamine rhodamine B sulfonyl) (ammonium salt) (rhodamine-PE) were purchased from Avanti Polar Lipids (Birmingham, AL). Cholesterol (Chol), doxorubicin hydrochloride, FITC-conjugated anti-mouse IgG, 3- [4,5-dimethylthiazol-2-yl]-2,5-diphenltetrazolium bromide (MTT) and dimethyl sulfoxide (DMSO) were purchased from Sigma–Aldrich (St. Louis, MO, USA). Mouse anti-early endosome antigen 1 (EEA1) monoclonal antibody was purchased from BD Transduction Laboratories. LysoTracker® Green DND-26 was purchased from Invitrogen, USA. PD-10 desalting column was purchased from GE Healthcare (Piscataway, NJ). Dulbecco`s Phosphate Buffered Saline (DPBS) was purchased from Gibco (Invitrogen Corporation, Carlsbad, CA). t-Boc Amine PEG NHS Ester (TBOC-PEG-NHS, MW 3500) was purchased from JenKem Technology USA, Inc (Allen, TX). All other chemicals and organic solvents were purchased from Sigma-Aldrich. ^{1}H NMR spectra were recorded on a Bruker FT 400 MHz. The synthesized compounds were also identified by matrix-assisted laser desorption/ionization time-of-flight (MALDI-TOF) mass spectrometry (Voyager-DE PRO BioSpectrometry Workstation, Applied Biosystems). The mass spectrum was obtained in linear mode with CHCA as the matrix.

Human prostate adenocarcinoma cell line DU-145, human lung carcinoma cell line A549, and human breast cancer MCF-7 cells were obtained from American Type Culture Collection (Rockville, MD). BEAS-2B (human bronchial epithelium cell line) is a generous gift from Dr. Di, Y.P. Peter at University of Pittsburgh. Cells were cultured in DMEM medium

(ATCC) supplemented with 10% FBS (Invitrogen, Carlsbad, CA) and 1% penicillin-streptomycin at 37°C in a humidified atmosphere of 5% CO_2 in air. All reagents were from Sigma-Aldrich Corporation (St. Louis, MO) unless otherwise stated.

5.2.2 Synthesis and Chemical Characterization of SV119-PEG-DOA Conjugates and Intermediates

The synthetic procedure for preparing SV119-PEG-DOA is depicted schematically in Figure 32. Experimental details are delineated below.

Compound 2. NaH (0.8 g, 60% in oil, 20 mmol) was added to a solution of 1 (3.04 g, 10 mmol) and benzyl 2-bromoacetate (2.75 g, 12 mmol) in THF (50 mL) (Vangveravong et al. 2006). The mixture was stirred overnight at ambient temperature. After the addition of ether (75 mL), the organic solution was quenched with water (30 mL) and then washed with saturated NaCl solution (40 mL), and finally the organic solution was dried over Na_2SO_4. After removal of solvent, the crude product was purified by flash column chromatography with hexane-ethyl acetate(1: 1) to obtain 2 (4.33 g, 96%) as a pale yellow oil. ^{1}H NMR ($CDCl_3$) δ 7.98 (s, 1H), 7.37-7.21 (m, 6H), 6.77 (m, 2H), 5.17 (s, 2H), 5.00 (m, 1H), 3.83 (s, 3H), 3.42 (m, 2H), 3.27 (m, 2H), 2.33 (m, 2H), 2.30 (s, 3H), 2.13 (m, 1H), 1.98 (m, 2H), 1.51 (m, 3H), 1.17 (m, 2H). ESI-MS m/z 453.5 ([M+H]+).

Compound 3. Chemical Name: 2-(3-((2-methoxy-5-methylphenyl)carbamoyl)-9-aza-bicyclo[3.3.1]nonan-9-yl)acetic acid. Pd/C (10%, 500 mg) was added to a solution of 2 (3.62 g, 10 mmol) and stirred under 1 atm of H_2 in MeOH (50 mL). After evaporation of the solvents under vacuum, EtOAc (100 mL) was added. The mixture was washed by saturated NaCl solution (40 mL), and finally the organic solution was dried over Na_2SO_4. EtOAc was then

removed to obtain 3 (2.82 g, 100%) as a white solid. ^{1}H NMR ($CDCl_3$) δ 10.9 (brs, 1H), 7.96 (s, 1H), 7.15 (s, 1H), 6.79 (m, 2H), 4.96 (m, 1H), 3.83 (s, 3H), 3.32 (m, 2H), 3.04 (m, 2H), 2.35 (m, 2H), 2.29 (s, 3H), 2.08 (m, 1H), 1.64 (m, 3H), 1.50 (m, 4H). ESI-MS m/z 363.4 ([M+H]+).

Compound 4. A mixture of Boc-aspartic acid (2.47 g, 10 mmol), oleyl amine (8.01 g, 30 mmol) and DCC (6.18 g, 30 mmol), DMAP (122 mg, 1 mmol) in anhydrous CH_2Cl_2 (60 mL) was stirred vigorously at room temperature for 5 h. After the reaction was completed, the mixture was filtered, and evaporated under reduced pressure, and the residue was purified by flash column chromatography (MeOH: $CHCl_3$ 1:9) to afford the product (4.40 g, 60%). ^{1}H NMR ($CDCl_3$) δ 7.93 (m, 1H), 5.37 (m, 4H), 4.17 (m, 1H), 3.24 (m, 4H), 1.98 (m, 9H), 1.51 (m, 4H), 1.47 (s, 9H), 1.26 (m, 45H), 0.87 (m, 6H). ESI-MS m/z 719.1 ([M+H]+).

DOA (dioleyl amido aspartic acid). To a solution of 4 (4.4 g, 6 mmol) in anhydrous CH_2Cl_2 (6 mL) was added trifluoroacetic acid (6 mL). After stirring for 2 h, the reaction mixture was diluted with CH_2Cl_2 (50 mL) and a saturated aqueous solution of Na_2CO_3 (20 mL) was then added until gas evolution ceased. The organic layer was separated and washed by brine. The organic layers were dried over anhydrous Na_2SO_4, filtered and concentrated under reduced pressure. The residue was purified by flash column chromatography (MeOH: $CHCl_3$ 1:9) to afford the product (3.70 g, 95%). ^{1}H NMR ($CDCl_3$) δ 7.53 (m, 1H), 6.33 (m, 1H), 5.37 (m, 4H), 3.67 (m, 1H), 3.22 (m, 4H), 1.98 (m, 9H), 1.50 (m, 4H), 1.26 (m, 45H), 0.87 (m, 6H). ESI-MS m/z 641.0 ([M+Na]+).

Compound 6. A mixture of Boc-NH_2-PEG-NHS (350 mg, 0.1 mmol) and DOA (63.1 mg, 0.1 mmol) in anhydrous CH_2Cl_2 (1 mL) was stirred vigorously at room temperature for 2 h. The solution was precipitated in cold diethyl ether and the precipitate was washed again by diethyl ether. Into the precipitate was added anhydrous CH_2Cl_2 (1 mL) and TFA (1 mL) and the

mixture was stirred for 2 h. The reaction mixture wan diluted with CH_2Cl_2 (10 mL) and a saturated aqueous solution of Na_2CO_3 (2 mL) was then added until gas evolution ceased. The organic layer was separated and precipitated in cold diethyl ether. The precipitate obtained was washed again by diethyl ether.

Compound 7. A mixture of compound 3 (72 mg, 0.2 mmol), PEG-DOA (300 mg, 0.1 mmol), DCC (41.2 mg, 0.2 mmol), and DMAP (12 mg, 0.1 mmol) in anhydrous CH_2Cl_2 (1 mL) was stirred vigorously at room temperature for 5 h. The solution was precipitated in cold diethyl ether and washed again with diethyl ether to obtain 7 (245mg, 73%).

Compound 8. A mixture of compound 1 (304 mg, 1 mmol), succinic anhydride (200 mg, 2 mmol), and DMAP (12 mg, 0.1 mmol) in anhydrous CH_2Cl_2 (1 mL) was stirred vigorously at room temperature for 5 h. The residue was purified by flash column chromatography (ethyl acetate) to afford the product. (3.70 g, 95%). ^{1}H NMR ($CDCl_3$) δ 10.9 (brs, 1H), 7.96 (s, 1H), 7.15 (s, 1H), 6.79 (m, 2H), 4.96 (m, 1H), 3.83 (s, 3H), 3.04 (m, 2H), 2.72 (m, 2H), 2.35 (m, 2H), 2.29 (s, 3H), 2.24 (m, 2H), 2.08 (m, 1H), 1.64 (m, 3H), 1.50 (m, 4H).

Compound 9. A mixture of compound 8 (75 mg, 0.2 mmol), PEG-DOA (300 mg, 0.1 mmol), DCC (41.2 mg, 0.2 mmol), and DMAP (12 mg, 0.1 mmol) in anhydrous CH_2Cl_2 (1 mL) was stirred vigorously at room temperature for 5 h. The solution was precipitated in cold diethyl ether and washed again with diethyl ether to obtain 9 (212mg, 65%).

5.2.3 Preparation of rhodamine-PE labeled liposomes

Rhodamine-PE labeled liposomes with or without SV119 were prepared by thin lipid film hydration followed by probe sonication. Unmodified liposomes were composed of SPC:Chol:DSPE-PEG2000:rhodamine-PE in a 7:3:0.5:0.05 molar ratio. Chloroform solution of

the lipid components was mixed and evaporated under a gentle stream of N_2 followed by vacuum for at least 4 h. The dried lipid films were hydrated with DPBS at 4 °C overnight with an initial total lipid concentration of 16 mM. After brief vortex, the suspension was then probe sonicated for 1h at the power of 3 watts. Liposomes were then passed through a PD-10 desalting column and used for fluorescence microscopic and quantitative liposome uptake studies. The preparation of SV119-liposomes followed the same procedures except that DSPE-PEG2000 was partially substituted by DOA-PEG(3500)-SV119 conjugate. The size distribution and ζ-potentials of the liposomes were monitored by dynamic light scattering method using the Malvern Zetasizer (Nano-ZS, Malvern Instruments Ltd., Worcestershire, UK).

5.2.4 Cellular uptake studies

Cells (2×10^4 per well) were seeded onto 48-well plates (Corning Inc., Corning, NY) and allowed to attach overnight. The complete medium was replaced with the serum-free DMEM containing rhodamine-PE labeled liposomes at a final total lipid concentration of 800 μM. Unmodified- or SV119- liposomes were incubated with cells at 37 °C for 1 h unless otherwise indicated. After incubation, the cells were then washed three times with ice cold PBS and lysed with 200 μl 0.3% Triton X-100 at room temperature for 0.5 h. Fluorescence intensity of cell lysate was determined by a Perkin-Elmer LS 50B luminescence spectrometer (Norwalk, CT) (lamda ex, 560nm;λ lamda emission, 588 nm). The results were expressed as arbitrary fluorescence intensity/mg of protein lysates. All the numbers were subtracted by the autofluorescence of cells incubated in serum-free medium without any formulations. The results are reported as the average values of four wells performed in the same plate on the same day.

To evaluate cellular uptake by microscopy, cells were fixed with 4% paraformaldehyde in DPBS at 4 °C for 20 min and washed three times by DPBS. Fluorescence images were obtained using a Nikon fluorescence phase contrast optical microscope.

To investigate the effect of free SV119 on uptake of SV119-liposomes, SV119 was conjugated with PEG550 to increase its water solubility (Figure 31). The effect of SV119 on SV119-liposome uptake was examined by incubating DU-145 cells with the liposomes in serum-free media for 1 hr at 37 °C in the presence of SV119-PEG550 (200 μM) or PEG550 (200 μM), and fluorescence microscopy study was carried out as described above.

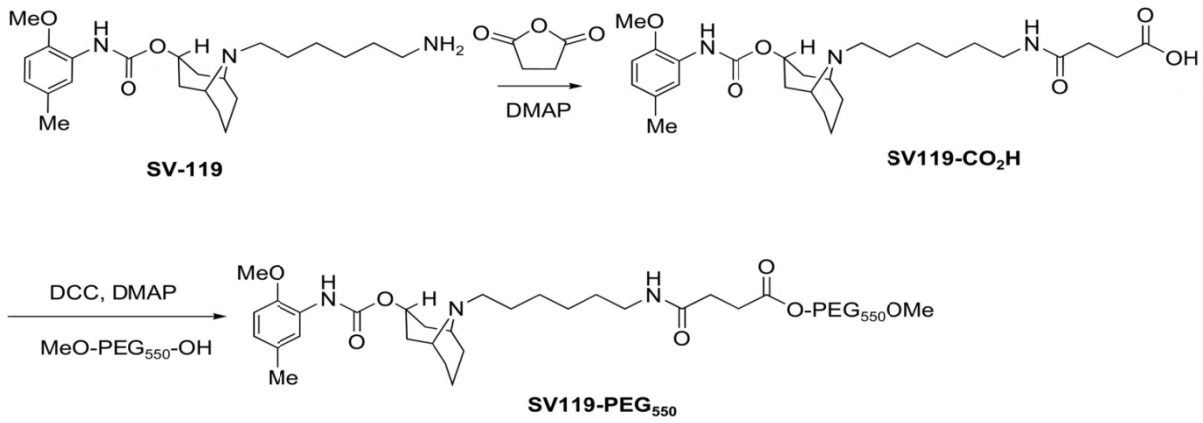

Figure 31 Scheme of synthesis for SV119-PEG550

5.2.5 Preparation of DOX-loaded liposomes

DOX was encapsulated into unmodified- and SV119- liposomes using an ammonium sulphate gradient method as previously described (Eliaz et al. 2001). The components of blank liposomes were similar to the liposomes described in section 2.3, and the percentage of SV119-PEG3500-DOA in total lipid of targeted liposomes was 5 mole%. Instead of DPBS, 250 mM ammonium sulfate solution was used to hydrate the lipid membrane. DOX (10mg/mL) dissolved in 5%

glucose was mixed with the liposomes and incubated at 37°C for 20 min. The drug: lipid ratio was kept at approximately 100 μg/μmol to achieve an encapsulation efficiency of greater than 90% (Eliaz et al. 2001). Nonentrapped DOX was removed by filtration through a PD-10 column. After solubilization of the liposomes in 1% (w/v) Triton X-100, the DOX concentration in liposomes was determined by measuring the absorbance at 480 nm using free DOX solution as a standard.

5.2.6 Cytotoxicity assay

The viability of cells treated by DOX encapsulated in SV119-liposomes or unmodified liposomes was measured by MTT colorimetric assay. DU-145 cells were trypsinized and resuspended in serum-free DMEM. Formulations were diluted in serum-free medium and mixed with DU-145 cell suspension, followed by incubation at 37 °C for 1h. Then the medium was removed by centrifugation. The cell pellets were resuspended in complete medium and plated on a 96-well plate at a density of 5×10^3 cells per well. Cells were cultured at 37 °C for another 72 h followed by MTT assay. Twenty microliters of MTT solution (5 mg/mL in PBS) was added to each well and the cells were incubated for 4 hr at 37°C. Then the media were removed and 150 μl DMSO was added to each well. Absorbance at 550/630 nm was measured in Ultramark Microplate Imaging System (Bio-Rad, Hercules, CA). Six wells were used for each sample, and the data are expressed as the percentage of viable cells compared to untreated control cells.

5.2.7 Intracellular localization

DU-145 cells grown on glass bottom dishes (In Vitro Scientific, Sunnyvale, CA) to 60%-70% confluence were incubated with rhodamine-PE labeled liposomes (with 3 mole% SV119-PEG-DOA) at 37°C for 3 h or 16 h. For detection of early endosomes, the cells were fixed with 4% paraformaldehyde and permeabilized with 0.2% saponin, stained with anti-EEA1 (1:100) followed by FITC-conjugated anti-mouse IgG (1:100). For live cell staining of lysosomes, Lyso-Tracker Green® (50 nM) was added to the medium 30 min before the conclusion of incubation. The stained cells were rapidly washed with ice cold PBS and observed using an Olympus FV1000 laser scanning confocal microscope (Olympus America Inc., Melville, NY).

5.2.8 Statistical analysis

Statistical analysis was done by two-tailed unpaired Student's t-test using the SPSS software, version 11.5 (SPSS. Inc., Chicago, IL) and data were expressed as mean ± SD. Differences with $p < 0.05$ were considered significant.

5.3 RESULTS

5.3.1 Synthesis of SV119-PEG3500-DOA

In order to develop lipid-based nanoparticles incorporating SV119 on the surface, we have designed and synthesized a SV119-derivatized PEG-lipid. DOA is a double-chain lipid

synthesized from oleyl amine and aspartic acid, and it can be inserted into the lipid bilayer of liposomes. The PEG moiety on liposomes provides steric hindrance, which renders the nanoparticles more stable and minimizes nonspecific binding of the liposomes to the cell surface (Lasic et al. 1995). After replacing the amine group with a carboxyl group, a SV119-PEG-DOA conjugate was synthesized by covalent linkage between the carboxyl group of SV119 and the terminal amine group of PEG. Figure 32 illustrates the synthesis scheme of SV119-PEG3500-DOA.

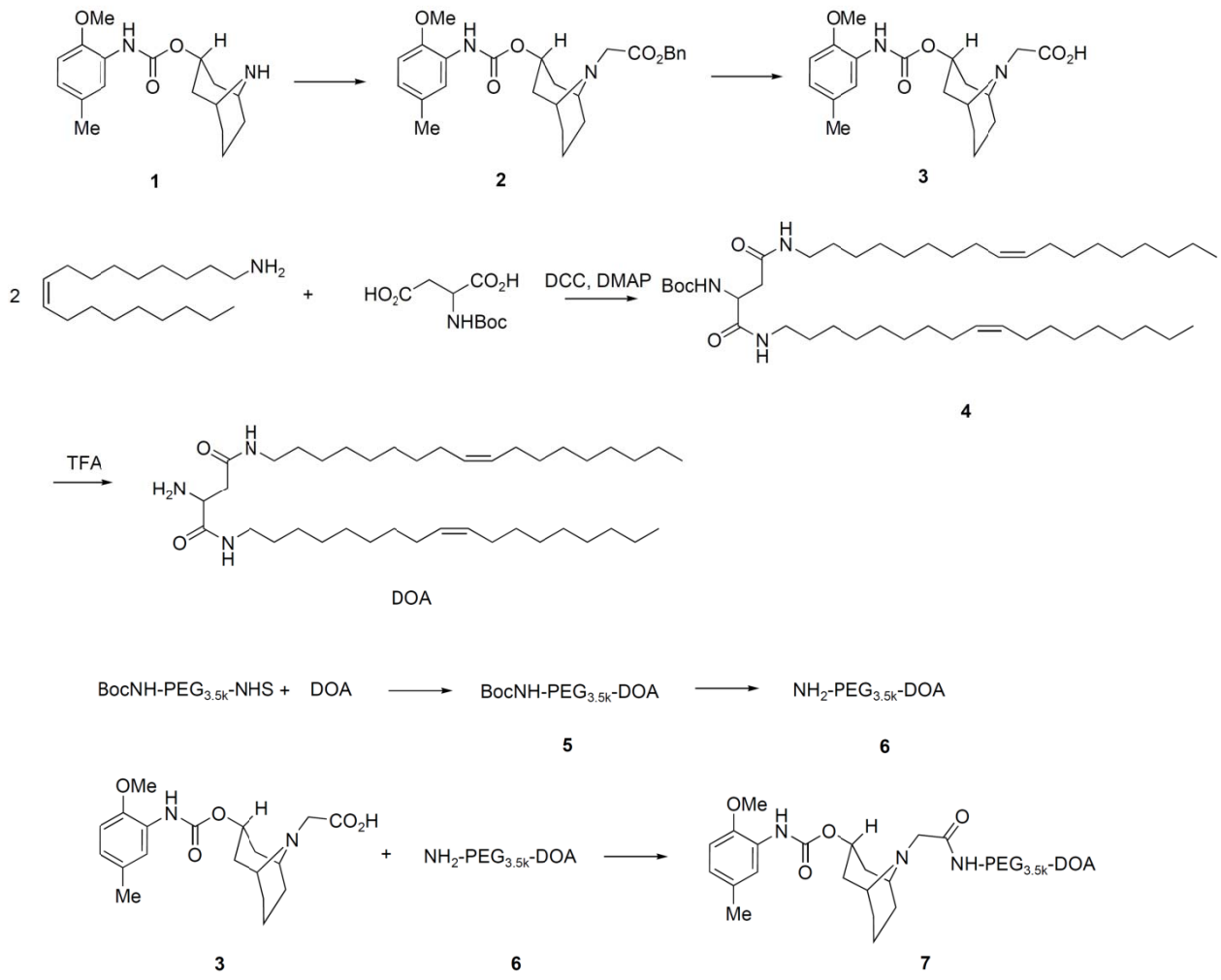

Figure 32 Scheme of synthesis for SV119-PEG3500-DOA.

Figure 33A shows the NMR spectrum of synthesized SV119-PEG3500-DOA. The peaks at 7.2-7.3 ppm were attributed to the benzene groups on SV119, the signals at 5.0-5.2 ppm were attributed to the double bond of DOA, the peaks between 3-4 were attributed to the PEG, and the signals at 1-2 ppm were attributed to the carbon chain of DOA. The molecular weight of synthesized product was determined by MALDI-TOF mass spectrometry. As shown in Figure 33B, the spectra exhibited a bell-shaped distribution of 44 Da-spaced lines centered at 4754.9 Da for SV119-PEG3500-DOA.

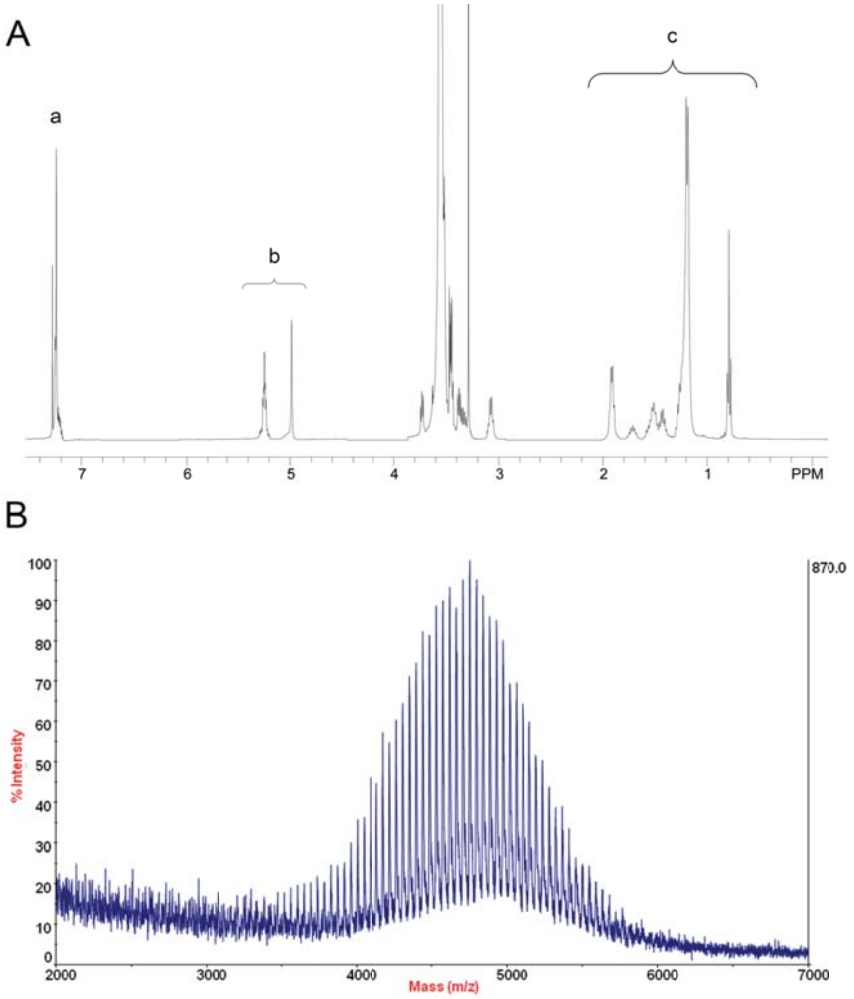

Figure 33 NMR spectrum (A) and MALDI-TOF mass spectrum (B) of SV119-PEG3500-DOA.

The peaks in panel A were attributed to benzene groups on SV119 (a), the double bonds of DOA (b), and the carbon chains of DOA (c).

Comparison with the mass spectrum of PEG3500 (Figure 34) and PEG3500-DOA (Figure 35) suggests the successful synthesis of SV119-PEG3500-DOA conjugate.

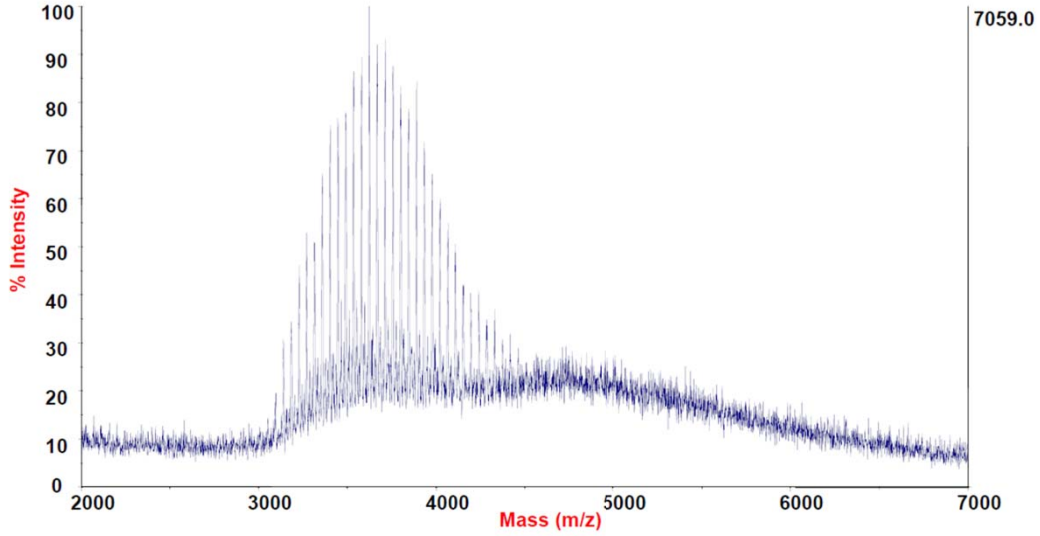

Figure 34 MALDI-TOF mass spectrometry of PEG3500.

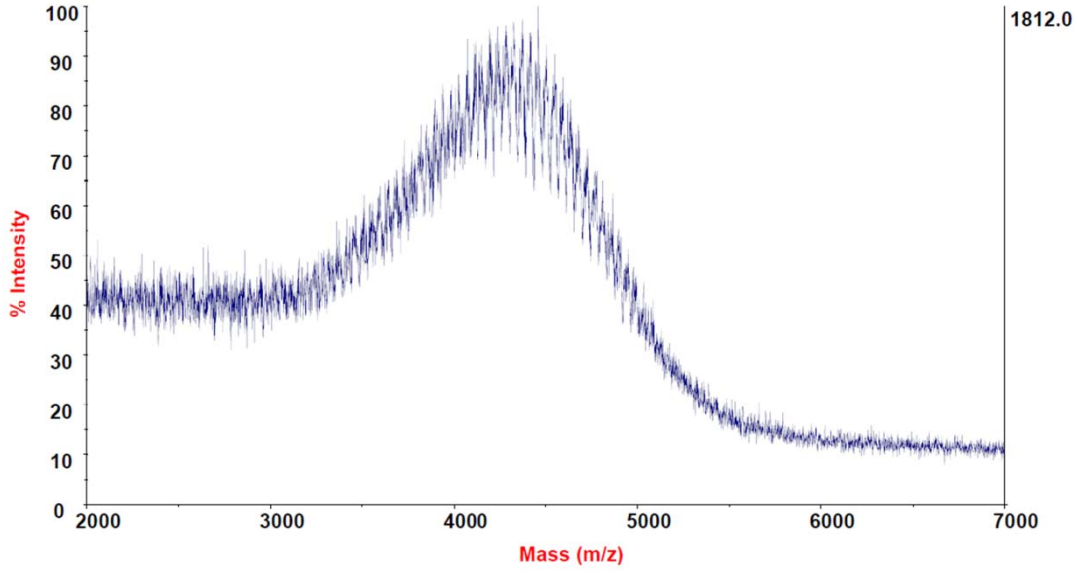

Figure 35 MALDI-TOF mass spectrometry of PEG3500-DOA.

5.3.2 Preparation of rhodamine-PE labeled liposomes

The synthesized SV119-PEG-DOA was used to formulate targeted liposomes. Liposomes are mainly composed of phospholipids and cholesterol. These molecules also are components of the cells and, thus, are believed to be biocompatible and non-toxic. In our experiment, it was shown that all the liposomal formulations have a mean diameter of approximately 90 nm (Table 4), which is optimal for penetrating the blood vessels surrounding the tumor and subsequent endocytosis by the tumor cells (Gabizon 1995).

Table 4 Size and zeta potential of SV119 decorated liposomes

SV119-PEG-DOA	0%	1%	3%	5%
Particle size (nm)	90.0 ± 0.2	90.7 ± 0.3	97.6 ± 0.2	89.2 ± 0.6
Zeta Potential (mV)	-2.0 ± 0.6	-2.4 ± 0.5	-2.2 ± 0.3	-3.1 ± 0.4

Note: Data are the mean ± standard deviation for n=3.

5.3.3 Cellular uptake studies

The targeting efficiency of SV119-liposomes was characterized in vitro. Cellular uptake was studied using DU-145 cells as target cells. DU-145 is a human prostate cancer cell line and these cells have been reported to over-express sigma-2 receptors (John et al. 1999). Human bronchial epithelial cells BEAS-2B were chosen to examine the liposomal uptake by normal cells. SV119-PEG3500-DOA was formulated into rhodamine-PE labeled liposomes to partially substitute PEG2000-DSPE, and the total amount of PEG-conjugated lipid in liposomes was kept at 5 mole percent. A longer spacer (PEG3500) was used between SV119 and DOA to minimize

the potential steric hindrance imposed by DSPE-PEG2000 and to increase the targeting efficiency (Zhou et al. 2002a).

Figure 36A shows the fluorescence images of DU-145 cells that were treated with rhodamine-PE labeled SV119-liposomes. After incubation with SV119-liposomes and unmodified liposomes for 1h, fluorescence was observed both on the cell membrane and inside the cells. Increasing the amounts of SV119 incorporated into the liposomes was associated with significant increase in rhodamine fluorescence intensity. This is in contrast to unmodified liposomes which showed minimal binding and cellular uptake by DU-145 cells (Figure 36A). Figure 36B shows the quantitative measurements of cell-associated fluorescence 1 h following treatment of DU145 cells with SV119-liposomes and unmodified liposomes. Consistent with the fluorescence imaging studies (Figure 36A), the amount of cell-associated fluorescence for DU-145 cells increased significantly with increasing amounts of ligand incorporated into the liposomes.

In addition, binding and uptake of SV119-liposomes was competitively blocked by the presence of SV119-PEG550 conjugate, but was not inhibited by the same concentration of PEG550 (Figure 37). These results demonstrate that the enhanced uptake of SV119-liposomes was mediated by SV119.

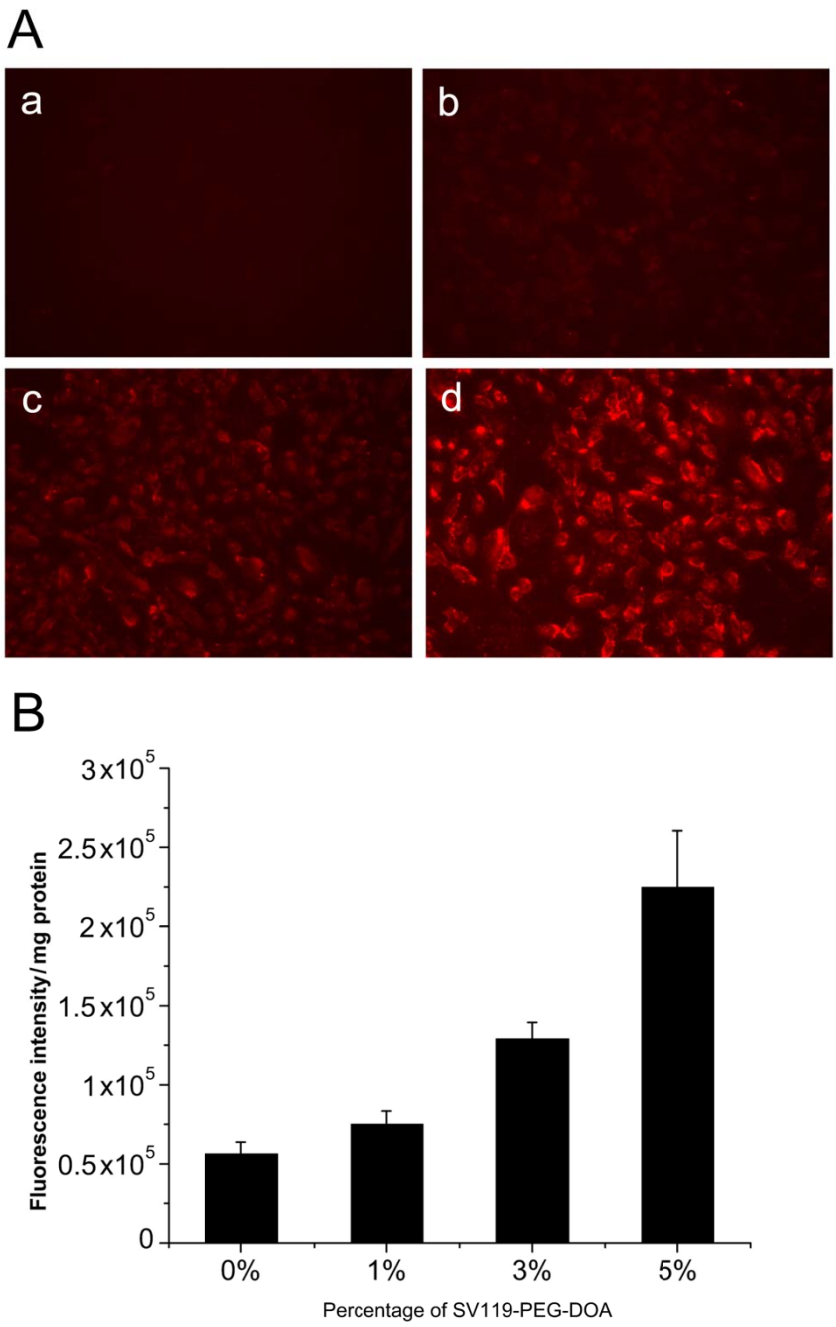

Figure 36 Enhanced cellular uptake of SV119-liposomes by DU-145 cells

Cellular uptake was examined by microscopic study (A) and quantitative analysis (B) (n = 4, mean ± SD). In panel A, the pencentage of SV119-PEG-DOA in total lipid was 0% (a), 1%(b), 3%(c) and 5%(d), respectively.

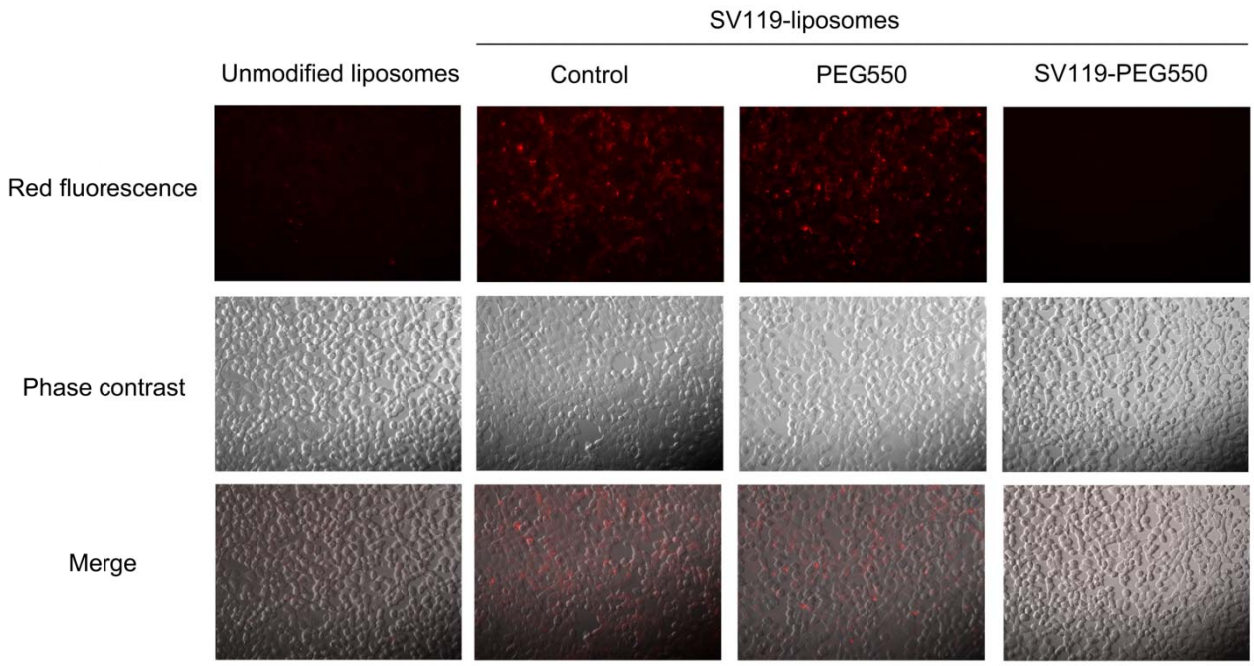

Figure 37 Effect of SV119 on the uptake of SV119-liposomes by DU-145 cells.

In order to demonstrate the cell-type specificity of the uptake of SV119-liposomes, normal human bronchial epithelial cells BEAS-2B were tested as a control. Results showed little binding and cellular uptake of both SV119-liposomes and unmodified liposomes by BEAS-2B cells (Figure 38A). No difference was found between SV119-liposomes and unmodified liposomes in cell-associated fluorescence intensity (Figure 38B). These observations suggest that SV119-mediated liposomal uptake is specific to the tumor cells.

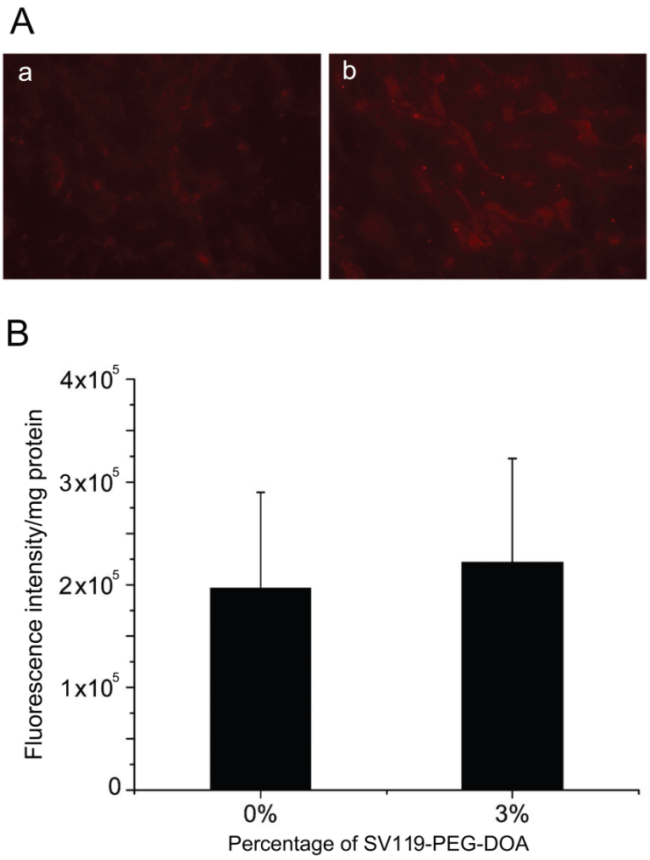

Figure 38 Cellular uptake of liposomes by BEAS-2B cells.

Cellular uptake was shown as microscopic images (A) and quantitative analysis (B). (n = 4, mean ± SD) The pencentage of SV119-PEG-DOA in total lipid was 0% (a) or 3% (b).

One of the unique features of sigma-2 receptor is its over-expression in multiple types of cancers. Thus, following the demonstration of specific targeting to DU145 cells, we examined the targeting capacity of SV119-liposomes using several other cancer cell lines, including PC-3 (prostate cancer), MCF-7 (breast cancer), A549 and 201T (lung cancer) cells. Similar to our observations in DU-145 cells, the cell-associated fluorescence intensity for SV119-liposomes was much higher than that for unmodified liposomes in all the tumor cell lines tested (Figure 39), suggesting the potential of using SV119-liposomes to target multiple types of tumors.

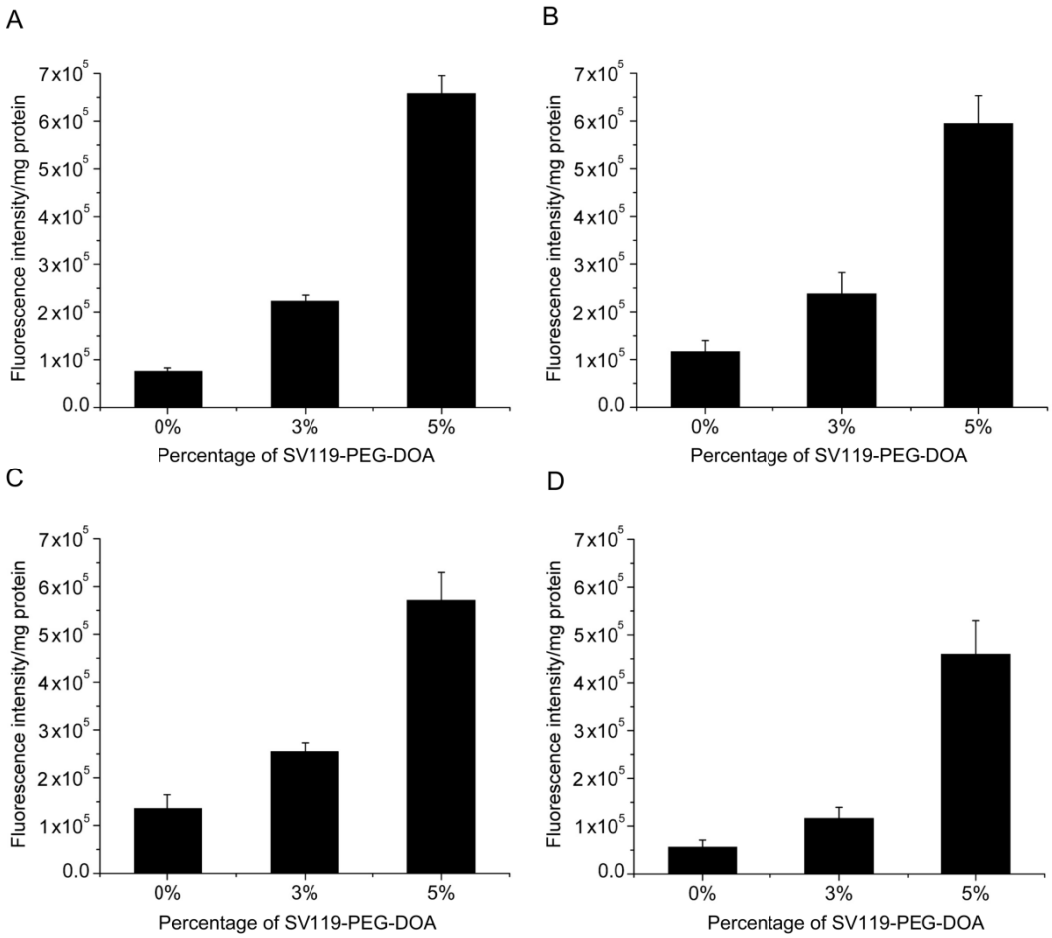

Figure 39 Uptake of SV119-liposomes by MCF-7 (A), PC-3 (B), 201T (C) and A549 cells (D).

(n = 4, mean ± SD)

Next we investigated the time course of liposomal uptake by DU-145 cells. As shown in Figure 40, the cell-associated fluorescence intensity was increased during prolonged incubation within 6 hours for both SV119-liposomes and unmodified liposomes. Note that the cellular uptake of SV119-liposomes was significantly higher at each time point compared with unmodified liposomes. This observation further supports our conclusion that incorporation of SV119 significantly enhances the uptake of liposomes into tumor cells.

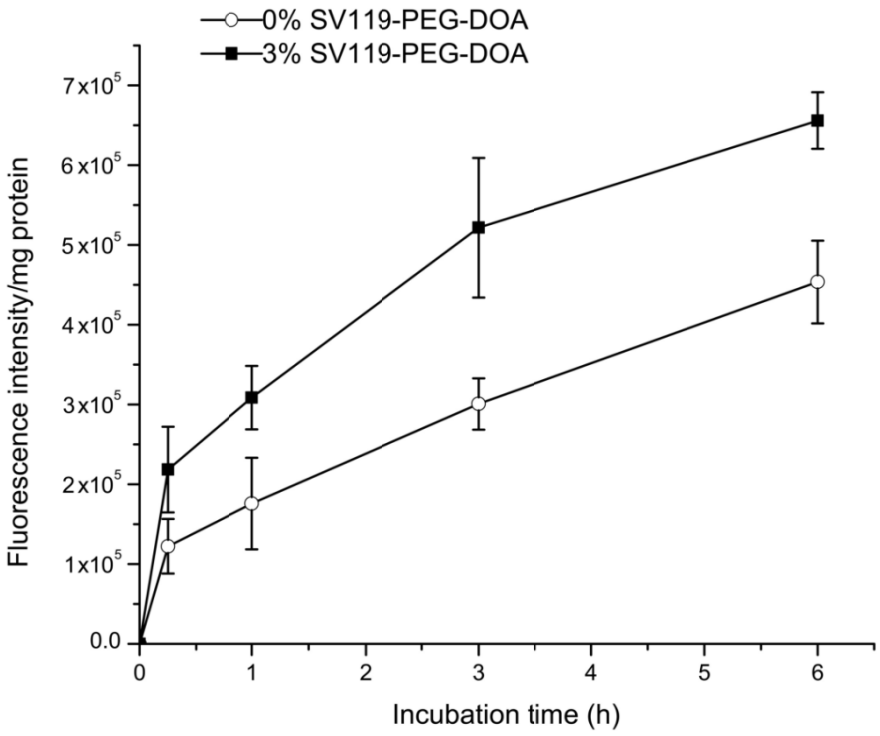

Figure 40 Time-course of cellular uptake of SV119-liposomes.

Rhodamine-PE labeled liposomes with 0% or 3% SV119-PEG-DOA were incubated with DU-145 cells for indicated time periods at 37 °C. (n = 4, mean ± SD).

Like many other sigma-2 receptor ligands (Mach et al. 2009), SV119 has a tertiary amine group. It is therefore possible that incorporation of SV119 onto the surface of liposomes may render the particles positively charged which may increase the nonspecific cellular uptake of SV119-liposomes. However, zeta potential analysis showed that incorporation of up to 5 mol% of lipid-PEG-derivatized SV119 into liposomes did not significantly alter the surface charge (Table 4), which excluded the possibility that the enhanced uptake was mediated by non-specific charge-charge interaction. Furthermore, to minimize the protonation of the amine nitrogen, a modified SV119 (mSV119) was synthesized by introducing an adjacent carbonyl group, and the mSV119 was similarly conjugated with PEG3500-DOA for the incorporation

into liposomes (Figure 41A). This modification did not affect the targeting efficiency of the ligand (Figure 41B). This result may shed new insights into the structure-activity relationship which may aid in the design of new sigma-2 receptor ligands.

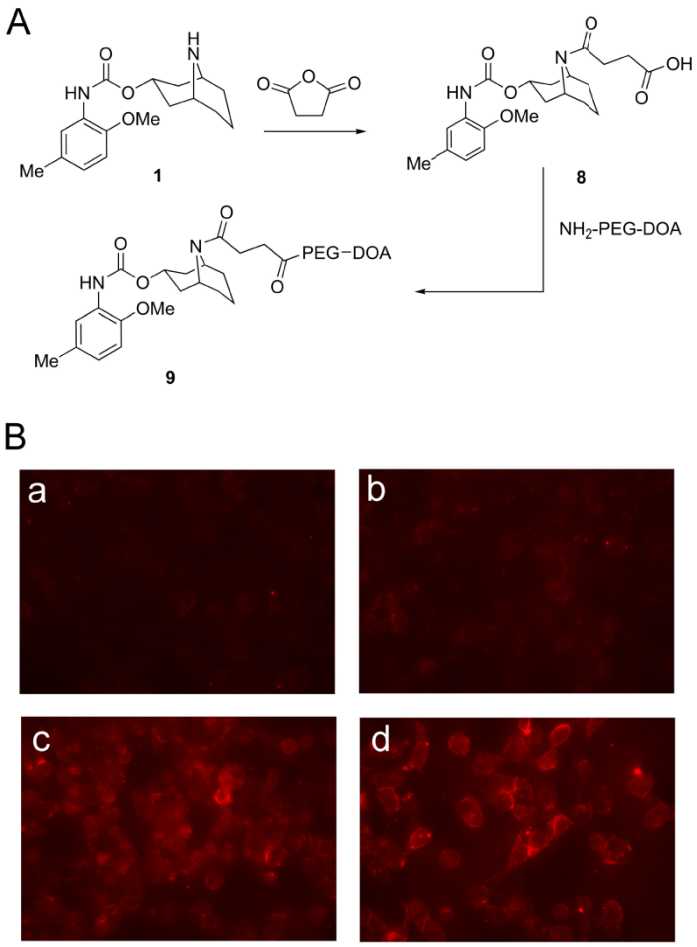

Figure 41 Uptake of liposomes decorated with modified SV119 (mSV119) by DU-145 cells.

Scheme of synthesis (A) and microscopic images (B) (n = 4, mean ± SD). In panel B, the pencentage of mSV119-PEG-DOA in total lipid was 0% (a), 1%(b), 3%(c) and 5%(d), respectively.

5.3.4 Intracellular localization

Despite the enhanced cellular uptake of SV119-liposomes, it is crucial to understand the intracellular fate of the liposomes in order to maximize the bioavailability of loaded drug.

Nanoparticles internalized via the endocytosis pathway often are sequestered in endosomes and lysosomes, which represent an intracellular barrier that limits the accessibility of encapsulated agents to their molecular targets. In this study, confocal microscopy was used to examine the intracellular localization of rhodamine-PE labeled SV119-liposomes in DU-145 cells. After 3 h of incubation, the liposomes showed a peri-nuclei punctuated distribution that is substantially co-localized with early endosomes (Figure 42A-C). After an additional 13 h incubation, the

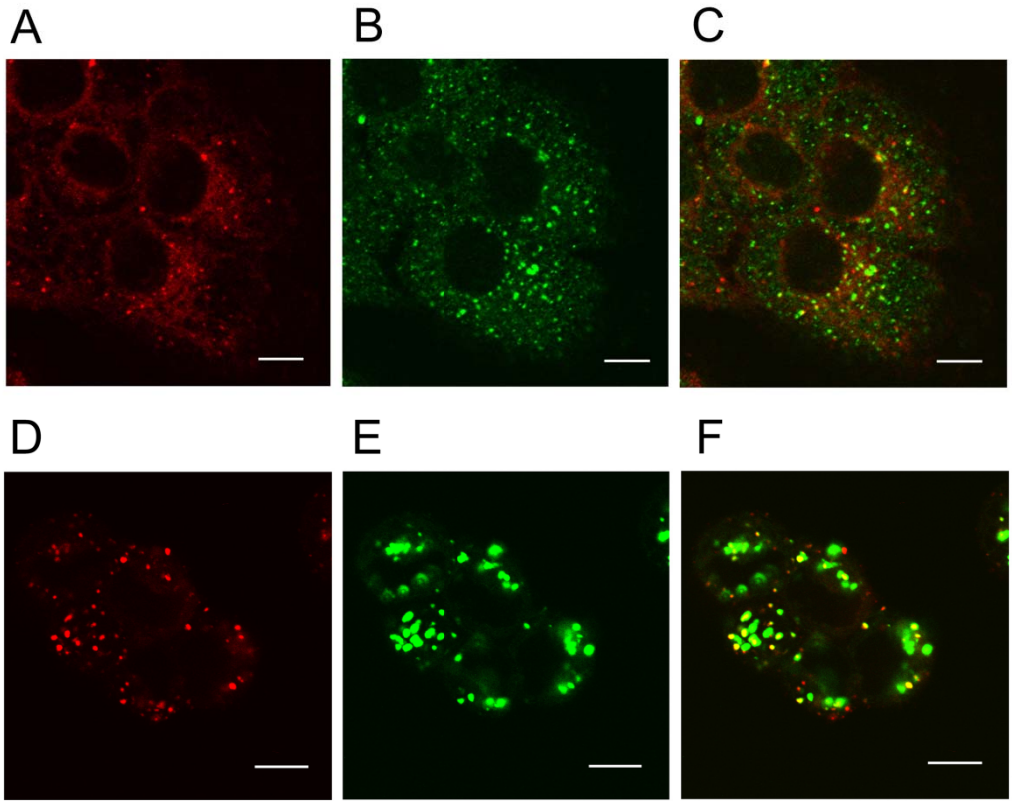

Figure 42 Localization of SV119-liposomes in DU-145 cells.

Cells were incubated with rhodamine-PE labeled SV119-liposomes for 3h (A-C) or 16h (D-F) in serum-free medium, stained with markers of early endosomes (anti-EEA1; A-C) or lysosomes (Lysotracker® ; D-F), and imaged by confocal microscopy. Red fluorescence represents rhodamine-PE labeled liposomes (A and D), green fluorescence represents early endosomes (B) or lysosomes (E). Yellow color observed in the red + green overlay (C and F) indicates co-localization of red liposomes with the green endosomes (C) or lysosomes (F). Scale bar = 10 μm.

liposomes were largely accumulated in the lysosomes, as evident by co-localization with markers of lysosomes (LysoTracker®; Figure 42D-F). These observations are consistent with the internalization via the endocytosis pathway. Future studies are warranted to improve the formulation to achieve more efficient release from endosomes and lysosomes.

5.3.5 Cytotoxicity of DOX-loaded liposomes

After demonstrating the efficiency and specificity of SV119 in mediating the uptake of liposomes by tumor cells, we investigated the utility of the SV119-liposomes for targeted delivery of anticancer agents. We chose DOX as the model drug since its liposomal formulation Doxil® is well-established and widely used in clinical chemotherapy. DU-145 cells were pre-treated with DOX-loaded SV119-liposomes (SV119-L[D]), DOX-loaded unmodified liposomes (L[D]) and free DOX for 1h, and the cells were then cultured for an additional 72 h before conducting the MTT assay. Results show that the cytotoxic effects of all treatments were dose-dependent at concentrations of 0.2~10 μg/mL (Figure 43). At each indicated concentration, the viability of cells treated with L[D] showed 1.5-3 folds enhancement compared with that of free DOX, suggesting the protection of the cells by encapsulation of the drug into liposomes. In addition, SV119-L[D] exhibited a ~2-fold higher cytotoxicity to DU-145 cells than L[D] (Figure 43), suggesting improved efficacy of the SV119-modified liposomes vs. unmodified liposomes for delivering DOX to the tumor cells. The increased cytotoxicity of SV119-L[D] is consistent with the enhanced uptake of SV119-liposomes as shown in Figure 36. This demonstrates the potential of SV119-liposome to be used as a carrier for the targeted delivery of chemotherapeutics to tumor cells.

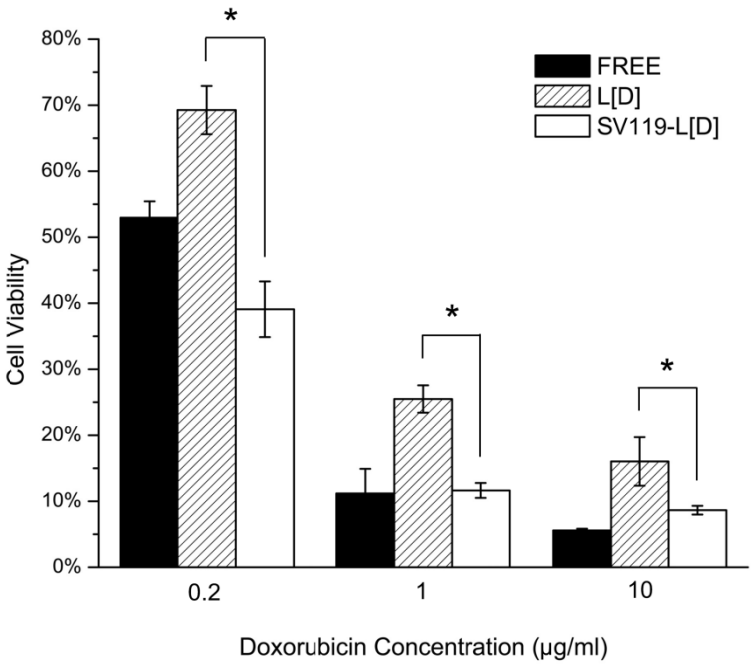

Figure 43 Cytotoxic effect of free and liposomal DOX on DU-145 prostate cancer cells.

Cells were treated with free DOX, DOX-loaded SV119-liposomes or DOX-loaded unmodified liposomes with DOX concentrations at 0.2, 1 or 10 µg/mL. Cytotoxicity was assessed by MTT assay. Cells receiving no treatment were defined as the maximal cell viability. Values presented are the mean± SD of six replicates. *P<.05 compared with control treatments with unmodified liposomes.

5.4 DISCUSSION

Recently, several selective sigma-2 receptor ligands have been developed and evaluated in vitro and in vivo. For example, Mach et al reported the synthesis of a series of N-substituted 9-azabicyclo[3.3.1]nonan-3a-yl phenylcarbamate analogs (Mach et al. 2009). Several high affinity sigma-2-selective ligands such as SV119 were identified through structure-activity relationship (SAR) studies. SV119 has a free amino group that is linked to a bridgehead nitrogen atom via a

linker group of 6 methylene units. SAR studies suggest that the amino group is a preferred substituent for assuring a high affinity for σ2 receptors and high σ1 : σ2 selectivity. Nevertheless, various SV119 conjugates were synthesized by chemical modification of this amino group. For example, coupling of SV119 to a fluorescence molecule via this amino group lead to the development of a sigma-2-selective probe, SW-120, which was used as an effective tool for the assessment of sigma-2 receptor expression levels in cultured tumor cells (Xu et al. 2011). In addition, a recent study by Spitzer et al showed that coupling of SV119 to a proapoptotic peptide via the amino group similarly led to the development of a conjugate that demonstrated selective cytotoxicity towards tumor cells that overexpress sigma-2 receptor (Spitzer et al. 2012).

We have demonstrated successful synthesis of the functional lipid, SV119-PEG-DOA, as well as its incorporation into a liposome formulation for targeted delivery to cancer cells. As compared with unmodified liposomes, the SV119-liposomes demonstrated enhanced uptake by multiple types of tumor cell lines including DU-145, MCF-7, PC-3, 201T and A549 cells. In addition, this enhanced uptake was shown to be dependent on ligand density and incubation time, and the uptake of SV119-liposomes was dramatically inhibited by the presence of free SV119. In contrast, enhanced uptake of SV119-liposomes was not observed in BEAS-2B normal cells, suggesting that enhanced uptake is specific for tumor cells. Furthermore, results of the MTT assay suggest that the incorporation of SV119 onto the surface of liposomes significantly enhanced the delivery and cytotoxicity of liposomal DOX in vitro. Recently, Xia and colleague reported that SV119 mediated selective delivery of SV119-gold nanocage conjugates to tumor cells (Wang et al. 2012c). Collectively, these data suggest that SV119-

conjugated nanoparticles may represent a promising delivery system for the targeted delivery of anticancer therapeutics to tumor cells.

6.0 SUMMARY AND PERSPECTIVES

6.1 The role of miR-29 in liver fibrosis

Liver fibrosis is a chronic disorder that is characterized by an alteration of the balance between fibrogenesis and fibrolysis, resulting in accumulation of excessive amounts of extracellular matrix (ECM) and distortion of the normal liver architecture. The activation and transformation of quiescent hepatic stellate cells (HSCs) into myofibroblast-like cells constitute a major mechanism for the increased production of ECM in the liver. The nuclear receptor farnesoid X receptor (FXR) shows potent antifibrotic activity in HSCs and protects animals in rodent models of liver fibrosis. However, the detailed mechanism remains incompletely understood. We report in this study that treatment with GW4064, a synthetic FXR ligand, led to upregulation of microRNA-29a (miR-29a) in HSCs isolated from wild-type mice, rats, and humans but not from FXR-/-mice. MiR-29a appears to play an inhibitory role in the regulation of ECM production as: 1) transfection of HSCs with miR-29a mimic resulted in drastic downregulation of the mRNA expression of a number of genes encoding ECM proteins; and 2) miR-29a significantly inhibited the expression of a reporter expression plasmid that contains the 3'-UTR of the corresponding ECM genes. My results suggest that miR-29a is a FXR target gene because miR-29a promoter activity was significantly increased by pharmacological or genetic activation of FXR. Functional analysis of human miR-29a gene promoter identified an

imperfect inverted repeat DNA motif, IR1 (-AGGTCAcAGACCT), as a likely FXR-responsive element that is involved in miR-29a regulation. Our study uncovers a new mechanism by which FXR negatively regulates the expression of ECM in HSCs.

Altered expression of miR-29b is implicated in the pathogenesis and progression of liver fibrosis. We and others previously demonstrated that miR-29b down-regulates the expression of several extracellular-matrix (ECM) genes including Col 1A1, Col 3A1 and Elastin via directly targeting their 3'-UTRs. However, whether or not miR-29b plays a role in the post-translational regulation of ECM biosynthesis has not been reported. Heat shock protein 47 (HSP47) and lysyl oxidase (LOX) are known to be essential for ECM maturation. In this study I have demonstrated that expression of HSP47 and LOX was significantly up-regulated in culture-activated primary rat HSCs, TGF-β stimulated LX-2 cells and liver tissue of CCl_4-treated mice, which was accompanied by a decrease of miR-29b level. In contrast, over-expression of miR-29b in LX-2 cells resulted in significant inhibition on HSP47 and LOX expression. Mechanistically, miR-29b inhibited the expression of a reporter gene that contains the respective full-length 3'-UTR from HSP47 and LOX gene, and this inhibitory effect was abolished by the deletion of a putative miR-29b targeting sequence from the 3'-UTRs. Transfection of LX-2 cells with miR-29b led to abnormal collagen structure as shown by electron-microscopy, presumably through down-regulation of the expression of molecules involved in ECM maturation including HSP47 and LOX. These results demonstrated that miR-29b plays a role in regulating the post-translational processing of ECM and fibril formation.

The study of miRNAs and their roles in physiology and diseased processes has become a rapidly evolving field, as evidenced by the increasing body of literature. However, our understanding of how miRNAs function in liver diseases remains limited. MiRNAs are only one

class of regulatory molecules in the cells; there are many transcriptional factors and nuclear receptors that are also involved in gene regulation. How the regulatory networks amongst miRNAs, transcription factors, and their target genes are governed is just beginning to be discovered and understood. As discussed before, FXR activation can lead to upregulation of miR-29a, which is one of the major effectors to downregulate fibrosis-related genes. This reflects the complicated interaction of different regulatory machineries in controlling important physiological and pathophysiological events.

It has become increasingly apparent that miRNA analysis may aid in disease diagnosis as well as the prediction of drug response and prognosis. Therapeutic applications using miRNA overexpression or downregulation may also represent a new strategy for the treatment of various diseases including liver diseases. MiRNAs are small molecules comprised of a known sequence that is often completely conserved among species, and these features are very attractive from a drug development standpoint. However, several issues need to be considered before the microRNA therapeutics enter the clinic. Firstly, safety is an important concern in drug development. In order to minimize the potential off target effects, the miRNAs that are more tissue restricted will be preferred, especially for chronic diseases. For example, inhibition of a hepatic-specific miRNA, miR-122, by LNA-anti-miR was shown to be safe and efficacious in the treatment of HCV-induced liver pathology. Secondly, intravenous gene delivery has to overcome three barriers at blood circulation, cellular and intracellular level, which include: (1) to decrease non-specific interactions with blood components and increase stability of microRNA in blood circulation; (2) to enhance the binding and uptake of microRNAs to the appropriate tissue or cells; and (3) effectively trigger the release of delivered microRNA from

endosomes to cytoplasm. These challenges will hopefully be addressed by appropriate design of delivery systems for microRNAs (Li et al. 2013b).

It is generally believed that a single miRNA can potentially regulate hundreds of target mRNAs due to the fact that the primary target recognition determinant is only seven to eight nucleotides long in the seed region. This notion was further validated by a transcriptome analysis of tissues isolated from mice with targeted deletion of miRNAs. Thus, the potential off-target of miRNA therapeutics needs to be thoroughly examined in animal and human studies.

Liver cirrhosis is the leading cause of hepatocellular carcinoma (HCC), which is the fifth most common cancer in the world. Thus the second half of my dissertation work was mainly focused on the development of nanocarriers for tumor-targeted drug delivery.

6.2 Tumor-targeted drug delivery with micelles

Paclitaxel (PTX) is a potent chemotherapeutic agent, however, the clinical application of PTX is often limited by its poor water solubility and the toxicity of solubilizers used in its formulation. Many stable and non-toxic formulations of PTX such as PEG-derivatized Vitamin E polymeric micelles have been developed, which exhibit favorable biological activity in addition to solubilizing PTX. We have previously developed a series of PEG-Vitamin E conjugates with various lengths of PEG and different number of Vitamin E chains, among which the PEG_{5K}-VE_2 has been shown to be the most effective PTX micellar formulation. However, the PEG_{5K}-VE_2 formulation is still limited by the insufficient drug loading. Herein we report that the loading capacity for PTX could be significantly improved via incorporation of a drug-interactive motif (Fmoc) into the system. The PEG_{5K}-(Fmoc)-VE_2 (PEG-FVE_2) micelles have a low CMC value

of 4 μg/ml and show a morphology of both spherical and worm-like structures on electron microscope. The Fmoc/PTX physical interaction was demonstrated by a fluorescence quenching assay. PTX-loaded PEG-FVE_2 micelles exerted more potent cytotoxicity than free PTX or Taxol formulation in several tumor cell lines. Finally, intravenous injection of PTX-loaded PEG-FVE_2 micelles showed superior anticancer activity and minimal toxicity compared with Taxol formulation in a mouse model of breast cancer.

Polymeric micelles have been extensively studied over the last decade as versatile and efficient drug delivery systems for cancer therapy. The design of polymer structure is increasingly sophisticated to improve the drug loading capacity, tumor-specific uptake as well as anticancer effect. Various strategies have been developed to increase the drug/carrier interaction of polymeric micelles to maximize the drug loading capacity, such as hydrotropic polymers and Fmoc-conjugated surfactants. In addition, several biologically active carriers have been developed as dual-functional carriers to improve the anticancer effect. More systematic studies on the structure-activity relationship of polymeric micellar systems are needed to better understand the mechanism of drug-carrier interaction and the effect of polymer structure on the drug loading capacity. In addition, computational modeling may offer help in the tailored design of a polymeric carrier for each drug. These studies shall lead to the development of further improved micellar systems to advance the treatment of cancers.

APPENDIX A

SEQUENCES OF PRIMERS FOR AMPLIFICATION OF 3'-UTR AND REAL-TIME PCR

Gene	Forward primer	Reverse primer
Col1A1 3'-UTR	ACGAGCTCAAACTCCCTCCATCCCAATC	ACACGCGTCCACCCCAGGGATAAAAACT
Mutated Col1A1 3'-UTR	ACGAGCTCAAACTCCCTCCATCCCAATC	ACACGCGTATGGCCAGGCTTTGACCATTTG
Col3A1 3'-UTR	ACGAGCTCTTATAAGCCAAACTCTCTGAAAC	ACACGCGTTGATGTTTATTTATTATATCACCATTA
Mutated Col3A1 3'-UTR	ACGAGCTCTTATAAGCCAAACTCTCTGAAAC	ACACGCGTGAGACAGGGTGAAGTTGGAATTGG
ELN1 3'-UTR	ACACGCGTCTGACTCGCGACCTCGTCA	ACAAGCTTCACAGCGAAACACAAAGAGG
Mutated ELN1 3'-UTR	CCCACGCGTGGGGGTGCTACTGCTTGGTGGAG	CGAAGCTTCGCACCAATTTCTCTTGGAGATGG
miR-29a	TAGCACCATCTGAAATCGGTTA	UNIVERSAL PRIMER
rno-mir-29a precursor	CCCTTAGAGGATGACTGATTTC	AACCGATTTCAGATGGTGCT
rno-mir-29b precursor	GGAAGCTGGTTTCACATGGT	TCCTAAAACACTGATTTCAAATGG

rno-mir-29c precursor	ACACAGGCTGACCGATTTCT	CCCCTACATCATAACCGATTTC
hsa-mir-29a precursor	TGACTGATTTCTTTTGGTGTTCA	AACCGATTTCAGATGGTGCT
mmu-mir-29a precursor	CCCTTAGAGGATGACTGATTTC	AACCGATTTCAGATGGTGCT
Mus-HSP47	TGAACGCCATGTTCTTTAAGC	AGTATAGGAGCGGGTCACCA
Mus-LOX	GGAGGACACGTCCTGTGACT	CTGCCGCATAGGTGTCATAA
Rat-HSP47	CTGCCTGAGAGCGAGTGTC	AGGTGCCCAGAAGGAGAGAG
Rat-LOX	GCAAGCTTCTGTCTGGAGGA	TCATAACATCCGGGACTCAA
Homo-HSP47	GATGGGGAAGATGCAGAAGA	CTTGTCAATGGCCTCAGTCA
Homo-LOX	TCCTGTGACTATGGCTACCAC	GGCAGTCTATGTCTGCACCA
HSP47 WT 3'-UTR	CGACGCGTCGCTCAGGGTGCACA CAGGAT	CCCAAGCTTGGGCTTCCACGCTC CAACAAAAT
HSP47 Mut 3'-UTR	CGACGCGTCGGTGAGGTACCAGC CTTGGAT	CCCAAGCTTGGGCTTCCACGCTC CAACAAAAT
LOX WT 3'-UTR	CGAGCTCGATGGACACATCTGGT GCTGA	CGACGCGTCGAAGATTTAATGC ATTTTACATTCAGA
LOX Mut 3'-UTR-L	CGAGCTCGAAACACATTACCATT GGTGTCAA	ACGTACTACGTGTAATTTCATTT TCTTGAATTTAGGT
LOX Mut 3'-UTR-R	CGTAGTACGTTCTCAAGTAAGAT TTTCCAGTGC	CGACGCGTCGGCTTAGAGGATA AATGAAATGTTTAGT

BIBLIOGRAPHY

Ackley D.C., Rockich K.T., and Baker T. R. (2004) "Metabolic Stability Assessed by Liver Microsomes and Hepatocytes." Methods in Pharmacology and Toxicology. Optimization in Drug Discovery. Editors: Yan Z., and Caldwell G.W. pp 151-162

Adam, O., K. Theobald, D. Lavall, M. Grube, H. K. Kroemer, S. Ameling, H. J. Schafers, M. Bohm and U. Laufs (2011). "Increased lysyl oxidase expression and collagen cross-linking during atrial fibrillation." J Mol Cell Cardiol **50**(4): 678-85.

Aggarwal, B. B., A. Kumar and A. C. Bharti (2003). "Anticancer potential of curcumin: preclinical and clinical studies." Anticancer Res **23**(1A): 363-98.

Aggarwal, B. B. and S. Shishodia (2006). "Molecular targets of dietary agents for prevention and therapy of cancer." Biochem Pharmacol **71**(10): 1397-421.

Agrawal, N., P. V. N. Dasaradhi, A. Mohmmed, P. Malhotra, R. K. Bhatnagar and S. K. Mukherjee (2003). "RNA interference: Biology, mechanism, and applications." Microbiol Mol Biol Rev **67**(4): 657-85.

Ahn, K. S., G. Sethi and B. B. Aggarwal (2007). "Embelin, an inhibitor of X chromosome-linked inhibitor-of-apoptosis protein, blocks nuclear factor-kappaB (NF-kappaB) signaling pathway leading to suppression of NF-kappaB-regulated antiapoptotic and metastatic gene products." Mol Pharmacol **71**(1): 209-19.

Ambros, V. (2001). "microRNAs: Tiny regulators with great potential." Cell **107**(7): 823-26.

Anand, P., H. B. Nair, B. Sung, A. B. Kunnumakkara, V. R. Yadav, R. R. Tekmal and B. B. Aggarwal (2010). "Design of curcumin-loaded PLGA nanoparticles formulation with enhanced cellular uptake, and increased bioactivity in vitro and superior bioavailability in vivo." Biochem Pharmacol **79**(3): 330-8.

Anisfeld, A. M., H. R. Kast-Woelbern, H. Lee, Y. Zhang, F. Y. Lee and P. A. Edwards (2005). "Activation of the nuclear receptor FXR induces fibrinogen expression: a new role for bile acid signaling." J Lipid Res **46**(3): 458-68.

Anuchapreeda, S., P. Limtrakul, P. Thanarattanakorn, S. Sittipreechacharn and P. Chanarat (2006). "Inhibitory effect of curcumin on WT1 gene expression in patient leukemic cells." Arch Pharm Res **29**(1): 80-7.

Aydar E., C. P. Palmer and M. B. Djamgoz (2004) "Sigma receptors and cancer: possible involvement of ion channels." Cancer Res **64**(15):5029-35.

Banerjee, R., P. Tyagi, S. Li and L. Huang (2004). "Anisamide-targeted stealth liposomes: A potent carrier for targeting doxorubicin to human prostate cancer cells." Int J Cancer **112**(4): 693-700.

Barad, O., E. Meiri, A. Avniel, R. Aharonov, A. Barzilai, I. Bentwich, U. Einav, S. Glad, P. Hurban, Y. Karov, E. K. Lobenhofer, E. Sharon, Y. M. Shiboleth, M. Shtutman, Z. Bentwich and P. Einat (2004). "MicroRNA expression detected by oligonucleotide microarrays: System establishment and expression profiling in human tissues." Genome Res **14**(12): 2486-94.

Barkan, B., S. Starinsky, E. Friedman, R. Stein and Y. Kloog (2006). "The Ras Inhibitor Farnesylthiosalicylic Acid as a Potential Therapy for Neurofibromatosis Type 1." Clin Cancer Res **12**(18): 5533-42.

Bataller, R. and D. A. Brenner (2005). "Liver fibrosis." J Clin Invest **115**(2): 209-18.

Bauduin, P., A. Renoncourt, A. Kopf, D. Touraud and W. Kunz (2005). "Unified concept of solubilization in water by hydrotropes and cosolvents." Langmuir **21**(15): 6769-75.

Benahmed, A., M. Ranger and J. C. Leroux (2001). "Novel polymeric micelles based on the amphiphilic diblock copolymer poly(N-vinyl-2-pyrrolidone)-block-poly(D,L-lactide)." Pharm Res **18**(3): 323-8.

Berezovskaya, O., A. D. Schimmer, A. B. Glinskii, C. Pinilla, R. M. Hoffman, J. C. Reed and G. V. Glinsky (2005). "Increased expression of apoptosis inhibitor protein XIAP contributes to anoikis resistance of circulating human prostate cancer metastasis precursor cells." Cancer Res **65**(6): 2378-86.

Bertolotti, M., C. Gabbi, C. Anzivino, L. Carulli, P. Loria and N. Carulli (2008). "Nuclear Receptors as Potential Molecular Targets in Cholesterol Accumulation Conditions: Insights from Evidence on Hepatic Cholesterol Degradation and Gallstone Disease in Humans." Curr Med Chem **15**(22): 2271-84.

Bhandari, U., N. Jain and K. K. Pillai (2007). "Further studies on antioxidant potential and protection of pancreatic beta-cells by Embelia ribes in experimental diabetes." Exp Diabetes Res **2007**: 15803.

Blum, R. and Y. Kloog (2005). "Tailoring Ras-pathway--inhibitor combinations for cancer therapy." Drug Resist Updat **8**(6): 369-80.

Bos, J. L. (1989). "Ras oncogenes in human cancer: a review." Cancer Res **49**(17): 4682-9.

Broxterman, H. J. and N. H. Georgopapadakou (2005). "Anticancer therapeutics: "addictive" targets, multi-targeted drugs, new drug combinations." Drug Resist Updat **8**(4): 183-97.

Cao, N. and S. S. Feng (2008). "Doxorubicin conjugated to D-alpha-tocopheryl polyethylene glycol 1000 succinate (TPGS): Conjugation chemistry, characterization, in vitro and in vivo evaluation." Biomaterials **29**(28): 3856-65.

Cao, X., S. L. Pfaff and F. H. Gage (2007). "A functional study of miR-124 in the developing neural tube." Genes Dev **21**(5): 531-6.

Carstens, M. G., P. H. de Jong, C. F. van Nostrum, J. Kemmink, R. Verrijk, L. G. de Leede, D. J. Crommelin and W. E. Hennink (2008). "The effect of core composition in biodegradable oligomeric micelles as taxane formulations." Eur J Pharm Biopharm **68**(3): 596-606.

Chandran, T., U. Katragadda, Q. Teng and C. Tan (2010). "Design and evaluation of micellar nanocarriers for 17-allyamino-17-demethoxygeldanamycin (17-AAG)." Int J Pharm **392**(1-2): 170-7.

Chandrasekharan, P., D. Maity, C. X. Yong, K. H. Chuang, J. Ding and S. S. Feng (2011). "Vitamin E (D-alpha-tocopheryl-co-poly(ethylene glycol) 1000 succinate) micelles-superparamagnetic iron oxide nanoparticles for enhanced thermotherapy and MRI." Biomaterials **32**(24): 5663-72.

Charman, W., C. Lai, D. Craik, B. Finnin and B. Reed (1993). "Self-Association of Nicotinamide in Aqueous-Solution: N.M.R. Studies of Nicotinamide and the Mono- and Di-methyl-Substituted Amide Analogs." Aust J Chem **46**(3): 377-85.

Chau, B. N. and D. A. Brenner (2011). "What goes up must come down: the emerging role of microRNA in fibrosis." Hepatology **53**(1): 4-6.

Chiang, J. Y. L. (2002). "Bile acid regulation of gene expression: Roles of nuclear hormone receptors." Endocr Rev **23**(4): 443-63.

Chitra, M., E. Sukumar, V. Suja and C. S. Devi (1994). "Antitumor, anti-inflammatory and analgesic property of embelin, a plant product." Chemotherapy **40**(2): 109-13.

Chou, J., J. H. Lin, A. Brenot, J.-w. Kim, S. Provot and Z. Werb (2013). "GATA3 suppresses metastasis and modulates the tumour microenvironment by regulating microRNA-29b expression." Nat Cell Biol **15**(2): 201-13.

Choucair, A. and A. Eisenberg (2003). "Control of amphiphilic block copolymer morphologies using solution conditions." Eur Phys J E Soft Matter **10**(1): 37-44.

Christian, D. A., A. Tian, W. G. Ellenbroek, I. Levental, K. Rajagopal, P. A. Janmey, A. J. Liu, T. Baumgart and D. E. Discher (2009). "Spotted vesicles, striped micelles and Janus assemblies induced by ligand binding." Nat Mater **8**(10): 843-9.

Chua, F., J. Gauldie and G. J. Laurent (2005). "Pulmonary fibrosis: searching for model answers." Am J Respir Cell Mol Biol **33**(1): 9-13.

Chung, J. E., M. Yokoyama, T. Aoyagi, Y. Sakurai and T. Okano (1998). "Effect of molecular architecture of hydrophobically modified poly(N-isopropylacrylamide) on the formation of thermoresponsive core-shell micellar drug carriers." J Control Release **53**(1-3): 119-30.

Claudel, T., E. Sturm, H. Duez, I. P. Torra, A. Sirvent, V. Kosykh, J. C. Fruchart, J. Dallongeville, D. W. Hum, F. Kuipers and B. Staels (2002). "Bile acid-activated nuclear receptor FXR suppresses apolipoprotein A-I transcription via a negative FXR response element." J Clin Invest **109**(7): 961-71.

Cobos, E. J., J. M. Entrena, F. R. Nieto, C. M. Cendan and E. Del Pozo (2008). "Pharmacology and Therapeutic Potential of Sigma(1) Receptor Ligands." Curr Neuropharmacol **6**(4): 344-66.

Coburn, G. A. and B. R. Cullen (2003). "siRNAs: a new wave of RNA-based therapeutics." J Antimicrob Chemother **51**(4): 753-56.

Coffman, R. and D. Kildsig (1996). "Hydrotropic solubilization— mechanistic studies." Pharmaceut Res **13**(10): 1460-63.

Colabufo, N. A., F. Berardi, M. Contino, S. Ferorellia, M. Niso, R. Perrone, A. Pagliarulo, P. Saponaro and V. Pagliarulo (2006). "Correlation between sigma(2) receptor protein expression and histopathologic grade in human bladder cancer." Cancer Lett **237**(1): 83-88.

Collnot, E. M., C. Baldes, U. F. Schaefer, K. J. Edgar, M. F. Wempe and C. M. Lehr (2010). "Vitamin E TPGS P-glycoprotein inhibition mechanism: influence on conformational flexibility, intracellular ATP levels, and role of time and site of access." Mol Pharm **7**(3): 642-51.

Crottès D., H. Guizouarn, P. Martin, F. Borgese and O. Soriani (2013) "The sigma-1 receptor: a regulator of cancer cell electrical plasticity?" Front. Physiol. 4:175

Croy, S. R. and G. S. Kwon (2006). "Polymeric micelles for drug delivery." Curr Pharm Des **12**(36): 4669-84.

Cui, Y. (2010). "Parallel stacking of caffeine with riboflavin in aqueous solutions: The potential mechanism for hydrotropic solubilization of riboflavin." Int J Pharmaceut **397**(1–2): 36-43.

Cushing, L., P. P. Kuang, J. Qian, F. Shao, J. Wu, F. Little, V. J. Thannickal, W. V. Cardoso and J. Lu (2011). "miR-29 is a major regulator of genes associated with pulmonary fibrosis." Am J Respir Cell Mol Biol **45**(2): 287-94.

da Silva, R. C., M. Spitzer, L. s. H. M. da Silva and W. Loh (1999). "Investigations on the mechanism of aqueous solubility increase caused by some hydrotropes." Thermochim Acta **328**(1–2): 161-67.

Dai, Y., L. Qiao, K. W. Chan, M. Yang, J. Ye, J. Ma, B. Zou, Q. Gu, J. Wang, R. Pang, H. Y. Lan and B. C. Wong (2009). "Peroxisome proliferator-activated receptor-gamma contributes to the inhibitory effects of Embelin on colon carcinogenesis." Cancer Res **69**(11): 4776-83.

Danhier, F., N. Magotteaux, B. Ucakar, N. Lecouturier, M. Brewster and V. Preat (2009). "Novel self-assembling PEG-p-(CL-co-TMC) polymeric micelles as safe and effective delivery system for Paclitaxel." Eur J Pharm Biopharm **73**(2): 230-38.

Danquah, M., F. Li, C. B. Duke, 3rd, D. D. Miller and R. I. Mahato (2009). "Micellar delivery of bicalutamide and embelin for treating prostate cancer." Pharm Res **26**(9): 2081-92.

Danson, S., D. Ferry, V. Alakhov, J. Margison, D. Kerr, D. Jowle, M. Brampton, G. Halbert and M. Ranson (2004). "Phase I dose escalation and pharmacokinetic study of pluronic polymer-bound doxorubicin (SP1049C) in patients with advanced cancer." Br J Cancer **90**(11): 2085-91.

Davis, M. E., Z. G. Chen and D. M. Shin (2008). "Nanoparticle therapeutics: an emerging treatment modality for cancer." Nat Rev Drug Discov **7**(9): 771-82.

Deeb, D., H. Jiang, X. Gao, S. Al-Holou, A. L. Danyluk, S. A. Dulchavsky and S. C. Gautam (2007). "Curcumin [1,7-Bis(4-hydroxy-3-methoxyphenyl)-1–6-heptadine-3,5-dione; C21H20O6] Sensitizes Human Prostate Cancer Cells to Tumor Necrosis Factor-Related Apoptosis-Inducing Ligand/Apo2L-Induced Apoptosis by Suppressing Nuclear Factor-κB via Inhibition of the Prosurvival Akt Signaling Pathway." J Pharmacol Exp Ther **321**(2): 616-25.

Di Paolo, D., F. Pastorino, C. Brignole, D. Marimpietri, M. Loi, M. Ponzoni and G. Pagnan (2008). "Drug delivery systems: application of liposomal anti-tumor agents to neuroectodermal cancer treatment." Tumori **94**(2): 246-53.

Dintaman, J. M. and J. A. Silverman (1999). "Inhibition of P-glycoprotein by D-alpha-tocopheryl polyethylene glycol 1000 succinate (TPGS)." Pharm Res **16**(10): 1550-6.

Dong, H., M. Paquette, A. Williams, R. T. Zoeller, M. Wade and C. Yauk (2010). "Thyroid hormone may regulate mRNA abundance in liver by acting on microRNAs." PLoS One **5**(8): e12136.

Dong, Y. and S. S. Feng (2005). "Poly(d,l-lactide-co-glycolide)/montmorillonite nanoparticles for oral delivery of anticancer drugs." Biomaterials **26**(30): 6068-76.

Downes, M., M. A. Verdecia, A. J. Roecker, R. Hughes, J. B. Hogenesch, H. R. Kast-Woelbern, M. E. Bowman, J.-L. Ferrer, A. M. Anisfeld, P. A. Edwards, J. M. Rosenfeld, J. G. A. Alvarez, J. P. Noel, K. C. Nicolaou and R. M. Evans (2003). "A Chemical, Genetic, and Structural Analysis of the Nuclear Bile Acid Receptor FXR." Mol Cell **11**(4): 1079-92.

Downward, J. (2003). "Targeting RAS signalling pathways in cancer therapy." Nat Rev Cancer **3**(1): 11-22.

El-Serag H. B. (2011). "Hepatocellular Carcinoma." N Engl J Med **365**:1118-1127

Eliaz, R. E. and F. C. Szoka, Jr. (2001). "Liposome-encapsulated doxorubicin targeted to CD44: a strategy to kill CD44-overexpressing tumor cells." Cancer Res **61**(6): 2592-601.

Eloranta, J. J. and G. A. Kullak-Ublick (2008). "The role of FXR in disorders of bile acid homeostasis." Physiology (Bethesda) **23**: 286-95.

Fattovich. G., T. Stroffolini, I. Zagni and F. Donato (2004). "Hepatocellular carcinoma in cirrhosis: incidence and risk factors." Gastroenterology. **127**(5 Suppl 1):S35-50.

Fiorucci, S., E. Antonelli, G. Rizzo, B. Renga, A. Mencarelli, L. Riccardi, S. Orlandi, R. Pellicciari and A. Morelli (2004). "The nuclear receptor SHP mediates inhibition of hepatic stellate cells by FXR and protects against liver fibrosis." Gastroenterology **127**(5): 1497-512.

Fiorucci, S., G. Rizzo, E. Antonelli, B. Renga, A. Mencarelli, L. Riccardi, A. Morelli, M. Pruzanski and R. Pellicciari (2005a). "Cross-talk between farnesoid-X-receptor (FXR)and peroxisome proliferator-activated receptor gamma contributes to the antifibrotic activity of FXR ligands in rodent models of liver cirrhosis." J Pharmacol Exp Ther **315**(1): 58-68.

Fiorucci, S., G. Rizzo, E. Antonelli, B. Renga, A. Mencarelli, L. Riccardi, S. Orlandi, M. Pruzanski, A. Morelli and R. Pellicciari (2005b). "A farnesoid X receptor-small heterodimer partner regulatory cascade modulates tissue metalloproteinase inhibitor-1 and matrix metalloprotease expression in hepatic stellate cells and promotes resolution of liver fibrosis." J Pharmacol Exp Ther **314**(2): 584-95.

Fogelgren, B., N. Polgár, K. M. Szauter, Z. Újfaludi, R. Laczkó, K. S. K. Fong and K. Csiszar (2005). "Cellular Fibronectin Binds to Lysyl Oxidase with High Affinity and Is Critical for Its Proteolytic Activation." J Biol Chem **280**(26): 24690-97.

Forman, B. M., E. Goode, J. Chen, A. E. Oro, D. J. Bradley, T. Perlmann, D. J. Noonan, L. T. Burka, T. McMorris, W. W. Lamph, R. M. Evans and C. Weinberger (1995).

"Identification of a nuclear receptor that is activated by farnesol metabolites." Cell **81**(5): 687-93.

Forman, J. J., A. Legesse-Miller and H. A. Coller (2008). "A search for conserved sequences in coding regions reveals that the let-7 microRNA targets Dicer within its coding sequence." Proc Natl Acad Sci U S A **105**(39): 14879-84.

Friedman, S. L. (2008). "Hepatic stellate cells: protean, multifunctional, and enigmatic cells of the liver." Physiol Rev **88**(1): 125-72.

Fuchs, M. (2012). "Non-alcoholic Fatty liver disease: the bile Acid-activated farnesoid x receptor as an emerging treatment target." J Lipids **2012**: 934396.

Furui, K., T. Takahara, H. Ito, Y. Nakayama, C. Miyabayashi, K. Higuchi, A. Watanabe and A. Ooshima (1995). "Gene expression of lysyl oxidase in CCl_4-induced liver injury." Int Hepatol Commun **3**(1000): 3-3.

Gabizon, A. A. (1995). "Liposome Circulation Time and Tumor Targeting - Implications for Cancer-Chemotherapy." Adv Drug Deliver Rev **16**(2-3): 285-94.

Galli, A., D. W. Crabb, E. Ceni, R. Salzano, T. Mello, G. Svegliati-Baroni, F. Ridolfi, L. Trozzi, C. Surrenti and A. Casini (2002). "Antidiabetic thiazolidinediones inhibit collagen synthesis and hepatic stellate cell activation in vivo and in vitro." Gastroenterology **122**(7): 1924-40.

Gana-Weisz, M., J. Halaschek-Wiener, B. Jansen, G. Elad, R. Haklai and Y. Kloog (2002). "The Ras inhibitor S-trans,trans-farnesylthiosalicylic acid chemosensitizes human tumor cells without causing resistance." Clin Cancer Res **8**(2): 555-65.

Gao, X., Y. Huang, A. M. Makhov, M. Epperly, J. Lu, S. Grab, P. Zhang, L. Rohan, X. Q. Xie, P. Wipf, J. Greenberger and S. Li (2013). "Nanoassembly of surfactants with interfacial drug-interactive motifs as tailor-designed drug carriers." Mol Pharm **10**(1): 187-98.

Gao, Y., L. B. Li and G. Zhai (2008). "Preparation and characterization of Pluronic/TPGS mixed micelles for solubilization of camptothecin." Colloids Surf B Biointerfaces **64**(2): 194-9.

Gao, Z., A. N. Lukyanov, A. Singhal and V. P. Torchilin (2002). "Diacyllipid-Polymer Micelles as Nanocarriers for Poorly Soluble Anticancer Drugs." Nano Letters **2**(9): 979-82.

Gaucher, G., M. H. Dufresne, V. P. Sant, N. Kang, D. Maysinger and J. C. Leroux (2005). "Block copolymer micelles: preparation, characterization and application in drug delivery." J Control Release **109**(1-3): 169-88.

Ge, X., L. Yin, H. Ma, T. Li, J. Y. Chiang and Y. Zhang (2011). "Aldo-keto reductase 1B7 is a target gene of FXR and regulates lipid and glucose homeostasis." J Lipid Res **52**(8): 1561-8.

Geng, Y., P. Dalhaimer, S. Cai, R. Tsai, M. Tewari, T. Minko and D. E. Discher (2007). "Shape effects of filaments versus spherical particles in flow and drug delivery." Nat Nanotechnol **2**(4): 249-55.

Georges, P. C., J. J. Hui, Z. Gombos, M. E. McCormick, A. Y. Wang, M. Uemura, R. Mick, P. A. Janmey, E. E. Furth and R. G. Wells (2007). "Increased stiffness of the rat liver precedes matrix deposition: implications for fibrosis." Am J Physiol Gastrointest Liver Physiol **293**(6): G1147-54.

Ghiassi-Nejad, Z. and S. L. Friedman (2008). "Advances in antifibrotic therapy." Expert Rev Gastroenterol Hepatol **2**(6): 803-16.

Ghildiyal, M. and P. D. Zamore (2009). "Small silencing RNAs: an expanding universe." Nat Rev Genet **10**(2): 94-108.

Giacomelli, C., V. Schmidt and R. Borsali (2007). "Specific interactions improve the loading capacity of block copolymer micelles in aqueous media." Langmuir **23**(13): 6947-55.

Gong, H., C. M. Liu, D. P. Liu and C. C. Liang (2005). "The role of small RNAs in human diseases: Potential troublemaker and therapeutic tools." Med Res Rev **25**(3): 361-81.

Gressner, A. M. (1995). "Cytokines and Cellular Crosstalk Involved in the Activation of Fat-Storing Cells." J Hepatol **22**: 28-36.

Gressner, A. M., S. Lotfi, G. Gressner, E. Haltner and J. Kropf (1993). "Synergism between Hepatocytes and Kupffer Cells in the Activation of Fat-Storing Cells (Perisinusoidal Lipocytes)." J Hepatol **19**(1): 117-32.

Grewal, T., M. Koese, F. Tebar and C. Enrich (2011). "Differential Regulation of RasGAPs in Cancer." Genes Cancer **2**(3): 288-97.

Grosshans, H. and F. J. Slack (2002). "Micro-RNAs: small is plentiful." J Cell Biol **156**(1): 17-21.

Guo, C. J., Q. Pan, D. G. Li, H. Sun and B. W. Liu (2009). "miR-15b and miR-16 are implicated in activation of the rat hepatic stellate cell: An essential role for apoptosis." J Hepatol **50**(4): 766-78.

Guo, W. and F. G. Giancotti (2004). "Integrin signalling during tumour progression." Nat Rev Mol Cell Biol **5**(10): 816-26.

Halaschek-Wiener, J., V. Wacheck, H. Schlagbauer-Wadl, K. Wolff, Y. Kloog and B. Jansen (2000). "A novel Ras antagonist regulates both oncogenic Ras and the tumor suppressor p53 in colon cancer cells." Mol Med **6**(8): 693-704.

Hamaguchi, T., K. Kato, H. Yasui, C. Morizane, M. Ikeda, H. Ueno, K. Muro, Y. Yamada, T. Okusaka, K. Shirao, Y. Shimada, H. Nakahama and Y. Matsumura (2007). "A phase I and pharmacokinetic study of NK105, a paclitaxel-incorporating micellar nanoparticle formulation." Br J Cancer **97**(2): 170-6.

Han, Y. C., C. Y. Park, G. Bhagat, J. Zhang, Y. Wang, J. B. Fan, M. Liu, Y. Zou, I. L. Weissman and H. Gu (2010). "microRNA-29a induces aberrant self-renewal capacity in hematopoietic progenitors, biased myeloid development, and acute myeloid leukemia." J Exp Med **207**(3): 475-89.

He, F. T., J. Li, Y. Mu, R. Kuruba, Z. Ma, A. Wilson, S. Alber, Y. Jiang, T. Stevens, S. Watkins, B. Pitt, W. Xie and S. Li (2006). "Downregulation of endothelin-1 by farnesoid X receptor in vascular endothelial cells." Circ Res **98**(2): 192-99.

He, L. and G. J. Hannon (2004). "MicroRNAs: Small RNAs with a big role in gene regulation." Nat Rev Genet **5**(8): 522-31.

Hisatomi, K., H. Mukae, N. Sakamoto, Y. Ishimatsu, T. Kakugawa, S. Hara, H. Fujita, S. Nakamichi, H. Oku, Y. Urata, H. Kubota, K. Nagata and S. Kohno (2012). "Pirfenidone inhibits TGF-beta1-induced over-expression of collagen type I and heat shock protein 47 in A549 cells." BMC Pulm Med **12**(1): 24.

Ho, S. N., H. D. Hunt, R. M. Horton, J. K. Pullen and L. R. Pease (1989). "Site-directed mutagenesis by overlap extension using the polymerase chain reaction." Gene **77**(1): 51-9.

Holy, J. (2004). "Curcumin inhibits cell motility and alters microfilament organization and function in prostate cancer cells." Cell Motil Cytoskeleton **58**(4): 253-68.

Holy, J. M. (2002). "Curcumin disrupts mitotic spindle structure and induces micronucleation in MCF-7 breast cancer cells." Mutat Res **518**(1): 71-84.

Hong HH, Pischon N, Santana RB, Palamakumbura AH, Chase HB, et al. (2004) "A role for lysyl oxidase regulation in the control of normal collagen deposition in differentiating osteoblast cultures." J Cell Physiol 200: 53-62.

Horwitz, S. B. (1994). "Taxol (paclitaxel): mechanisms of action." Ann Oncol **5 Suppl 6**: S3-6.

Hosokawa, N., C. Hohenadl, M. Satoh, K. Kuhn and K. Nagata (1998). "HSP47, a collagen-specific molecular chaperone, delays the secretion of type III procollagen transfected in human embryonic kidney cell line 293: A possible role for HSP47 in collagen modification." J Biochem **124**(3): 654-62.

Hu, P. F., H. Chen, W. Zhong, Y. Lin, X. Zhang, Y. X. Chen and W. F. Xie (2009). "Adenovirus-mediated transfer of siRNA against PAI-1 mRNA ameliorates hepatic fibrosis in rats." J Hepatol **51**(1): 102-13.

Huang, Y., J. Lu, X. Gao, J. Li, W. Zhao, M. Sun, D. B. Stolz, R. Venkataramanan, L. C. Rohan and S. Li (2012). "PEG-derivatized embelin as a dual functional carrier for the delivery of paclitaxel." Bioconjug Chem **23**(7): 1443-51.

Huh, K. M., S. C. Lee, Y. W. Cho, J. Lee, J. H. Jeong and K. Park (2005). "Hydrotropic polymer micelle system for delivery of paclitaxel." J Control Release **101**(1-3): 59-68.

Ishida, Y., H. Kubota, A. Yamamoto, A. Kitamura, H. P. Bächinger and K. Nagata (2006). " Type I collagen in Hsp47-null cells is aggregated in endoplasmic reticulum and deficient in N-propeptide processing and fibrillogenesis." Mol Biol Cell **17**(5): 2346-55.

Iwakiri, Y. (2012). "Endothelial dysfunction in the regulation of cirrhosis and portal hypertension." Liver Int **32**(2): 199-213.

Jackson, L. E., B. Faris, B. M. Martin, H. V. Jones, C. B. Rich, J. A. Foster and C. Franzblau (1991). "The effect of β-aminopropionitrile on elastin gene expression in smooth muscle cell cultures." Biochem Biophys Res Commun **179**(2): 939-44.

Jansen, B., H. Schlagbauer-Wadl, H. Kahr, E. Heere-Ress, B. X. Mayer, H. Eichler, H. Pehamberger, M. Gana-Weisz, E. Ben-David, Y. Kloog and K. Wolff (1999). "Novel Ras antagonist blocks human melanoma growth." Proc Natl Acad Sci U S A **96**(24): 14019-24.

Jha, A., M. Mehra and R. Shankar (2011). "The regulatory epicenter of miRNAs." J Biosci **36**(4): 621-38.

Ji, J., L. Zhao, A. Budhu, M. Forgues, H. L. Jia, L. X. Qin, Q. H. Ye, J. Yu, X. Shi, Z. Y. Tang and X. W. Wang (2010). "Let-7g targets collagen type I alpha2 and inhibits cell migration in hepatocellular carcinoma." J Hepatol **52**(5): 690-7.

Ji, J. L., J. S. Zhang, G. C. Huang, J. Qian, X. Q. Wang and S. Mei (2009). "Over-expressed microRNA-27a and 27b influence fat accumulation and cell proliferation during rat hepatic stellate cell activation." Febs Letters **583**(4): 759-66.

Jia L. and X. Liu. (2007) "The conduct of drug metabolism studies considered good practice (II): in vitro experiments." Curr Drug Metab **8**(8):822-9.

Jiang, M. C., H. F. Yang-Yen, J. J. Yen and J. K. Lin (1996). "Curcumin induces apoptosis in immortalized NIH 3T3 and malignant cancer cell lines." Nutr Cancer **26**(1): 111-20.

Jiang, T., X. X. Wang, P. Scherzer, P. Wilson, J. Tallman, H. Takahashi, J. Li, M. Iwahashi, E. Sutherland, L. Arend and M. Levi (2007). "Farnesoid X receptor modulates renal lipid metabolism, fibrosis, and diabetic nephropathy." Diabetes **56**(10): 2485-93.

Jiang, X., E. Tsitsiou, S. E. Herrick and M. A. Lindsay (2010). "MicroRNAs and the regulation of fibrosis." Febs Journal **277**(9): 2015-21.

Jiao, J. J., S. L. Friedman and C. Aloman (2009). "Hepatic fibrosis." Curr Opin Gastroenterol **25**(3): 223-29.

John, C. S., W. D. Bowen, T. Saga, S. Kinuya, B. J. Vilner, J. Baumgold, C. H. Paik, R. C. Reba, R. D. Neumann, V. M. Varma and J. G. Mcafee (1993). "A malignant-melanoma imaging agent - synthesis, characterization, in-vitro binding and biodistribution of iodine-125-(2-piperidinylaminoethyl)4-iodobenzamide." J Nucl Med **34**(12): 2169-75.

John, C. S., B. J. Vilner, B. C. Geyer, T. Moody and W. D. Bowen (1999). "Targeting sigma receptor-binding benzamides as in vivo diagnostic and therapeutic agents for human prostate tumors." Cancer Res **59**(18): 4578-83.

Kadener, S., J. Rodriguez, K. C. Abruzzi, Y. L. Khodor, K. Sugino, M. T. Marr, S. Nelson and M. Rosbash (2009). "Genome-wide identification of targets of the drosha-pasha/DGCR8 complex." RNA **15**(4): 537-45.

Kadler, K. E., A. Hill and E. G. Canty-Laird (2008). "Collagen fibrillogenesis: fibronectin, integrins, and minor collagens as organizers and nucleators." Curr Opin Cell Biol **20**(5): 495-501.

Kagan, H. M. (2000). "Intra- and extracellular enzymes of collagen biosynthesis as biological and chemical targets in the control of fibrosis." Acta Tropica **77**(1): 147-52.

Kagan, H. M. and F. Ryvkin (2011). Lysyl oxidase and lysyl oxidase-like enzymes. The Extracellular Matrix: an Overview. R. P. Mecham. Berlin Heidelber, Springer

Kagan, H. M. and P. C. Trackman (1991). "Properties and function of lysyl oxidase." Am J Respir Cell Mol Biol **5**(3): 206-10.

Kapinas, K., C. Kessler, T. Ricks, G. Gronowicz and A. M. Delany (2010). "miR-29 modulates wnt signaling in human osteoblasts through a positive feedback loop." J Biol Chem **285**(33): 25221-31.

Karkare, S., S. Daniel and D. Bhatnagar (2004). "RNA interference silencing the transcriptional message - Aspects and applications." Appl Biochem Biotechnol **119**(1): 1-12.

Kashiwagi, H., J. E. McDunn, P. O. Simon, P. S. Goedegebuure, J. Xu, L. Jones, K. Chang, F. Johnston, K. Trinkaus, R. S. Hotchkiss, R. H. Mach and W. G. Hawkins (2007).

"Selective sigma-2 ligands preferentially bind to pancreatic adenocarcinomas: applications in diagnostic imaging and therapy." Mol Cancer **6:** 48.

Kato, K., K. Chin, T. Yoshikawa, K. Yamaguchi, Y. Tsuji, T. Esaki, K. Sakai, M. Kimura, T. Hamaguchi, Y. Shimada, Y. Matsumura and R. Ikeda (2012). "Phase II study of NK105, a paclitaxel-incorporating micellar nanoparticle, for previously treated advanced or recurrent gastric cancer." Invest New Drugs **30**(4): 1621-7.

Kim, D. W., S. Y. Kim, H. K. Kim, S. W. Kim, S. W. Shin, J. S. Kim, K. Park, M. Y. Lee and D. S. Heo (2007). "Multicenter phase II trial of Genexol-PM, a novel Cremophor-free, polymeric micelle formulation of paclitaxel, with cisplatin in patients with advanced non-small-cell lung cancer." Ann Oncol **18**(12): 2009-14.

Kim, J. Y., S. Kim, M. Papp, K. Park and R. Pinal (2010a). "Hydrotropic solubilization of poorly water-soluble drugs." J Pharm Sci **99**(9): 3953-65.

Kim, J. Y., S. Kim, R. Pinal and K. Park (2011). "Hydrotropic polymer micelles as versatile vehicles for delivery of poorly water-soluble drugs." J Control Release **152**(1): 13-20.

Kim, S., Y. Shi, J. Y. Kim, K. Park and J. X. Cheng (2010b). "Overcoming the barriers in micellar drug delivery: loading efficiency, in vivo stability, and micelle-cell interaction." Expert Opin Drug Deliv **7**(1): 49-62.

Kim, S. H., J. P. Tan, F. Nederberg, K. Fukushima, J. Colson, C. Yang, A. Nelson, Y. Y. Yang and J. L. Hedrick (2010c). "Hydrogen bonding-enhanced micelle assemblies for drug delivery." Biomaterials **31**(31): 8063-71.

Kim, T. Y., D. W. Kim, J. Y. Chung, S. G. Shin, S. C. Kim, D. S. Heo, N. K. Kim and Y. J. Bang (2004). "Phase I and pharmacokinetic study of Genexol-PM, a cremophor-free, polymeric micelle-formulated paclitaxel, in patients with advanced malignancies." Clin Cancer Res **10**(11): 3708-16.

Kim, Y., S. Peyrol, C.-K. So, C. D. Boyd and K. Csiszar (1999). "Coexpression of the lysyl oxidase-like gene (LOXL) and the gene encoding type III procollagen in induced liver fibrosis." J Cell Biochem **72**(2): 181-88.

Kutter, C. and P. Svoboda (2008). "miRNA, siRNA, piRNA Knowns of the unknown." Rna Biol **5**(4): 181-88.

Kwiecinski, M., A. Noetel, S. Schievenbusch, I. Strack, N. Elfimova, U. Drebber, U Töx, H. P. Dienes and M. Odenthal (2010). "microRNA-29 regulates the expression of profibrogenic mediators in hepatic stellate cells." Z Gastroenterol **48**(01): P1_22.

Kwiecinski, M., I. Strack, A. Noetel, S. Schievenbusch, M. Scheffler, N. Elfimova, H. P. Dienes and M. Odenthal (2009). "MicroRNA-29: a novel antifibrogenic mediator in liver fibrogenesis." J Hepatol **50**: S110.

Lai, E. C. (2002). "Micro RNAs are complementary to 3 ' UTR sequence motifs that mediate negative post-transcriptional regulation." Nat Genet **30**(4): 363-64.

Lakner, A. M., N. M. Steuerwald, T. L. Walling, S. Ghosh, T. Li, I. H. McKillop, M. W. Russo, H. L. Bonkovsky and L. W. Schrum (2012). "Inhibitory effects of microRNA 19b in hepatic stellate cell-mediated fibrogenesis." Hepatology **56**(1): 300-10.

Landauer, J. and H. McConnell (1952). "A Study of Molecular Complexes Formed by Aniline and Aromatic Nitrohydrocarbons1,2." J Am Chem Soc **74**(5): 1221-24.

Lang, Q., Q. Liu, N. Xu, K. L. Qian, J. H. Qi, Y. C. Sun, L. Xiao and X. F. Shi (2011). "The antifibrotic effects of TGF-beta1 siRNA on hepatic fibrosis in rats." Biochem Biophys Res Commun **409**(3): 448-53.

Langer, C. J., K. J. O'Byrne, M. A. Socinski, S. M. Mikhailov, K. Lesniewski-Kmak, M. Smakal, T. E. Ciuleanu, S. V. Orlov, M. Dediu, D. Heigener, A. J. Eisenfeld, L. Sandalic, F. B. Oldham, J. W. Singer and H. J. Ross (2008). "Phase III trial comparing paclitaxel poliglumex (CT-2103, PPX) in combination with carboplatin versus standard paclitaxel and carboplatin in the treatment of PS 2 patients with chemotherapy-naive advanced non-small cell lung cancer." J Thorac Oncol **3**(6): 623-30.

Lasic, D. and F. Martin (1995). Stealth Liposomes. Boca Raton, FL, CRC Press.

Latere Dwan'Isa, J. P., L. Rouxhet, V. Preat, M. E. Brewster and A. Arien (2007). "Prediction of drug solubility in amphiphilic di-block copolymer micelles: the role of polymer-drug compatibility." Pharmazie **62**(7): 499-504.

Lau, N. C., L. P. Lim, E. G. Weinstein and D. P. Bartel (2001). "An abundant class of tiny RNAs with probable regulatory roles in Caenorhabditis elegans." Science **294**(5543): 858-62.

Lee, D. Y., T. Shatseva, Z. Jeyapalan, W. W. Du, Z. Deng and B. B. Yang (2009). "A 3'-untranslated region (3'UTR) induces organ adhesion by regulating miR-199a* functions." PLoS ONE **4**(2): e4527.

Lee, J., S. C. Lee, G. Acharya, C. J. Chang and K. Park (2003). "Hydrotropic solubilization of paclitaxel: analysis of chemical structures for hydrotropic property." Pharm Res **20**(7): 1022-30.

Lee, K. S., H. C. Chung, S. A. Im, Y. H. Park, C. S. Kim, S. B. Kim, S. Y. Rha, M. Y. Lee and J. Ro (2008). "Multicenter phase II trial of Genexol-PM, a Cremophor-free, polymeric micelle formulation of paclitaxel, in patients with metastatic breast cancer." Breast Cancer Res Treat **108**(2): 241-50.

Lee, R. C., R. L. Feinbaum and V. Ambros (1993). "The C. elegans heterochronic gene lin-4 encodes small RNAs with antisense complementarity to lin-14." Cell **75**(5): 843-54.

Lee, R. J. and P. S. Low (1995). "Folate-mediated tumor cell targeting of liposome-entrapped doxorubicin in vitro." Biochim Biophys Acta **1233**(2): 134-44.

Lee, Y., M. Kim, J. J. Han, K. H. Yeom, S. Lee, S. H. Baek and V. N. Kim (2004a). "MicroRNA genes are transcribed by RNA polymerase II." EMBO J **23**(20): 4051-60.

Lee, Y. S., K. Nakahara, J. W. Pham, K. Kim, Z. Y. He, E. J. Sontheimer and R. W. Carthew (2004b). "Distinct roles for Drosophila Dicer-1 and Dicer-2 in the siRNA/miRNA silencing pathways." Cell **117**(1): 69-81.

Lewis, B. P., I. H. Shih, M. W. Jones-Rhoades, D. P. Bartel and C. B. Burge (2003). "Prediction of mammalian microRNA targets." Cell **115**(7): 787-98.

Li. G, Q. Xie, Y. Shi, D. Li, M. Zhang, S Jiang, H. Zhou, H. Lu and Y. Jin (2006). "Inhibition of connective tissue growth factor by siRNA prevents liver fibrosis in rats." J Gene Med **8**(7):889-900.

Li, J., M. Ghazwani, Y. Zhang, J. Lu, J. Fan, C. R. Gandhi and S. Li (2013a). "miR-122 Regulates Collagen Production via Targeting Hepatic Stellate Cells and Suppressing P4HA1 Expression." J Hepatol **58**(3):522-28

Li, J., A. Wilson, X. Gao, R. Kuruba, Y. H. Liu, S. Poloyac, B. Pitt, W. Xie and S. Li (2009a). "Coordinated regulation of dimethylarginine dimethylaminohydrolase-1 and cationic amino acid transporter-1 by farnesoid X receptor in mouse liver and kidney and its implication in the control of blood levels of asymmetric dimethylarginine." J Pharmacol Exp Ther **331**(1): 234-43.

Li, J., A. Wilson, R. Kuruba, Q. Zhang, X. Gao, F. He, L. M. Zhang, B. R. Pitt, W. Xie and S. Li (2008a). "FXR-mediated regulation of eNOS expression in vascular endothelial cells." Cardiovasc Res **77**(1): 169-77.

Li, J., Y. Zhang, R. Kuruba, X. Gao, C. R. Gandhi, W. Xie and S. Li (2011a). "Roles of microRNA-29a in the antifibrotic effect of farnesoid X receptor in hepatic stellate cells." Mol Pharmacol **80**(1): 191-200.

Li, J., J. Lu, Y. Zhang, M. Ghazwani, P. Zhang, X. Gao, and S. Li (2013b) "RNAi in Liver Diseases." in Advanced Delivery and Therapeutic Applications of RNAi (eds K. Cheng and R. I. Mahato), John Wiley and Sons, Ltd, Chichester, UK. doi: 10.1002/9781118610749.ch15

Li, S. D. and L. Huang (2006b). "Targeted Delivery of Antisense Oligodeoxynucleotide and Small Interference RNA into Lung Cancer Cells." Mol Pharm **3**(5): 579-88.

Li, S. D., S. Chono and L. Huang (2008b). "Efficient oncogene silencing and metastasis inhibition via systemic delivery of siRNA." Mol Ther **16**(5): 942-46.

Li, W. Q., C. Chen, M. D. Xu, J. Guo, Y. M. Li, Q. M. Xia, H. M. Liu, J. He, H. Y. Yu and L. Zhu (2011b). "The rno-miR-34 family is upregulated and targets ACSL1 in dimethylnitrosamine-induced hepatic fibrosis in rats." FEBS J **278**(9): 1522-32.

Li, X., Z. Yang, K. Yang, Y. Zhou, X. Chen, Y. Zhang, F. Wang, Y. Liu and L. Ren (2009b). "Self-assembled polymeric micellar nanoparticles as nanocarriers for poorly soluble anticancer drug ethaselen." Nanoscale Res Lett **4**(12): 1502-11.

Li, Y., D. Li, S. Yuan, Z. Wang, F. Tang, R. Nie, J. Weng, L. Ma and B. Tang (2013c). "Embelin-induced MCF-7 breast cancer cell apoptosis and blockade of MCF-7 cells in the G2/M phase via the mitochondrial pathway." Oncol Lett **5**(3): 1005-09.

Li, Y. T., K. E. Swales, G. J. Thomas, T. D. Warner and D. Bishop-Bailey (2007). "Farnesoid X receptor ligands inhibit vascular smooth muscle cell inflammation and migration." Arterioscler Thromb Vasc Biol **27**(12): 2606-11.

Liao, D. Q. and A. M. Weiner (1995). "Concerted evolution of the tandemly repeated genes encoding primate U2 small nuclear RNA (the RNU2 locus) does not prevent rapid diversification of the (CT)(n)center dot(GA)(n) microsatellite embedded within the U2 repeat unit." Genomics **30**(3): 583-93.

Liu, J., H. Lee and C. Allen (2006). "Formulation of drugs in block copolymer micelles: drug loading and release." Curr Pharm Des **12**(36): 4685-701.

Liu, Y., L. Huang and F. Liu (2010). "Paclitaxel nanocrystals for overcoming multidrug resistance in cancer." Mol Pharm **7**(3): 863-9.

Lu, J., Y. Huang, W. Zhao, Y. Chen, J. Li, X. Gao, R. Venkataramanan and S. Li (2013a). "Design and characterization of PEG-Derivatized Vitamin E as a nanomicellar formulation for delivery of paclitaxel." Mol Pharm.

Lu, J. Q., Y. X. Huang, W. C. Zhao, R. T. Marquez, X. J. Meng, J. Li, X. Gao, R. Venkataramanan, Z. Wang and S. Li (2013b). "PEG-derivatized embelin as a nanomicellar carrier for delivery of paclitaxel to breast and prostate cancers." Biomaterials **34**(5): 1591-600.

Lukyanov, A. N., Z. Gao, L. Mazzola and V. P. Torchilin (2002). "Polyethylene glycol-diacyllipid micelles demonstrate increased acculumation in subcutaneous tumors in mice." Pharm Res **19**(10): 1424-9.

Lukyanov, A. N. and V. P. Torchilin (2004). "Micelles from lipid derivatives of water-soluble polymers as delivery systems for poorly soluble drugs." Adv Drug Deliver Rev **56**(9): 1273-89.

Luna, C., G. Li, J. Qiu, D. L. Epstein and P. Gonzalez (2009). "Role of miR-29b on the regulation of the extracellular matrix in human trabecular meshwork cells under chronic oxidative stress." Mol Vis **15**: 2488-97.

Mach, R. H., C. R. Smith, I. AlNabulsi, B. R. Whirrett, S. R. Childers and K. T. Wheeler (1997). "Sigma-2 receptors as potential biomarkers of proliferation in breast cancer." Cancer Res **57**(1): 156-61.

Mach, R. H. and K. T. Wheeler (2009). "Development of molecular probes for imaging sigma-2 receptors in vitro and in vivo." Cent Nerv Syst Agents Med Chem **9**(3): 230-45.

Maloney, P. R., D. J. Parks, C. D. Haffner, A. M. Fivush, G. Chandra, K. D. Plunket, K. L. Creech, L. B. Moore, J. G. Wilson, M. C. Lewis, S. A. Jones and T. M. Willson (2000). "Identification of a chemical tool for the orphan nuclear receptor FXR." J Med Chem **43**(16): 2971-74.

Manabe, I., T. Shindo and R. Nagai (2002). "Gene expression in fibroblasts and fibrosis: involvement in cardiac hypertrophy." Circ Res **91**(12): 1103-13.

Manju, S. and K. Sreenivasan (2011a). "Conjugation of curcumin onto hyaluronic acid enhances its aqueous solubility and stability." J Colloid Interface Sci **359**(1): 318-25.

Manju, S. and K. Sreenivasan (2011b). "Synthesis and characterization of a cytotoxic cationic polyvinylpyrrolidone-curcumin conjugate." J Pharm Sci **100**(2): 504-11.

Mann, J., D. C. Chu, A. Maxwell, F. Oakley, N. L. Zhu, H. Tsukamoto and D. A. Mann (2011). "MeCP2 controls an epigenetic pathway that promotes myofibroblast transdifferentiation and fibrosis." Gastroenterology **138**(2): 705-14, 14 e1-4.

Marek, C. J., S. J. Tucker, D. K. Konstantinou, L. J. Elrick, D. Haefner, C. Sigalas, G. I. Murray, B. Goodwin and M. C. Wright (2005). "Pregnenolone-16 alpha-carbonitrile inhibits rodent liver fibrogenesis via PXR (pregnane X receptor)-dependent and PXR-independent mechanisms." Biochem J **387**: 601-08.

Marutani, T., A. Yamamoto, N. Nagai, H. Kubota and K. Nagata (2004). "Accumulation of type IV collagen in dilated ER leads to apoptosis in HSP47-knockout mouse embryos via induction of CHOP." J Cell Sci **117**(24): 5913-22.

Masuda, H., M. Fukumoto, K. Hirayoshi and K. Nagata (1994). "Coexpression of the collagen-binding stress protein HSP47 gene and the alpha 1(I) and alpha 1(III) collagen genes in carbon tetrachloride-induced rat liver fibrosis." J Clin Invest **94**(6): 2481-8.

Matsumoto, R., T.-P. Su, R. R. Matsumoto and W. D. Bowen (2007). Sigma Receptors: Historical Perspective and Background. Sigma receptors: Chemistry, cell biology and clinical implications. , Springer US**:** 1-23.

Matsumura, Y., T. Hamaguchi, T. Ura, K. Muro, Y. Yamada, Y. Shimada, K. Shirao, T. Okusaka, H. Ueno, M. Ikeda and N. Watanabe (2004). "Phase I clinical trial and pharmacokinetic evaluation of NK911, a micelle-encapsulated doxorubicin." Br J Cancer **91**(10): 1775-81.

Mattick, J. S. and I. V. Makunin (2005). "Small regulatory RNAs in mammals." Hum Mol Genet **14**: R121-R32.

Maurice, T. and T. P. Su (2009). "The pharmacology of sigma-1 receptors." Pharmacol Ther **124**(2): 195-206.

Mendell, J. T. (2005). "MicroRNAs - Critical regulators of development, cellular physiology and malignancy." Cell Cycle **4**(9): 1179-84.

Mi, Y., Y. Liu and S. S. Feng (2011). "Formulation of Docetaxel by folic acid-conjugated d-alpha-tocopheryl polyethylene glycol succinate 2000 (Vitamin E TPGS(2k)) micelles for targeted and synergistic chemotherapy." Biomaterials **32**(16): 4058-66.

Miller, V. M., C. M. Gouvion, B. L. Davidson and H. L. Paulson (2004). "Targeting Alzheimer's disease genes with RNA interference: an efficient strategy for silencing mutant alleles." Nucleic Acids Res **32**(2): 661-68.

Miyahara, T., L. Schrum, R. Rippe, S. G. Xiong, H. F. Yee, K. Motomura, F. A. Anania, T. M. Willson and H. Tsukamoto (2000). "Peroxisome proliferator-activated receptors and hepatic stellate cell activation." J Biol Chem **275**(46): 35715-22.

Moffatt, S., C. Papasakelariou, S. Wiehle and R. Cristiano (2006). "Successful in vivo tumor targeting of prostate-specific membrane antigen with a highly efficient J591//PEI//DNA molecular conjugate." Gene Ther **13**(9): 761-72.

Mori, T., R. Doi, A. Kida, K. Nagai, K. Kami, D. Ito, E. Toyoda, Y. Kawaguchi and S. Uemoto (2007). "Effect of the XIAP inhibitor Embelin on TRAIL-induced apoptosis of pancreatic cancer cells." J Surg Res **142**(2): 281-6.

Moss, E. G. (2002). "MicroRNAs: Hidden in the genome." Curr Biol **12**(4): R138-R40.

Mu, L., A. Chrastina, T. Levchenko and V. P. Torchilin (2005a). " Micelles from poly(ethylene glycol)–phosphatidyl ethanolamine conjugates (PEG-PE) as pharmaceutical nanocarriers for poorly soluble drug camptothecin." J Biomed Nanotechnol **1**(2): 190-95.

Mu, L., T. A. Elbayoumi and V. P. Torchilin (2005b). "Mixed micelles made of poly(ethylene glycol)–phosphatidylethanolamine conjugate and d-α-tocopheryl polyethylene glycol 1000 succinate as pharmaceutical nanocarriers for camptothecin." Int J Pharmaceut **306**(1–2): 142-49.

Mu, L. and S. S. Feng (2002). "Vitamin E TPGS used as emulsifier in the solvent evaporation/extraction technique for fabrication of polymeric nanospheres for controlled release of paclitaxel (Taxol)." J Control Release **80**(1-3): 129-44.

Mukherjee, A., T. K. Prasad, N. M. Rao and R. Banerjee (2005). "Haloperidol-associated stealth liposomes: a potent carrier for delivering genes to human breast cancer cells." J Biol Chem **280**(16): 15619-27.

Murakami, Y., H. Toyoda, M. Tanaka, M. Kuroda, Y. Harada, F. Matsuda, A. Tajima, N. Kosaka, T. Ochiya and K. Shimotohno (2011). "The progression of liver fibrosis is related with overexpression of the miR-199 and 200 families." Plos One **6**(1): e16081.

Musacchio, T., V. Laquintana, A. Latrofa, G. Trapani and V. P. Torchilin (2009). "PEG-PE micelles loaded with paclitaxel and surface-modified by a PBR-ligand: synergistic anticancer effect." Mol Pharm **6**(2): 468-79.

Muthu, M. S., S. A. Kulkarni, J. Q. Xiong and S. S. Feng (2011). "Vitamin E TPGS coated liposomes enhanced cellular uptake and cytotoxicity of docetaxel in brain cancer cells." Int J Pharmaceut **421**(2): 332-40.

Nagai, N., M. Hosokawa, S. Itohara, E. Adachi, T. Matsushita, N. Hokawa and K. Nagata (2000). "Embryonic lethality of molecular chaperone HSP47 knockout mice is associated with defects in collagen biosynthesis." J Cell Biol **150**(6): 1499-505.

Nagata, K. (1996). "HSP47: A collagen-specific molecular chaperone." Trends Biochem Sci **21**(1): 23-26.

Nakagawa, O., X. Ming, L. Huang and R. L. Juliano (2010). " Targeted intracellular delivery of antisense oligonucleotides via conjugation with small-molecule ligands." J Am Chem Soc **132**(26): 8848-49.

Nakayama, S., H. Mukae, N. Sakamoto, T. Kakugawa, S. Yoshioka, H. Soda, H. Oku, Y. Urata, T. Kondo, H. Kubota, K. Nagata and S. Kohno (2008). "Pirfenidone inhibits the expression of HSP47 in TGF-beta1-stimulated human lung fibroblasts." Life Sci **82**(3-4): 210-7.

Nathans, R., C. Y. Chu, A. K. Serquina, C. C. Lu, H. Cao and T. M. Rana (2009). " Cellular microRNA and P bodies modulate host-HIV-1 interactions." Mol Cell **34**(6): 696-709.

Nie, S., Y. Xing, G. J. Kim and J. W. Simons (2007). "Nanotechnology applications in cancer." Annu Rev Biomed Eng **9**: 257-88.

Nikolovska-Coleska, Z., L. Xu, Z. Hu, Y. Tomita, P. Li, P. P. Roller, R. Wang, X. Fang, R. Guo, M. Zhang, M. E. Lippman, D. Yang and S. Wang (2004). "Discovery of embelin as a cell-permeable, small-molecular weight inhibitor of XIAP through structure-based

computational screening of a traditional herbal medicine three-dimensional structure database." J Med Chem **47**(10): 2430-40.

Nishiyama, N., Y. Kato, Y. Sugiyama and K. Kataoka (2001). "Cisplatin-loaded polymer-metal complex micelle with time-modulated decaying property as a novel drug delivery system." Pharmaceut Res **18**(7): 1035-41.

Odot, J., P. Albert, A. Carlier, M. Tarpin, J. Devy and C. Madoulet (2004). "In vitro and in vivo anti-tumoral effect of curcumin against melanoma cells." Int J Cancer **111**(3): 381-7.

Olaso, E. and S. L. Friedman (1998). "Molecular regulation of hepatic fibrogenesis." J Hepatol **29**(5): 836-47.

Ooya, T., S. Lee, K. Huh and K. Park (2006). "Hydrotropic nanocarriers for poorly soluble drugs." Nanocarrier Technologies. M. R. Mozafari, Springer Netherlands**:** 51-73.

Opanasopit, P., M. Yokoyama, M. Watanabe, K. Kawano, Y. Maitani and T. Okano (2004). "Block copolymer design for camptothecin incorporation into polymeric micelles for passive tumor targeting." Pharm Res **21**(11): 2001-8.

Paddison, P. J., J. M. Silva, D. S. Conklin, M. Schlabach, M. M. Li, S. Aruleba, V. Balija, A. O'Shaughnessy, L. Gnoj, K. Scobie, K. Chang, T. Westbrook, M. Cleary, R. Sachidanandam, W. R. McCombie, S. J. Elledge and G. J. Hannon (2004). "A resource for large-scale RNA-interference-based screens in mammals." Nature **428**(6981): 427-31.

Palamakumbura, A. H. and P. C. Trackman (2002). "A fluorometric assay for detection of lysyl oxidase enzyme activity in biological samples." Anal Biochem **300**(2): 245-51.

Parr, M. J., D. Masin, P. R. Cullis and M. B. Bally (1997). "Accumulation of liposomal lipid and encapsulated doxorubicin in murine Lewis lung carcinoma: the lack of beneficial effects by coating liposomes with poly(ethylene glycol)." J Pharmacol Exp Ther **280**(3): 1319-27.

Parsons, C. J., M. Takashima and R. A. Rippe (2007). "Molecular mechanisms of hepatic fibrogenesis." J Gastroen Hepatol **22**: S79-S84.

Payne, S. L., M. J. Hendrix and D. A. Kirschmann (2007). "Paradoxical roles for lysyl oxidases in cancer--a prospect." J Cell Biochem **101**(6): 1338-54.

Perera, R. F. and A. Ray (2007). "MicroRNAs in the search for understanding human diseases." Biodrugs **21**(2): 97-104.

Pogribny, I. P., A. Starlard-Davenport, V. P. Tryndyak, T. Han, S. A. Ross, I. Rusyn and F. A. Beland (2010). "Difference in expression of hepatic microRNAs miR-29c, miR-34a,

miR-155, and miR-200b is associated with strain-specific susceptibility to dietary nonalcoholic steatohepatitis in mice." Lab Invest: doi: 10.1038/labinvest.2010.113.

Popov, Y. and D. Schuppan (2009). "Targeting liver fibrosis: strategies for development and validation of antifibrotic therapies." Hepatology **50**(4): 1294-306.

Poy, M. N., L. Eliasson, J. Krutzfeldt, S. Kuwajima, X. S. Ma, P. E. MacDonald, S. Pfeffer, T. Tuschl, N. Rajewsky, P. Rorsman and M. Stoffel (2004). "A pancreatic islet-specific microRNA regulates insulin secretion." Nature **432**(7014): 226-30.

Prescott, W. A., Jr. and C. E. Johnson (2005). "Antiinflammatory therapies for cystic fibrosis: past, present, and future." Pharmacotherapy **25**(4): 555-73.

Qin, X. F., D. S. An, I. S. Y. Chen and D. Baltimore (2003). "Inhibiting HIV-1 infection in human T cells by lentiviral-mediated delivery of small interfering RNA against CCR5." Proc. Natl. Acad. Sci. U. S. A. **100**(1): 183-88.

Rasool, A. A., A. A. Hussain and L. W. Dittert (1991). "Solubility enhancement of some water-insoluble drugs in the presence of nicotinamide and related compounds." J Pharm Sci **80**(4): 387-93.

Riley, D. J., J. S. Kerr, R. A. Berg, B. D. Ianni, G. G. Pietra, N. H. Edelman and D. J. Prockop (1982). "Beta-aminopropionitrile prevents bleomycin-induced pulmonary fibrosis in the hamster." Am. Rev. Respir. Dis. **125**(1): 67-73.

Ringsdorf, H. (1975). "Structure and properties of pharmacologically active polymers." J Polym Sci Pol Sym **51**(1): 135-53.

Rockey, D. C. (2008). "Current and future anti-fibrotic therapies for chronic liver disease." Clin Liver Dis **12**(4): 939-62, xi.

Rocnik, E. F., E. van der Veer, H. Cao, R. A. Hegele and J. G. Pickering (2002). "Functional linkage between the endoplasmic reticulum protein Hsp47 and procollagen expression in human vascular smooth muscle cells." J Biol Chem **277**(41): 38571-78.

Roderburg, C., G. W. Urban, K. Bettermann, M. Vucur, H. Zimmermann, S. Schmidt, J. Janssen, C. Koppe, P. Knolle, M. Castoldi, F. Tacke, C. Trautwein and T. Luedde (2011). "Micro-RNA profiling reveals a role for miR-29 in human and murine liver fibrosis." Hepatology **53**(1): 209-18.

Safavy, A., K. P. Raisch, S. Mantena, L. L. Sanford, S. W. Sham, N. R. Krishna and J. A. Bonner (2007). "Design and development of water-soluble curcumin conjugates as potential anticancer agents." J Med Chem **50**(24): 6284-88.

Sage, J., L. Yuan, L. Martin, M. G. Mattei, J. L. Guenet, J. G. Liu, C. Hoog, M. Rassoulzadegan and F. Cuzin (1997). "The Sycp1 loci of the mouse genome: Successive retropositions of a meiotic gene during the recent evolution of the genus." Genomics **44**(1): 118-26.

Sanghvi, R., D. Evans and S. H. Yalkowsky (2007). "Stacking complexation by nicotinamide: a useful way of enhancing drug solubility." Int J Pharm **336**(1): 35-41.

Sato, Y., K. Murase, J. Kato, M. Kobune, T. Sato, Y. Kawano, R. Takimoto, K. Takada, K. Miyanishi, T. Matsunaga, T. Takayama and Y. Niitsu (2008). "Resolution of liver cirrhosis using vitamin A-coupled liposomes to deliver siRNA against a collagen-specific chaperone." Nat Biotechnol **26**(4): 431-42.

Satoh, J. and H. Tabunoki (2011). "Comprehensive analysis of human microRNA target networks." BioData Min **4**: 17.

Savic, R., L. Luo, A. Eisenberg and D. Maysinger (2003). "Micellar nanocontainers distribute to defined cytoplasmic organelles." Science **300**(5619): 615-8.

Scherr, M., D. Steinmann and M. Eder (2004). "RNA interference (RNAi) in hematology." Ann Hematol **83**(1): 1-8.

Sekiya, Y., T. Ogawa, K. Yoshizato, K. Ikeda and N. Kawada (2011). "Suppression of hepatic stellate cell activation by microRNA-29b." Biochem Biophys Res Commun **412**(1): 74-79.

Sengupta, S., J. A. den Boon, I. H. Chen, M. A. Newton, S. A. Stanhope, Y. J. Cheng, C. J. Chen, A. Hildesheim, B. Sugden and P. Ahlquist (2008). "MicroRNA 29c is down-regulated in nasopharyngeal carcinomas, up-regulating mRNAs encoding extracellular matrix proteins." Proc Natl Acad Sci U S A **105**(15): 5874-8.

Sezgin, Z., N. Yuksel and T. Baykara (2006). "Preparation and characterization of polymeric micelles for solubilization of poorly soluble anticancer drugs." Eur J Pharm Biopharm **64**(3):261-8.

Shahani, K. and J. Panyam (2011). "Highly loaded, sustained-release microparticles of curcumin for chemoprevention." J Pharm Sci **100**(7): 2599-609.

Shan, S. W., D. Y. Lee, Z. Deng, T. Shatseva, Z. Jeyapalan, W. W. Du, Y. Zhang, J. W. Xuan, S. P. Yee, V. Siragam and B. B. Yang (2009). "MicroRNA miR-17 retards tissue growth and represses fibronectin expression." Nat Cell Biol **11**(8): 1031-38.

Sharma, R. A., A. J. Gescher and W. P. Steward (2005). "Curcumin: the story so far." Eur J Cancer **41**(13): 1955-68.

Shen, H., L. Zhang and A. Eisenberg (1999). "Multiple pH-Induced Morphological Changes in Aggregates of Polystyrene-block-poly(4-vinylpyridine) in DMF/H_2O Mixtures." J Am Chem Soc **121**(12): 2728-40.

Shiah, J. G., Y. Sun, P. Kopečková, C. M. Peterson, R. C. Straight and J. Kopeček (2001). "Combination chemotherapy and photodynamic therapy of targetable N-(2-hydroxypropyl)methacrylamide copolymer–doxorubicin/mesochlorin e6-OV-TL 16 antibody immunoconjugates." J Control Release **74**(1–3): 249-53.

Shirai, K., M. Matsuoka and K. Fukunishi (1999). "Fluorescence quenching by intermolecular pi-pi interactions of 2,5-bis(N,N-dialkylamino)-3,6-dicyanopyrazines." Dyes Pigments **42**(1): 95-101.

Shishodia, S., H. M. Amin, R. Lai and B. B. Aggarwal (2005). "Curcumin (diferuloylmethane) inhibits constitutive NF-kappaB activation, induces G1/S arrest, suppresses proliferation, and induces apoptosis in mantle cell lymphoma." Biochem Pharmacol **70**(5): 700-13.

Siegel, R. C., K. H. Chen, J. S. Greenspan and J. M. Aguiar (1978). "Biochemical and immunochemical study of lysyl oxidase in experimental hepatic fibrosis in the rat." Proc Natl Acad Sci U S A **75**(6): 2945-9.

Simone, E. A., T. D. Dziubla, D. E. Discher and V. R. Muzykantov (2009). "Filamentous polymer nanocarriers of tunable stiffness that encapsulate the therapeutic enzyme catalase." Biomacromolecules **10**(6): 1324-30.

Sinal, C. J., M. Tohkin, M. Miyata, J. M. Ward, G. Lambert and F. J. Gonzalez (2000). "Targeted disruption of the nuclear receptor FXR/BAR impairs bile acid and lipid homeostasis." Cell **102**(6): 731-44.

Singh, D., R. Singh, P. Singh and R. S. Gupta (2009). "Effects of embelin on lipid peroxidation and free radical scavenging activity against liver damage in rats." Basic Clin Pharmacol Toxicol **105**(4): 243-8.

Sioud, M. (2004). "Therapeutic siRNAs." Trends Pharmacol Sci **25**(1): 22-8.

Soga, O., C. F. van Nostrum, M. Fens, C. J. Rijcken, R. M. Schiffelers, G. Storm and W. E. Hennink (2005). "Thermosensitive and biodegradable polymeric micelles for paclitaxel delivery." J Control Release **103**(2): 341-53.

Sommer, P., C. Gleyzal, M. Raccurt, M. Delbourg, M. Serrar, P. Joazeiro, S. Peyrol, H. Kagan, P. C. Trackman and J. A. Grimaud (1993). "Transient expression of lysyl oxidase by liver myofibroblasts in murine schistosomiasis." Lab Invest **69**(4): 460-70.

Spitzer, D., P. O. Simon, Jr., H. Kashiwagi, J. Xu, C. Zeng, S. Vangveravong, D. Zhou, K. Chang, J. E. McDunn, J. R. Hornick, P. Goedegebuure, R. S. Hotchkiss, R. H. Mach and

W. G. Hawkins (2012). "Use of multifunctional sigma-2 receptor ligand conjugates to trigger cancer-selective cell death signaling." Cancer Res **72**(1): 201-9.

Sugiyama, T., H. Cam, A. Verdel, D. Moazed and S. I. S. Grewal (2005). "RNA-dependent RNA polymerase is an essential component of a self-enforcing loop coupling heterochromatin assembly to siRNA production." P Natl Acad Sci U.S.A. **102**(1): 152-57.

Sutton, D., N. Nasongkla, E. Blanco and J. Gao (2007). "Functionalized micellar systems for cancer targeted drug delivery." Pharm Res **24**(6): 1029-46.

Suzuki, C., Y. Daigo, N. Ishikawa, T. Kato, S. Hayama, T. Ito, E. Tsuchiya and Y. Nakamura (2005). "ANLN plays a critical role in human lung carcinogenesis through the activation of RHOA and by involvement in the phosphoinositide 3-kinase/AKT pathway." Cancer Res **65**(24): 11314-25.

Taccioli, C., E. Fabbri, R. Visone, S. Volinia, G. A. Calin, L. Y. Fong, R. Gambari, A. Bottoni, M. Acunzo, J. Hagan, M. V. Iorio, C. Piovan, G. Romano and C. M. Croce (2009). "UCbase & miRfunc: a database of ultraconserved sequences and microRNA function." Nucleic Acids Res **37**: D41-D48.

Takamizawa, J., H. Konishi, K. Yanagisawa, S. Tomida, H. Osada, H. Endoh, T. Harano, Y. Yatabe, M. Nagino, Y. Nimura, T. Mitsudomi and T. Takahashi (2004). "Reduced expression of the let-7 microRNAs in human lung cancers in association with shortened postoperative survival." Cancer Res **64**(11): 3753-56.

Tamm, I., S. M. Kornblau, H. Segall, S. Krajewski, K. Welsh, S. Kitada, D. A. Scudiero, G. Tudor, Y. H. Qui, A. Monks, M. Andreeff and J. C. Reed (2000). "Expression and prognostic significance of IAP-family genes in human cancers and myeloid leukemias." Clin Cancer Res **6**(5): 1796-803.

Tang, H., C. J. Murphy, B. Zhang, Y. Shen, M. Sui, E. A. Van Kirk, X. Feng and W. J. Murdoch (2010). "Amphiphilic curcumin conjugate-forming nanoparticles as anticancer prodrug and drug carriers: in vitro and in vivo effects." Nanomedicine (Lond) **5**(6): 855-65.

Thabut, D. and V. Shah (2010). "Intrahepatic angiogenesis and sinusoidal remodeling in chronic liver disease: new targets for the treatment of portal hypertension?" J Hepatol **53**(5): 976-80.

Thirunavukkarasu, C., T. Uemura, L. F. Wang, S. C. Watkins and C. R. Gandhi (2005). "Normal rat hepatic stellate cells respond to endotoxin in LBP-independent manner to produce inhibitor(s) of DNA synthesis in hepatocytes." J Cell Physiol **204**(2): 654-65.

Torchilin, V. P. (2007). "Micellar nanocarriers: pharmaceutical perspectives." Pharm Res **24**(1): 1-16.

Triger, D. R., R. G. Malia and F. E. Preston (1988). "Platelet function and coagulation in patients with hepatobiliary disorders receiving cefotetan prophylaxis." Infection **16**(2): 105-8.

Trubetskoy, V. S. and V. P. Torchilin (1995). "Use of polyoxyethylene-lipid conjugates as long-circulating carriers for delivery of therapeutic and diagnostic agents." Adv Drug Deliver Rev **16**(2–3): 311-20.

Umesono, K., K. K. Murakami, C. C. Thompson and R. M. Evans (1991). "Direct repeats as selective response elements for the thyroid hormone, retinoic acid, and vitamin D3 receptors." Cell **65**(7): 1255-66.

van Rooij, E., L. B. Sutherland, J. E. Thatcher, J. M. DiMaio, R. H. Naseem, W. S. Marshall, J. A. Hill and E. N. Olson (2008). "Dysregulation of microRNAs after myocardial infarction reveals a role of miR-29 in cardiac fibrosis." P Natl Acad Sci U.S.A. **105**(35): 13027-32.

Vangveravong, S., J. Xu, C. Zeng and R. H. Mach (2006). " Synthesis of N-substituted 9-azabicyclo[3.3.1]nonan-3alpha-yl carbamate analogs as sigma2 receptor ligands." Bioorg Med Chem **14**(20): 6988-97.

Vargason, J. M., G. Szittya, J. Burgyan and T. M. T. Hall (2003). "Size selective recognition of siRNA by an RNA silencing suppressor." Cell **115**(7): 799-811.

Varma, M. V. and R. Panchagnula (2005). "Enhanced oral paclitaxel absorption with vitamin E-TPGS: effect on solubility and permeability in vitro, in situ and in vivo." Eur J Pharm Sci **25**(4-5): 445-53.

Venugopal, S. K., J. Jiang, T.-H. Kim, Y. Li, S.-S. Wang, N. J. Torok, J. Wu and M. A. Zern (2010). "Liver fibrosis causes downregulation of miRNA-150 and miRNA-194 in hepatic stellate cells, and their overexpression causes decreased stellate cell activation." Am J Physiol Gastrointest Liver Physiol **298**(1): G101-06.

Verschraegen, C. F., K. Skubitz, A. Daud, A. P. Kudelka, I. Rabinowitz, C. Allievi, A. Eisenfeld, J. W. Singer and F. B. Oldham (2009). "A phase I and pharmacokinetic study of paclitaxel poliglumex and cisplatin in patients with advanced solid tumors." Cancer Chemother Pharmacol **63**(5): 903-10.

Vilner, B. J., C. S. John and W. D. Bowen (1995). "Sigma-1 and sigma-2 receptors are expressed in a wide variety of human and rodent tumor-cell lines." Cancer Res **55**(2): 408-13.

Vitaglione, P., F. Morisco, N. Caporaso and V. Fogliano (2004). "Dietary antioxidant compounds and liver health." Crit Rev Food Sci Nutr **44**(7-8): 575-86.

Vogler, M., H. Walczak, D. Stadel, T. L. Haas, F. Genze, M. Jovanovic, U. Bhanot, C. Hasel, P. Moller, J. E. Gschwend, T. Simmet, K. M. Debatin and S. Fulda (2009). "Small molecule XIAP inhibitors enhance TRAIL-induced apoptosis and antitumor activity in preclinical models of pancreatic carcinoma." Cancer Res **69**(6): 2425-34.

Walters, D. K. and D. F. Jelinek (2002). "The effectiveness of double-stranded short inhibitory RNAs (siRNAs) may depend on the method of transfection." Antisense Nucleic Acid Drug Dev **12**(6): 411-18.

Wang B., R. Komers, R. Carew, C. E. Winbanks, B. Xu, M. Herman-Edelstein, P. Koh, M. Thomas, K. Jandeleit-Dahm, P. Gregorevic, M. E. Cooper, P. Kantharidis. (2012d) "Suppression of microRNA-29 expression by TGF-β1 promotes collagen expression and renal fibrosis." J Am Soc Nephrol **23**(2):252-65.

Wang, A. Z., F. Gu, L. Zhang, J. M. Chan, A. Radovic-Moreno, M. R. Shaikh and O. C. Farokhzad (2008a). "Biofunctionalized targeted nanoparticles for therapeutic applications." Expert Opin Biol Ther **8**(8): 1063-70.

Wang, J., D. A. Mongayt, A. N. Lukyanov, T. S. Levchenko and V. P. Torchilin (2004). "Preparation and in vitro synergistic anticancer effect of vitamin K3 and 1,8-diazabicyclo[5,4,0]undec-7-ene in poly(ethylene glycol)-diacyllipid micelles." Int J Pharm **272**(1-2): 129-35.

Wang, J., J. Sun, Q. Chen, Y. Gao, L. Li, H. Li, D. Leng, Y. Wang, Y. Sun, Y. Jing, S. Wang and Z. He (2012a). "Star-shape copolymer of lysine-linked di-tocopherol polyethylene glycol 2000 succinate for doxorubicin delivery with reversal of multidrug resistance." Biomaterials **33**(28): 6877-88.

Wang, J., R. Wang and L. B. Li (2009a). "Preparation and properties of hydroxycamptothecin-loaded nanoparticles made of amphiphilic copolymer and normal polymer." J Colloid Interface Sci **336**(2): 808-13.

Wang, X., J. Li, Y. Wang, L. Koenig, A. Gjyrezi, P. Giannakakou, E. H. Shin, M. Tighiouart, Z. Chen, S. Nie and D. M. Shin (2012b). "A folate receptor-targeting nanoparticle minimizes drug resistance in a human cancer model." ACS Nano **5**(8): 6184-94.

Wang, X. X., T. Jiang, Y. Shen, L. Adorini, M. Pruzanski, F. J. Gonzalez, P. Scherzer, L. Lewis, S. Miyazaki-Anzai and M. Levi (2009b). "The farnesoid X receptor modulates renal lipid metabolism and diet-induced renal inflammation, fibrosis, and proteinuria." Am J Physiol Renal Physiol **297**(6): F1587-96.

Wang, Y., J. Xu, X. Xia, M. Yang, S. Vangveravong, J. Chen, R. H. Mach and Y. Xia (2012c). "SV119-gold nanocage conjugates: a new platform for targeting cancer cells via sigma-2 receptors." Nanoscale **4**(2): 421-4.

Wang, Z. and L. Li (2008b). "Adenovirus-mediated RNA interference against collagen-specific molecular chaperone 47-KDa heat shock protein suppresses scar formation on mouse wounds." Cell Biol Int **32**(5): 484-93.

Weissig, V., K. R. Whiteman and V. P. Torchilin (1998). "Accumulation of protein-loaded long-circulating micelles and liposomes in subcutaneous Lewis lung carcinoma in mice." Pharm Res **15**(10): 1552-6.

Weisz, B., K. Giehl, M. Gana-Weisz, Y. Egozi, G. Ben-Baruch, D. Marciano, P. Gierschik and Y. Kloog (1999). "A new functional Ras antagonist inhibits human pancreatic tumor growth in nude mice." Oncogene **18**(16): 2579-88.

Wheeler, K. T., L. M. Wang, C. A. Wallen, S. R. Childers, J. M. Cline, P. C. Keng and R. H. Mach (2000). "Sigma-2 receptors as a biomarker of proliferation in solid tumours." Br J Cancer **82**(6): 1223-32.

Wilken, R., M. S. Veena, M. B. Wang and E. S. Srivatsan (2011). "Curcumin: A review of anti-cancer properties and therapeutic activity in head and neck squamous cell carcinoma." Mol Cancer **10**: 12.

Win, K. Y. and S. S. Feng (2006). "In vitro and in vivo studies on vitamin E TPGS-emulsified poly(D,L-lactic-co-glycolic acid) nanoparticles for paclitaxel formulation." Biomaterials **27**(10): 2285-91.

Woo, J.-H., Y.-H. Kim, Y.-J. Choi, D.-G. Kim, K.-S. Lee, J. H. Bae, D. S. Min, J.-S. Chang, Y.-J. Jeong, Y. H. Lee, J.-W. Park and T. K. Kwon (2003). "Molecular mechanisms of curcumin-induced cytotoxicity: induction of apoptosis through generation of reactive oxygen species, down-regulation of Bcl-XL and IAP, the release of cytochrome c and inhibition of Akt." Carcinogenesis **24**(7): 1199-208.

Xia, Z., K. Abe, A. Furusu, M. Miyazaki, Y. Obata, Y. Tabata, T. Koji and S. Kohno (2008). "Suppression of renal tubulointerstitial fibrosis by small interfering RNA targeting heat shock protein 47." Am J Nephrol **28**(1): 34-46.

Xiao, K., J. Luo, W. L. Fowler, Y. Li, J. S. Lee, L. Xing, R. H. Cheng, L. Wang and K. S. Lam (2009). "A self-assembling nanoparticle for paclitaxel delivery in ovarian cancer." Biomaterials **30**(30): 6006-16.

Xiao, K., J. Luo, Y. Li, J. S. Lee, G. Fung and K. S. Lam (2011). "PEG-oligocholic acid telodendrimer micelles for the targeted delivery of doxorubicin to B-cell lymphoma." J Control Release **155**(2): 272-81.

Xin, F., M. Li, C. Balch, M. Thomson, M. Fan, Y. Liu, S. M. Hammond, S. Kim and K. P. Nephew (2009). "Computational analysis of microRNA profiles and their target genes suggests significant involvement in breast cancer antiestrogen resistance." Bioinformatics **25**(4): 430-4.

Xu, H., H. Abe, M. Naito, Y. Fukumori, H. Ichikawa, S. Endoh and K. Hata (2010). "Efficient dispersing and shortening of super-growth carbon nanotubes by ultrasonic treatment with ceramic balls and surfactants." Adv Powder Technol **21**(5): 551-55.

Xu, J., C. Zeng, W. Chu, F. Pan, J. M. Rothfuss, F. Zhang, Z. Tu, D. Zhou, D. Zeng, S. Vangveravong, F. Johnston, D. Spitzer, K. C. Chang, R. S. Hotchkiss, W. G. Hawkins, K. T. Wheeler and R. H. Mach (2011). "Identification of the PGRMC1 protein complex as the putative sigma-2 receptor binding site." Nat Commun **2**: 380.

Xu, L., A. Y. Hui, E. Albanis, M. J. Arthur, S. M. O'Byrne, W. S. Blaner, P. Mukherjee, S. L. Friedman and F. J. Eng (2005). "Human hepatic stellate cell lines, LX-1 and LX-2: new tools for analysis of hepatic fibrosis." Gut **54**(1): 142-51.

Yallapu, M. M., M. Jaggi and S. C. Chauhan (2010). "beta-Cyclodextrin-curcumin self-assembly enhances curcumin delivery in prostate cancer cells." Colloids Surf B Biointerfaces **79**(1): 113-25.

Yan, A., A. Von Dem Bussche, A. B. Kane and R. H. Hurt (2007). "Tocopheryl polyethylene glycol succinate as a safe, antioxidant surfactant for processing carbon nanotubes and fullerenes." Carbon N Y **45**(13): 2463-70.

Yang, C., A. B. Attia, J. P. Tan, X. Ke, S. Gao, J. L. Hedrick and Y. Y. Yang (2012a). "The role of non-covalent interactions in anticancer drug loading and kinetic stability of polymeric micelles." Biomaterials **33**(10): 2971-9.

Yang, R., S. Zhang, D. Kong, X. Gao, Y. Zhao and Z. Wang (2012b). "Biodegradable polymer-curcumin conjugate micelles enhance the loading and delivery of low-potency curcumin." Pharm Res **29**(12): 3512-25.

Yang, T., Y. Wang, Z. Li, W. Dai, J. Yin, L. Liang, X. Ying, S. Zhou, J. Wang, X. Zhang and Q. Zhang (2012c). "Targeted delivery of a combination therapy consisting of combretastatin A4 and low-dose doxorubicin against tumor neovasculature." Nanomedicine **8**(1): 81-92.

Ye, Z., H. S. Houssein and R. I. Mahato (2007). "Bioconjugation of oligonucleotides for treating liver fibrosis." Oligonucleotides **17**(4): 349-404.

Yokoyama, M., S. Fukushima, R. Uehara, K. Okamoto, K. Kataoka*, Y. Sakurai and T. Okano (1998). "Characterization of physical entrapment and chemical conjugation of adriamycin in polymeric micelles and their design for in vivo delivery to a solid tumor." J Control Release **50**(1–3): 79-92.

Yokoyama, M., G. S. Kwon, T. Okano, Y. Sakurai, H. Ekimoto, K. Okamoto, H. Mashiba, T. Seto and K. Kataoka (1993). "Composition-dependent in vivo antitumor activity of

adriamycin-conjugated polymeric micelle against murine colon adenocarcinoma 26." Drug Deliv **1**(1): 11-19.

Yokoyama, M., G. S. Kwon, T. Okano, Y. Sakurai, T. Seto and K. Kataoka (1992). "Preparation of micelle-forming polymer-drug conjugates." Bioconjug Chem **3**(4): 295-301.

Yokoyama, M., T. Okano, Y. Sakurai, H. Ekimoto, C. Shibazaki and K. Kataoka (1991). "Toxicity and antitumor activity against solid tumors of micelle-forming polymeric anticancer drug and its extremely long circulation in blood." Cancer Res **51**(12): 3229-36.

Yokoyama, M., T. Okano, Y. Sakurai and K. Kataoka (1994). "Improved synthesis of adriamycin-conjugated poly (ethylene oxide)-poly (aspartic acid) block copolymer and formation of unimodal micellar structure with controlled amount of physically entrapped adriamycin." J Control Release **32**(3): 269-77.

Yokoyama, M., T. Okano, Y. Sakurai, S. Suwa and K. Kataoka (1996). "Introduction of cisplatin into polymeric micelle." J Control Release **39**(2-3): 351-56.

Yoysungnoen, P., P. Wirachwong, P. Bhattarakosol, H. Niimi and S. Patumraj (2006). "Effects of curcumin on tumor angiogenesis and biomarkers, COX-2 and VEGF, in hepatocellular carcinoma cell-implanted nude mice." Clin Hemorheol Microcirc **34**(1-2): 109-15.

Yu, L., A. Bridgers, J. Polli, A. Vickers, S. Long, A. Roy, R. Winnike and M. Coffin (1999). "Vitamin E-TPGS increases absorption flux of an HIV protease inhibitor by enhancing its solubility and permeability." Pharmaceut Res **16**(12): 1812-17.

Yu, Y., L. Zhang and A. Eisenberg (1998). "Morphogenic effect of solvent on crew-cut aggregates of apmphiphilic diblock copolymers." Macromolecules **31**(4): 1144-54.

Zamore, P. D. and N. Aronin (2003). "siRNAs knock down hepatitis." Nat Med **9**(3): 266-67.

Zhang, F., G. Y. Koh, D. P. Jeansonne, J. Hollingsworth, P. S. Russo, G. Vicente, R. W. Stout and Z. Liu (2011a). "A novel solubility-enhanced curcumin formulation showing stability and maintenance of anticancer activity." J Pharm Sci **100**(7): 2778-89.

Zhang, P., J. Lu, Y. Huang, W. Zhao, Y. Zhang, X. Zhang, J. Li, R. Venkataramanan, X. Gao and S. Li (2014). "Design and evaluation of a PEGylated lipopeptide equipped with drug-interactive motifs as an improved drug carrier " AAPS J **16**(1):114-24.

Zhang, Q., F. He, R. Kuruba, X. Gao, A. Wilson, J. Li, T. R. Billiar, B. R. Pitt, W. Xie and S. Li (2008). "FXR-mediated regulation of angiotensin type 2 receptor expression in vascular smooth muscle cells." Cardiovasc Res **77**(3): 560-9.

Zhang, X., J. Lu, Y. Huang, W. Zhao, Y. Chen, J. Li, X. Gao, R. Venkataramanan, M. Sun, D. B. Stolz, L. Zhang and S. Li (2013). "PEG-farnesylthiosalicylate conjugate as a nanomicellar carrier for delivery of paclitaxel." Bioconjug Chem **24**(3): 464-72.

Zhang, Y., C. H. Hagedorn and L. Wang (2011b). "Role of nuclear receptor SHP in metabolism and cancer." Biochim Biophys Acta **1812**(8): 893-908.

Zhang, Y. F., J. C. Wang, D. Y. Bian, X. Zhang and Q. Zhang (2010). "Targeted delivery of RGD-modified liposomes encapsulating both combretastatin A-4 and doxorubicin for tumor therapy: in vitro and in vivo studies." Eur J Pharm Biopharm **74**(3): 467-73.

Zhang, Z. and S. S. Feng (2006). "Nanoparticles of poly(lactide)/vitamin E TPGS copolymer for cancer chemotherapy: synthesis, formulation, characterization and in vitro drug release." Biomaterials **27**(2): 262-70.

Zhang, Z., S. Tan and S. S. Feng (2012). "Vitamin E TPGS as a molecular biomaterial for drug delivery." Biomaterials **33**(19): 4889-906.

Zhao, L., Y. Shi, S. Zou, M. Sun, L. Lil and G. Zhail (2011). "Formulation and in vitro evaluation of quercetin loaded polymeric micelles composed of pluronic P123 and D-α-tocopheryl polyethylene glycol succinate." J Biomed Nanotechnol **7**(3): 358-65.

Zhao, Y., Y. Wang, Q. Wang, Z. Liu, Q. Liu and X. Deng (2012). "Hepatic stellate cells produce vascular endothelial growth factor via phospho-p44/42 mitogen-activated protein kinase/cyclooxygenase-2 pathway." Mol Cell Biochem **359**(1-2): 217-23.

Zhou, W., X. Yuan, A. Wilson, L. J. Yang, M. Mokotoff, B. Pitt and S. Li (2002a). "Efficient intracellular delivery of oligonucleotides formulated in folate receptor-targeted lipid vesicles." Bioconjugate Chem **13**(6): 1220-25.

Zhou, Y., Y. P. Ching, K. H. Kok, H. F. Kung and D. Y. Jin (2002b). "Post-transcriptional suppression of gene expression in Xenopus embryos by small interfering RNA." Nucleic Acids Res **30**(7): 1664-69.

Zhu, X. C., Q. Z. Dong, X. F. Zhang, B. Deng, H. L. Jia, Q. H. Ye, L. X. Qin and X. Z. Wu (2012). "microRNA-29a suppresses cell proliferation by targeting SPARC in hepatocellular carcinoma." Int J Mol Med **30**(6): 1321-6.